SDC-91-170

SDC
SOLENOIDAL DETECTOR NOTES

CONCEPTUAL DESIGN REPORT: WINE RACK DESIGN OF THE SDC BARREL AND INTERMEDIATE MUON CHAMBER

Brandeis University
Harvard University
Tufts University

November 12, 1991

91
SDC-92-170

Conceptual Design Report

Wine Rack Design

of the
SDC Barrel and Intermediate
Muon Chambers

The Boston Area Group:

Brandeis University
Harvard University
Tufts University

Preliminary Version 0.2
November 12, 1991

Preface to Preliminary Version 0.2

We plan for this document to grow into a conceptual design report for the wine rack design of the SDC barrel and intermediate muon chambers, and eventually, if the wine rack design is selected, to be an important input to the Technical Proposal. At the present, it is in a rather early form, and is being issued to give the Technical Review Committee and the SDC muon group some preliminary information about this design.

The present report deals mainly with the general ideas of the design and a first report on the full-length prototype. Later versions will contain test results and more information on the proposed final design, including details of the supermodule.

This report has been prepared by physicists and engineers from Brandeis, Harvard, and Tufts Universities, and consulting engineers from Draper Laboratory.

Table of Contents

I. Introduction

II. Full-Length Prototype Design

A. Introduction

B. Drift Cell Design

C. Tube Design

D. Tube Assembly

E. Box Design

F. Alignment System

G. Box Assembly

H. Design Verification

Table of Figures

I-1 Extrusion cross sections.
I-2 Configuration of the prototype box.
I-3 Schematic of the supermodule box.
I-4 Layout of θ-measuring tubes in layer BW2.
I-5 Drift cell for the 8-cm drift version.
I-6 Illustration of the overlap between tubes in the same layer.
I-7 Maximum gravitational wire sag versus span.
I-8 Maximum tube deflection versus minor axis of the ellipse.
I-9 Maximum tube deflection versus span.
II.A-1 Layout of drift tubes in the prototype box.
II.A-2 Relationship of the prototype chamber to the full barrel muon system.
II.B-1 Drift cell for the 4-cm drift version.
II.B-2 Drift cell for the 4-cm drift version with wire displaced up 1 mm.
II.B-3 Drift cell for the 4-cm drift version with wire displaced right 1 mm.
II.C-1a Exploded isometric drawing of the prototype drift tube.
II.C-1b Assembly drawing of the drift tube.
II.C-2 Details of the field shaping board.
II.C-3 Details of wire and board support bridges.
II.C-4 Details of the end caps.
II.C-5 Details of the feed throughs.
II.C-6 Maximum sag versus wire tension.
II.D-1 Details of the drift tube assembly station.
II.D-2 Details of the wire locator.
II.E-1 Chamber box deflections versus stiffness ratio for an aluminum box.
II.E-2 Chamber box deflections versus stiffness ratio for a graphite/epoxy box.
II.E-3 Chamber box deflections versus stiffness ratio for tubes potted together.
II.E-4 Schematic of the prototype chamber box.
II.E-5 Prototype bulkhead adjustment eccentric.
II.E-6 End bulkhead.
II.E-7a Intermediate moveable bulkhead.
II.E-7b Intermediate fixed bulkhead (picture frame).

II.E-8 Schematic of the prototype box design.
II.E-9 End view of the prototype box.
II.E-10 Hatch configuration and connection details.
II.F-1 Schematic chamber deformation and compensation concept.
II.F-2 Schematic of the prototype alignment system.
II.F-3 LED mount for prototype alignment system.
II.F-4 Lens mount for prototype alignment system.
II.F-5 Quad-cell detector mount for prototype alignment system.
II.F-6 Comparative output of quad-cell and lateral effect detectors.
II.F-7 Light source tradeoffs.
II.G-1 Schematic of box assembly table.
II.G-2 Prototype box assembly table arrangement.
II.H-1 Transmission of x-rays.
II.H-2 x-ray film and fiducial holder.
II.H-3 x-ray photograph of a 50 μm tungsten wire inside an aluminum drift tube.

I. Introduction

Rationale and Overview

The SDC barrel and intermediate muon chambers are required to have the following properties:

1. They must have reasonably good resolution, approximately 250 μm per station. This is required to provide good redundant momentum measurements to several hundred GeV transverse momentum.
2. They must have good track pair resolution so that delta rays accompanying muons can be resolved.
3. They must be capable of accepting particles with angles of up to 55 degrees to the normal without significant loss of resolution.
4. They must be capable of having a single wire span a distance of up to 9 m.
5. In order to implement a simple first-level trigger, pairs of chambers must have wires that are accurately projective to the interaction point.
6. There should be a minimum of dead space within a layer so that the first level trigger is as robust as possible.
7. They must be easily industrialized. That is, they must be capable of being built at several sites with relatively unskilled labor with good quality control.
8. They must be relatively inexpensive.

The Boston Group (a collaboration of physicists and engineers from Brandeis, Harvard, and Tufts Universities, consulting with engineers from Draper Laboratory) has developed a design for these chambers which specifically addresses all of these requirements. The design had been dubbed the "wire rack" design for reasons that will be apparent.

The system consists of two parts which are manufactured separately: the drift tubes and the box that holds them. A drift tube consists of a single wire suspended in an oval-shaped aluminum extrusion. The electrostatic field is created by field-shaping boards on either side of the wire. The wire is suspended at several points along the tube, approximately every three meters, by being glued to a support. The position of the wire at the support is directly positioned relative to grooves on the

bottom of the extrusion in a single step using a positioning fixture. Figure I-1 shows 4 and 8 cm-drift versions of this tube. The initial full length prototype is being constructed with the 4 cm drift tubes, but the larger tubes, which are also being prototyped, are proposed for the production version.

The box is a semi-rigid structure with adjustable bulkheads at each point that the wire is supported within the drift tube. Figure I-2 shows the prototype box and Fig. I-3 shows a supermodule box. The adjustable bulkheads have NC-milled holes for the drift tubes, which are oversized except for two "rails" or keys which mate to the groves in the drift tubes. The holes are milled into the bulkheads so that the tubes face the interaction region within 8 degrees. This is illustrated in Figure I-4, which shows the layout of theta tubes for layer BW2. The bulkheads are aligned to each other with a simple optical system which is built into the bulkheads. It is intended that the boxes will be approximately 8 m by 9 m and will be assembled close to the SDC hall. After a box has been assembled, the drift tubes, which have been fabricated at several remote sites, are slid into the box with the same ease that one slides a wine bottle into a wine rack.

How then does this design address the above requirements? The first requirement of good resolution has two parts. The electrostatic field must be such that primary ionization electrons from a sufficient path length are reasonably isochronous. The shaped field created by the field shaping boards in this design insures this over most of the drift region. Figure I-5 shows a field lines, and isochronous surfaces for an 8 cm-drift tube. The second aspect of resolution is that the wire location is well-known at all points. The accuracy of the wire placement is assured by the single step placement of the wire relative to the locating grooves on the extrusion. The wire sag between supports is small, of order 125 μm. The grooves are then referenced to the keys in the NC-milled bulkheads. The bulkheads are then optically aligned to each other. Thus, there are only four steps in which errors can accumulate: wire to groove, groove to key, key to bulkhead, and bulkhead to bulkhead. Each of these steps can be controlled to within 25 to 50 μm, leading to an acceptably small accumulated error in the wire position.

The second requirement of good track pair separation and the third requirement of accepting tracks up to 55 degrees to the normal are met by having shaped fields and

having the tubes face the interaction region, so that ionization from high momentum tracks is highly isochronous over almost the entire path length.

The fourth requirement of a 9 m wire is met by the wire supports, and the fifth requirement of projective wires is met trivially by milling of holes in the bulkhead.

The sixth requirement of maximum robustness is met by feature which we believe to be unique to this design. The first level trigger matches two drift tubes with the projective wires. If tubes were just lined up in a brick style, then particles near the wall of a tube have a good chance of having an angle such that they do not pass through the projective tube. However, in this design we have overlapped the tubes in each layer such that every track with transverse momentum above 20 GeV/c will pass through a pair of projective tubes, unless it scatters by more than two standard deviations. An example of this is shown in Figure I-6.

The seventh requirement is met by having few, if any steps, that cannot be performed by unskilled labor. During drift tube production, only critical step for precision is the wire placement, which is done by a device which locates the wire automatically. After fabrication of a tube is completed, the position of the wire can checked by an X-ray device, which we are developing. The location of the tubes is guaranteed by the precision of the NC-milling and a built-in alignment system, which allows the alignment to be checked, and adjusted, if needed, in situ.

The eighth requirement of minimal cost is met by having a simple assembly procedure and by minimizing the number the channels. The latter is done by using cells with a maximum drift of 8 cm.

Basic Design Parameters

As will be discussed in Section II.B, the electrostatics of a field-shaped cell would make it quite difficult to meet a resolution requirement of 250 μm with unsupported wires over a 9 m span. There are several considerations that make spans of approximately 3 meters quite attractive. First, if a 50 μm tungsten wire is strung at 350 g tension, a value that we have found safe from experience with CDF upgrade muon tubes, then the maximum gravitational sag of the wire is limited to 125 μm and the additional electrostatic deflections are completely negligible. (See Section

II.B.) The maximum gravitational sag versus span for these conditions is shown in Fig. I-7. While any gravitational sag can be corrected for in the level 3 trigger or offline provided that the tension is known precisely, the very small sag removes the error in tension from our list of concerns.

In addition to keeping the wire straight to the order of 100 μm, we need to keep the extrusion straight to the order of 1 mm. This is because, in general, the precision of the drift cell is about an order of magnitude less sensitive to the location of the field shaping components than it is to the location of the sense wire. An oval shape has been chosen for exterior of the drift tube for reasons of strength. Figure I-8 shows the maximum tube deflection for a (8 cm-drift) tube versus the length of the minor axis of the ellipse which defines its outer boundary. A value of about 2 cm gives a maximum tube sag of about 1 mm in a 3.1 m span. Fixing the design of the tube, Fig. I-9 then shows the maximum tube deflection versus the unsupported tube span. It is clear from these two last figures that it would be difficult to implement this design with spans much longer than 3 meters.

These considerations, then, give us our basic design. In the following sections, we discuss some of these issues in more detail and describe the implementation of this design.

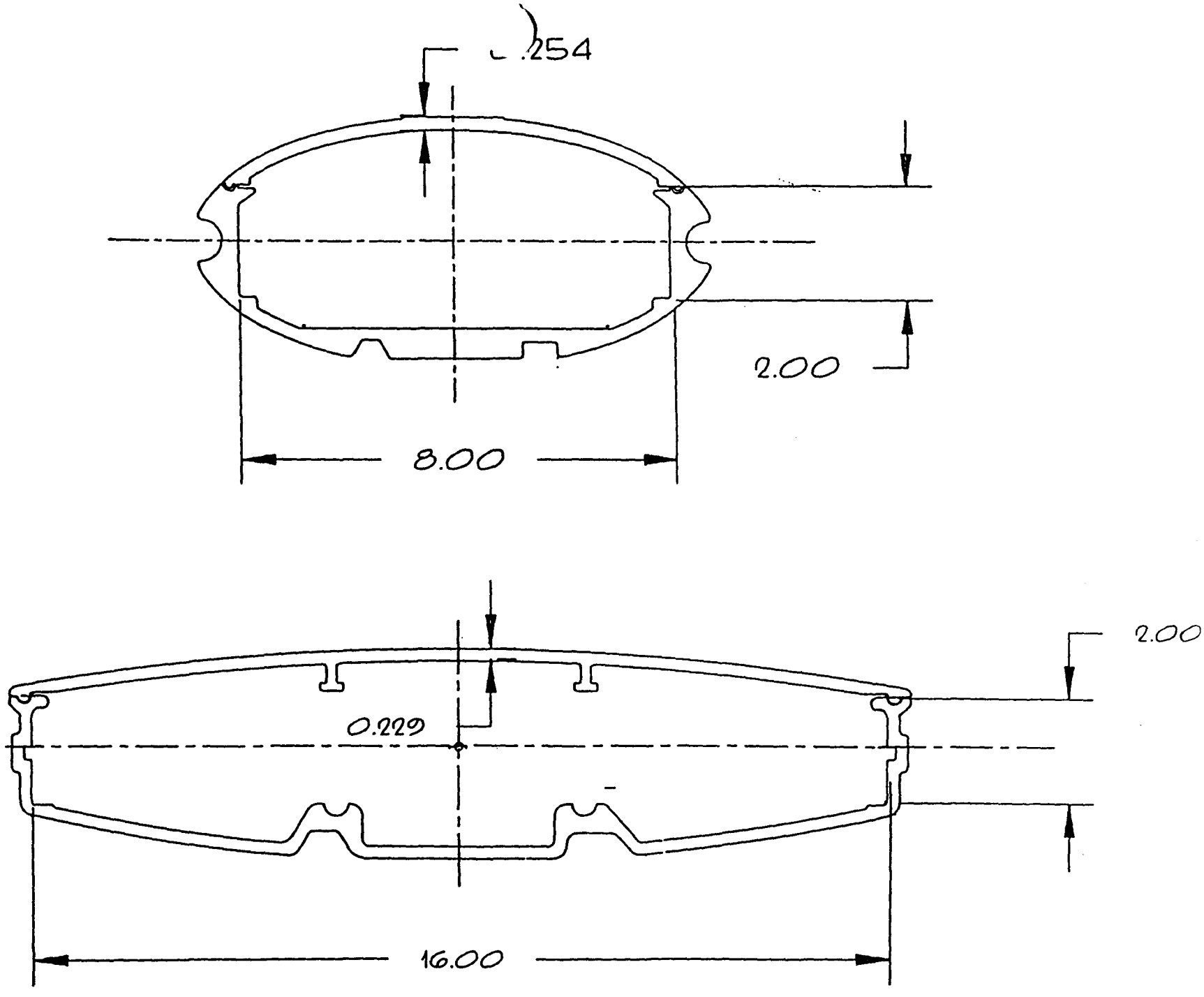

Figure I-1. Extrusion cross sections for the 4-cm drift and 8-cm drift versions of the drift tubes.

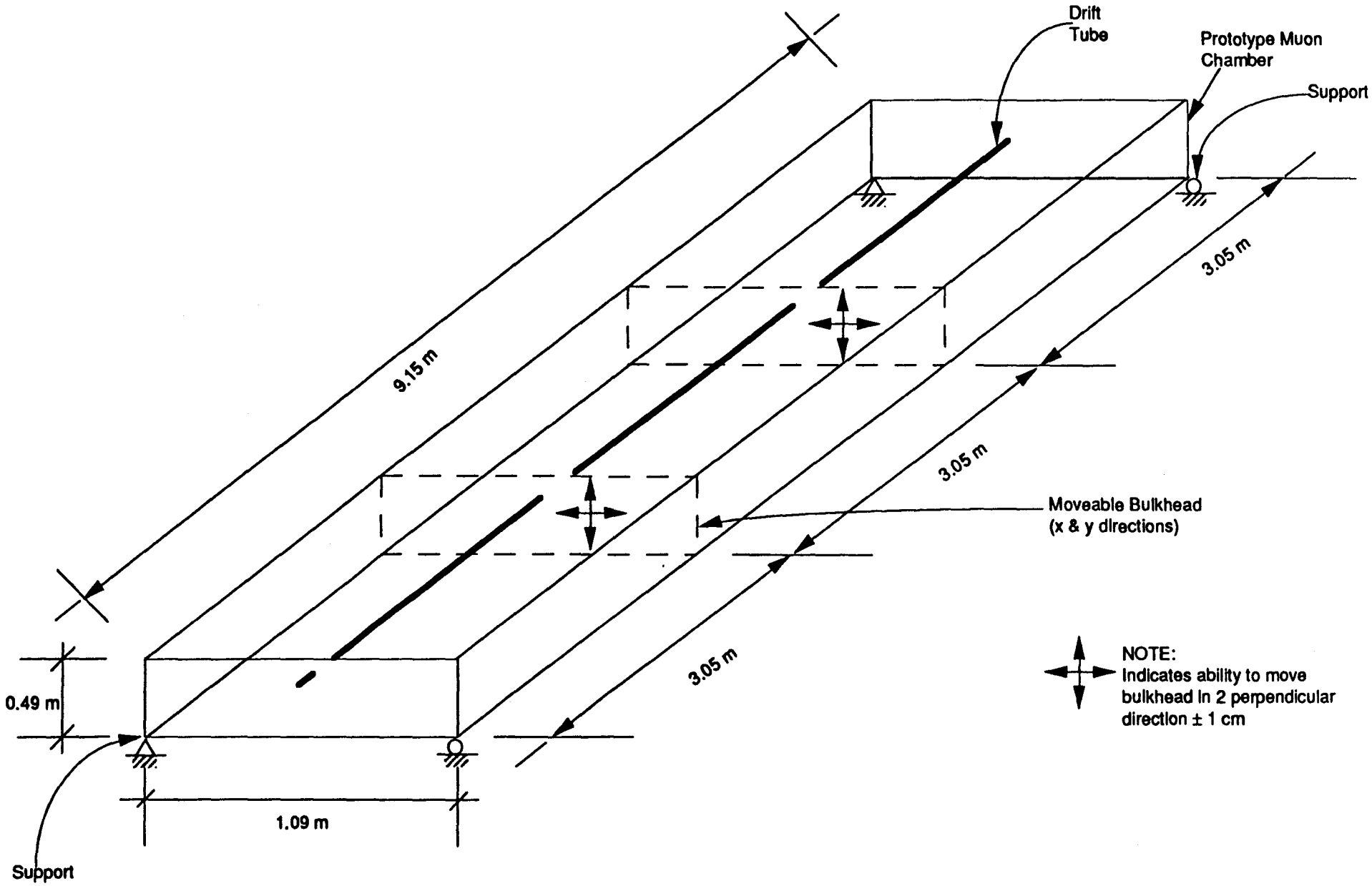

Figure I-2. Configuration of the prototype box

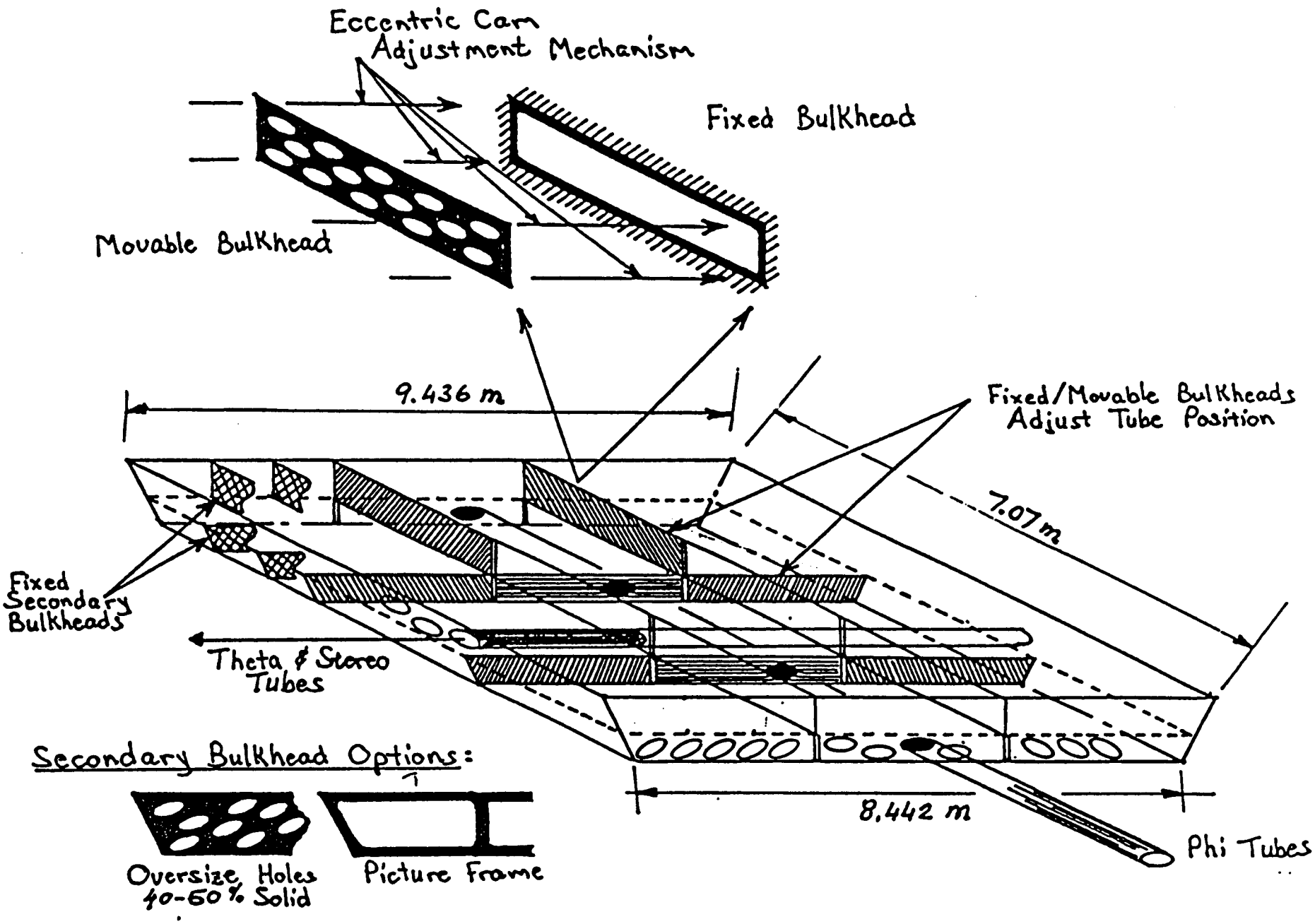

Figure I-3. Schematic of the supermodule box.

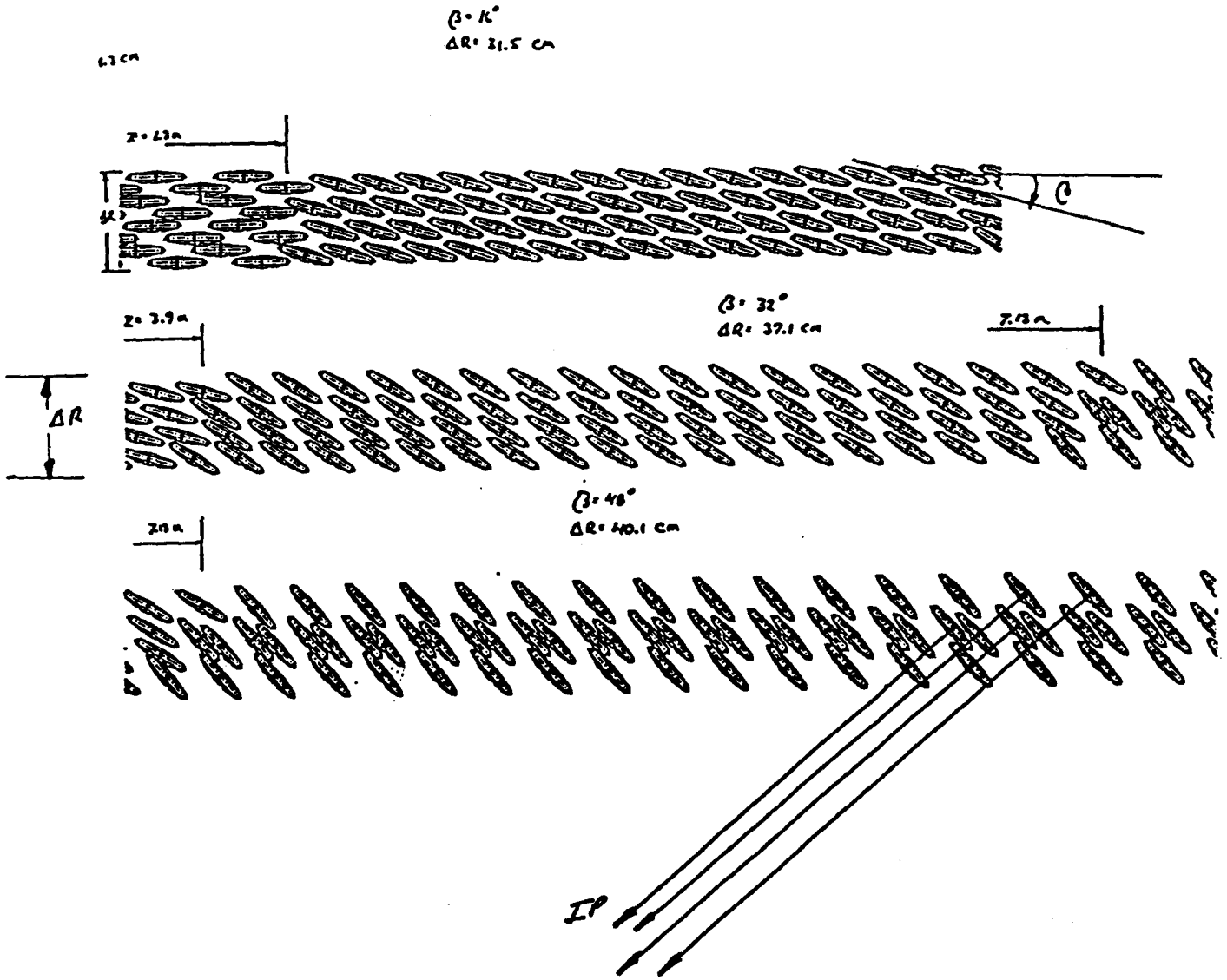

Figure I-4. Layout of θ-measuring tubes in layer BW2. The three rows are meant to be laid out end to end, starting from $\theta = 90^o$ at the left of the first row progressing to about $\theta = 35^o$ at the right of the third row. Wires in the first and third rows and the second and fourth rows are projective, with the latter pair at approximately a half-cell offset from the former. Note the progression from a brick-like structure at $\theta = 90^o$ to a shingle-like structure beginning at $\theta = 82^o$. Also note that the tubes become less dense at lower angles.

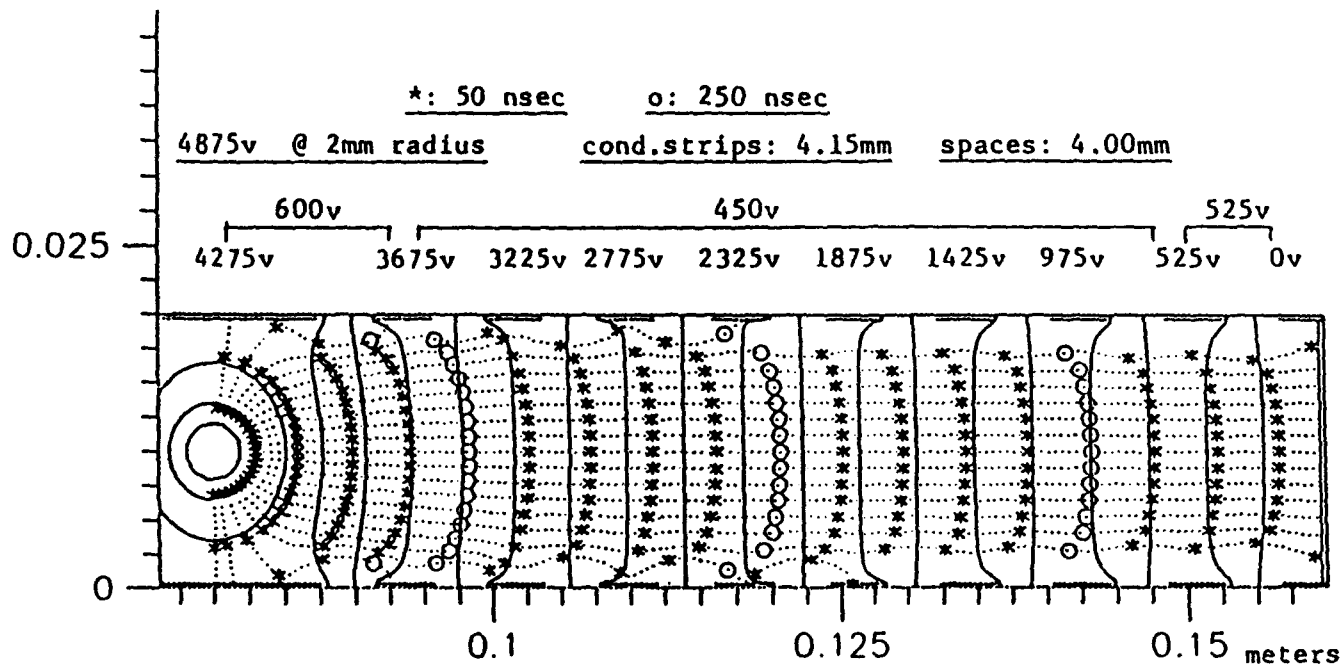

Figure I-5. Drift cell for the 8-cm drift version using an Ar-CF_4-CH_4 mixture in a 90:5:5 ratio with the voltages listed. Equipotentials are shown in solid lines, electric field lines in dotted lines, and isochrones in asterisks every 50 ns and open circles every 250 ns.

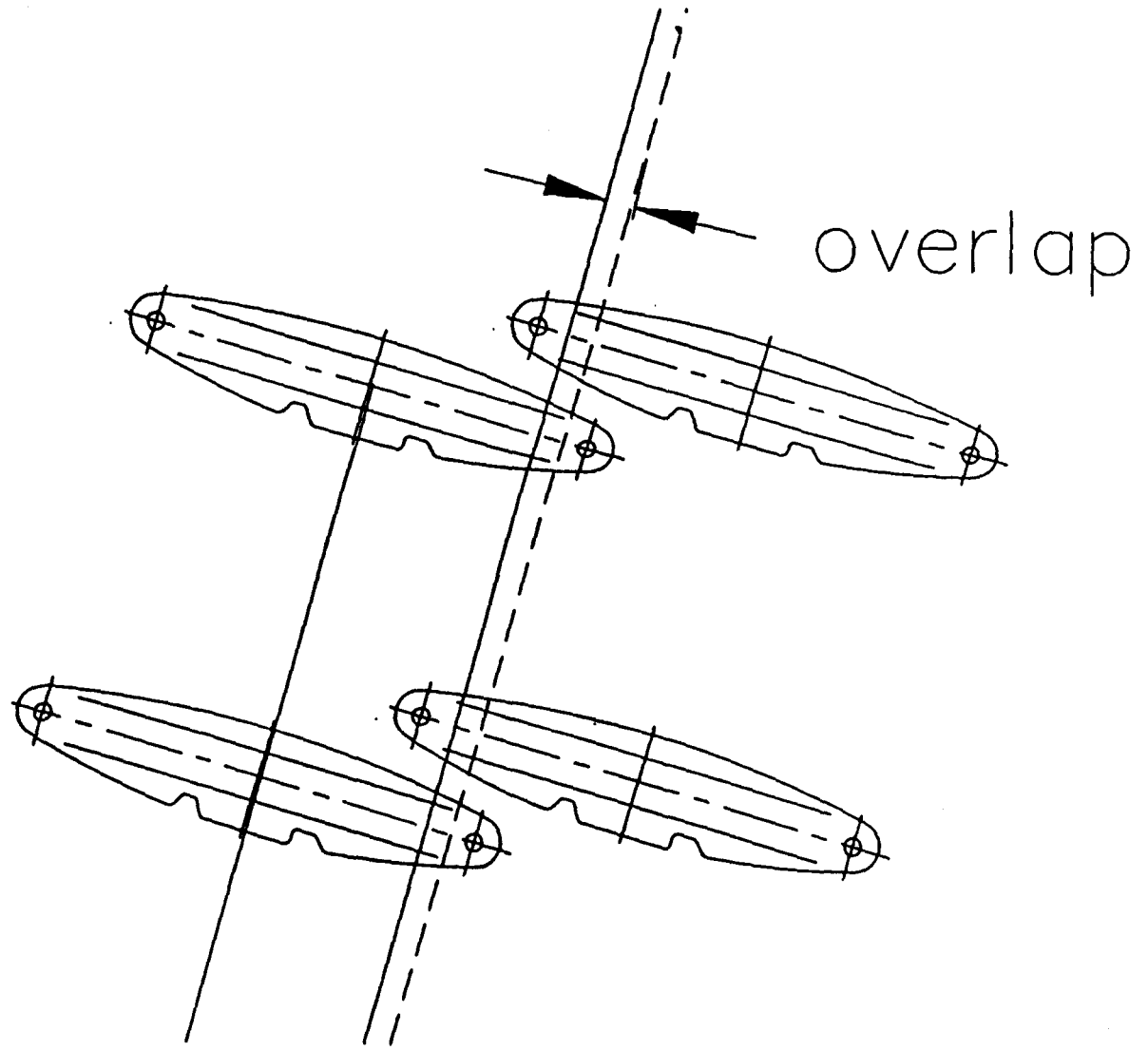

Figure I-6. Illustration of the overlap between tubes in the same layer.

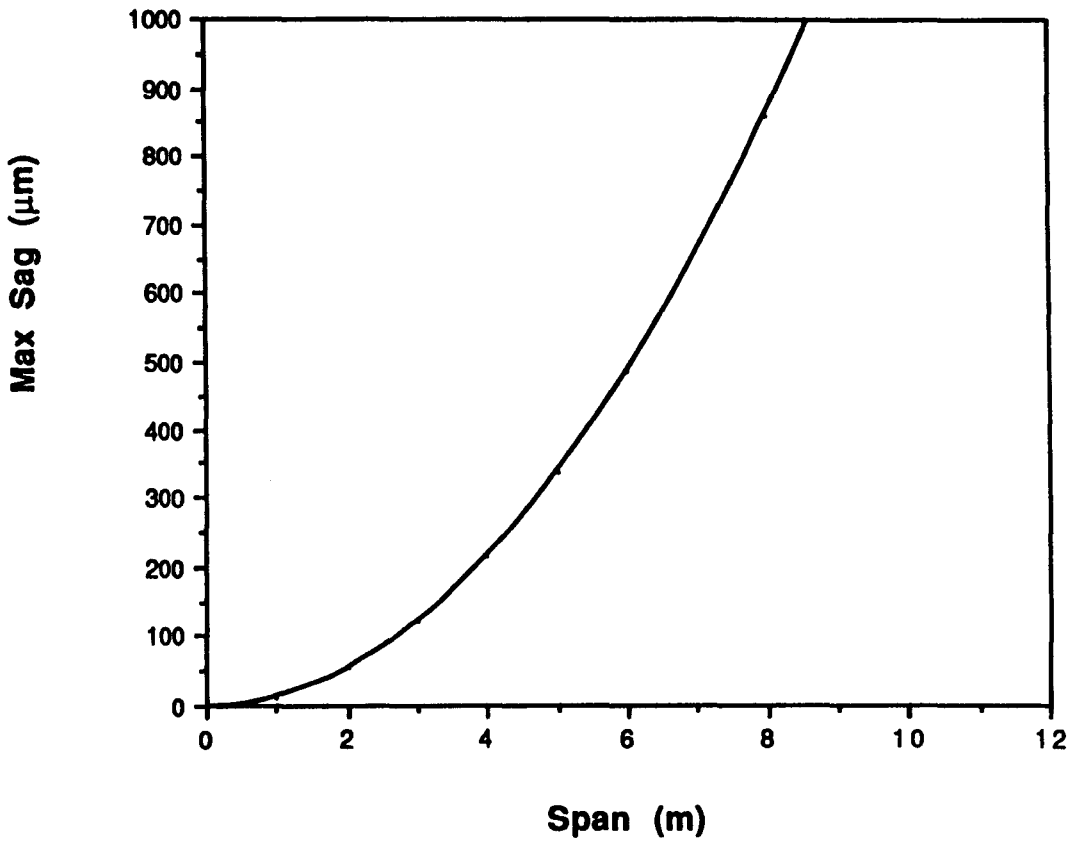

Figure I-7. Maximum gravitational wire sag versus span.

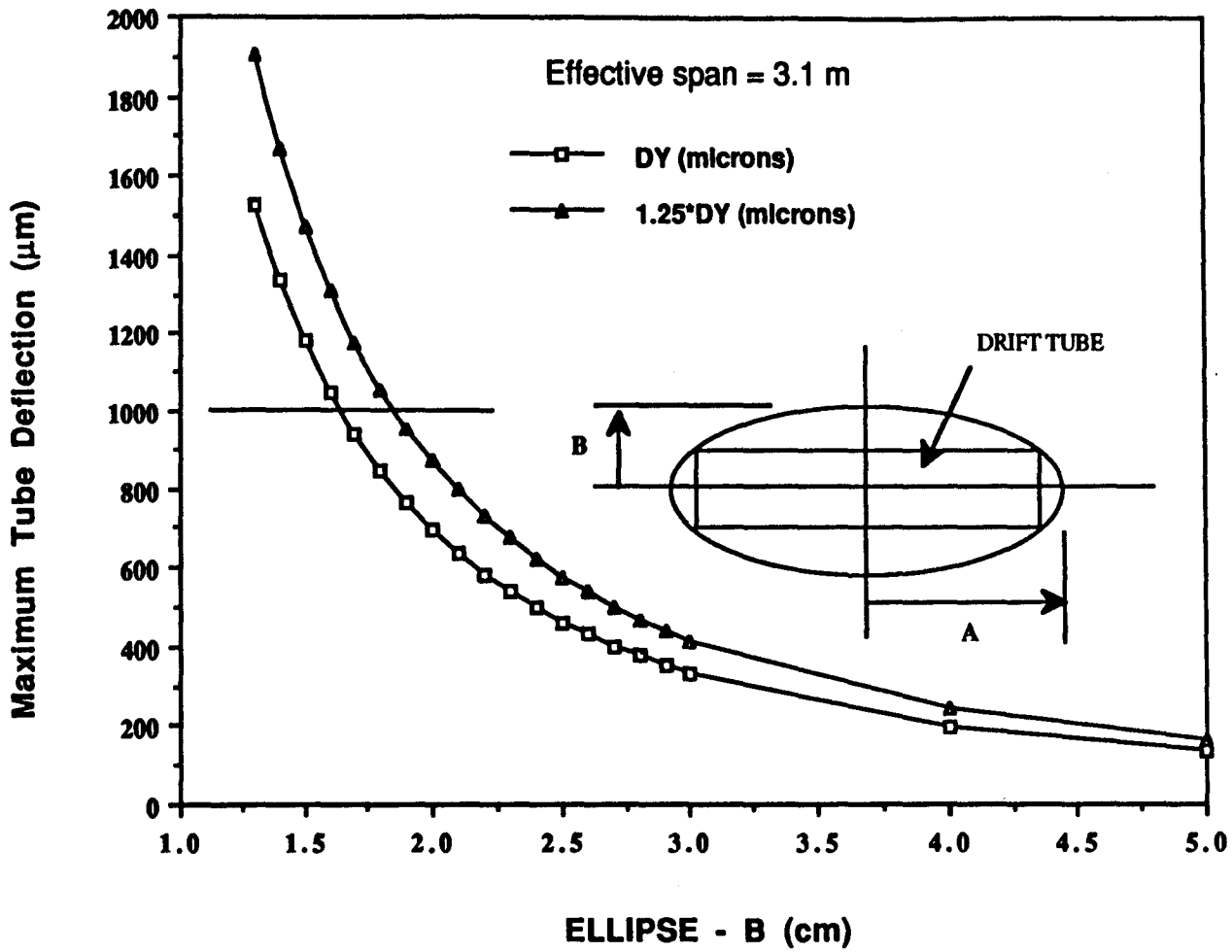

Figure I-8. Maximum tube deflection versus minor axis of the ellipse for 16 cm x 2 cm drift region.

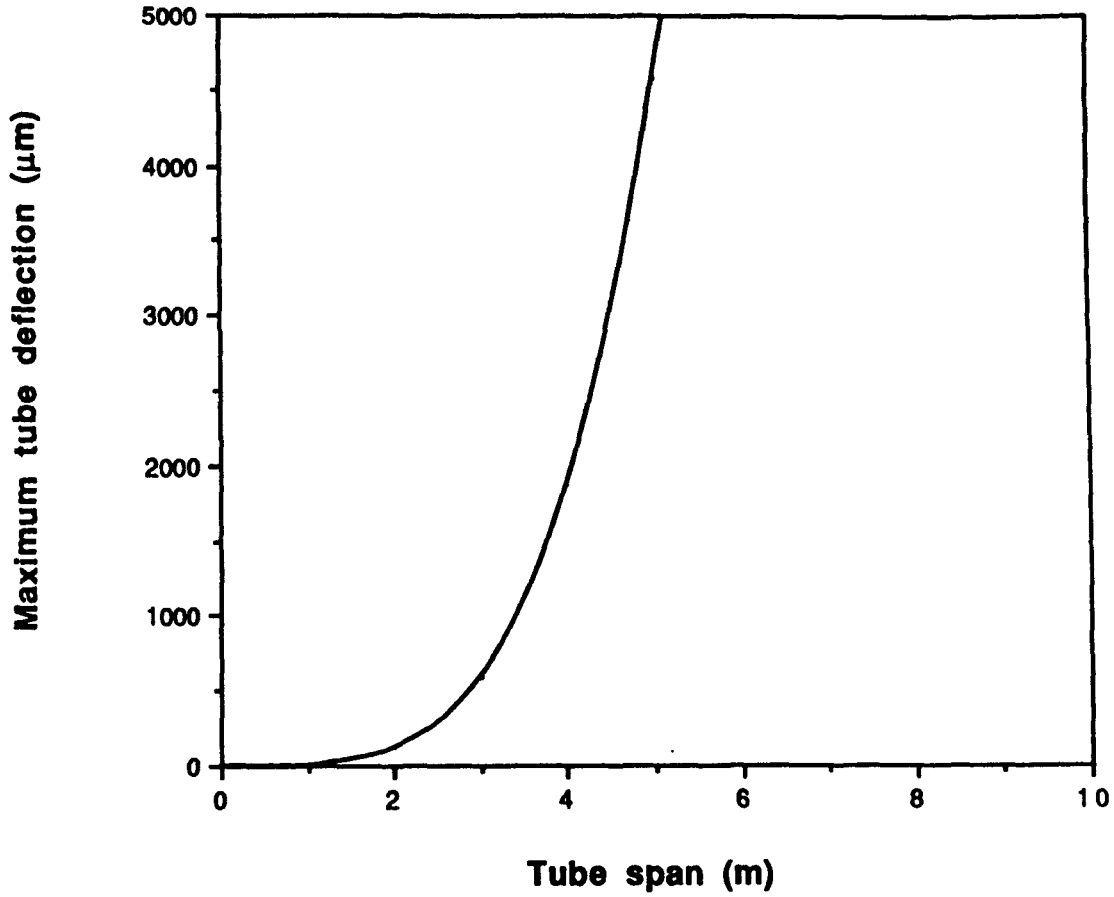

Figure I-9. Maximum tube deflection versus span.

II. Full-Length Prototype Design

A. INTRODUCTION

We are currently in the process of building a 48-cell, full-length prototype of the wine rack design. Figure II.A-1 shows the arrangement of tubes in the prototype box. The goals of this project are

1. to gain experience in the manufacture of drift tubes,
2. to gain experience in the manufacture of the box,
3. to provide a large enough array of tubes to test the performance of the proposed electronics,
3. to test the mechanical stability and precision of system, and
4. to test the bulkhead alignment system.

To achieve these goals, the prototype had to be full length and of reasonably large width. After we were well along in planning the prototype with 4 cm-drift tubes, we decided that the full system would require 8 cm-drift tubes for reasons of cost. We decided to go ahead with the full-length prototype using the smaller cells, because none of the goals depended on the cell width, except the properties of the drift cell itself. We simultaneously began designing the wider cell and ordered extrusions, so that we could also build a few short-sample and full-length drift tubes to test the cell properties and to see that no additional problems were caused by the wider cells.

The relationship of the prototype to the full barrel system is shown in Fig. II.A-2.

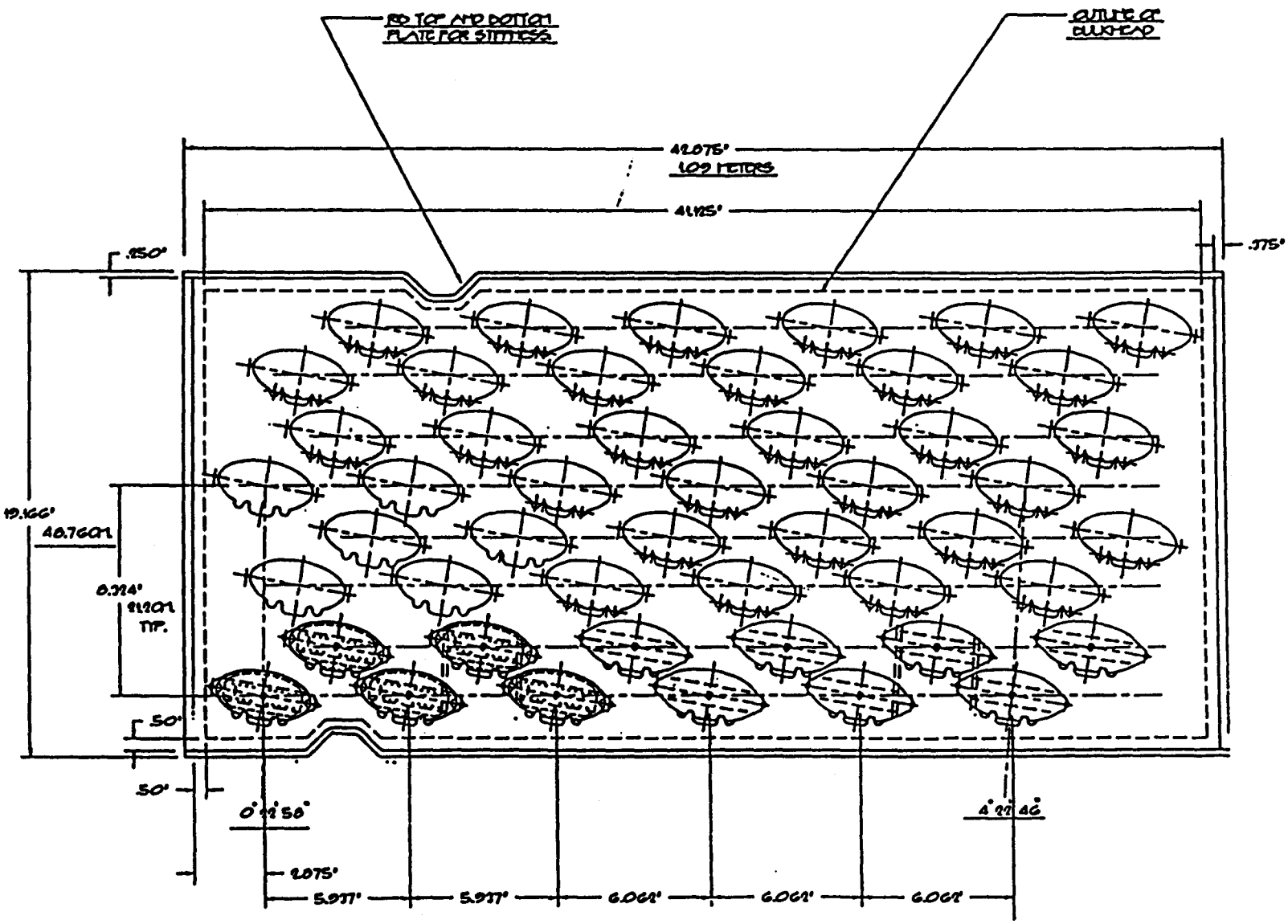

Figure II.A-1. Cross section of the prototype box showing layout of the drift tubes.

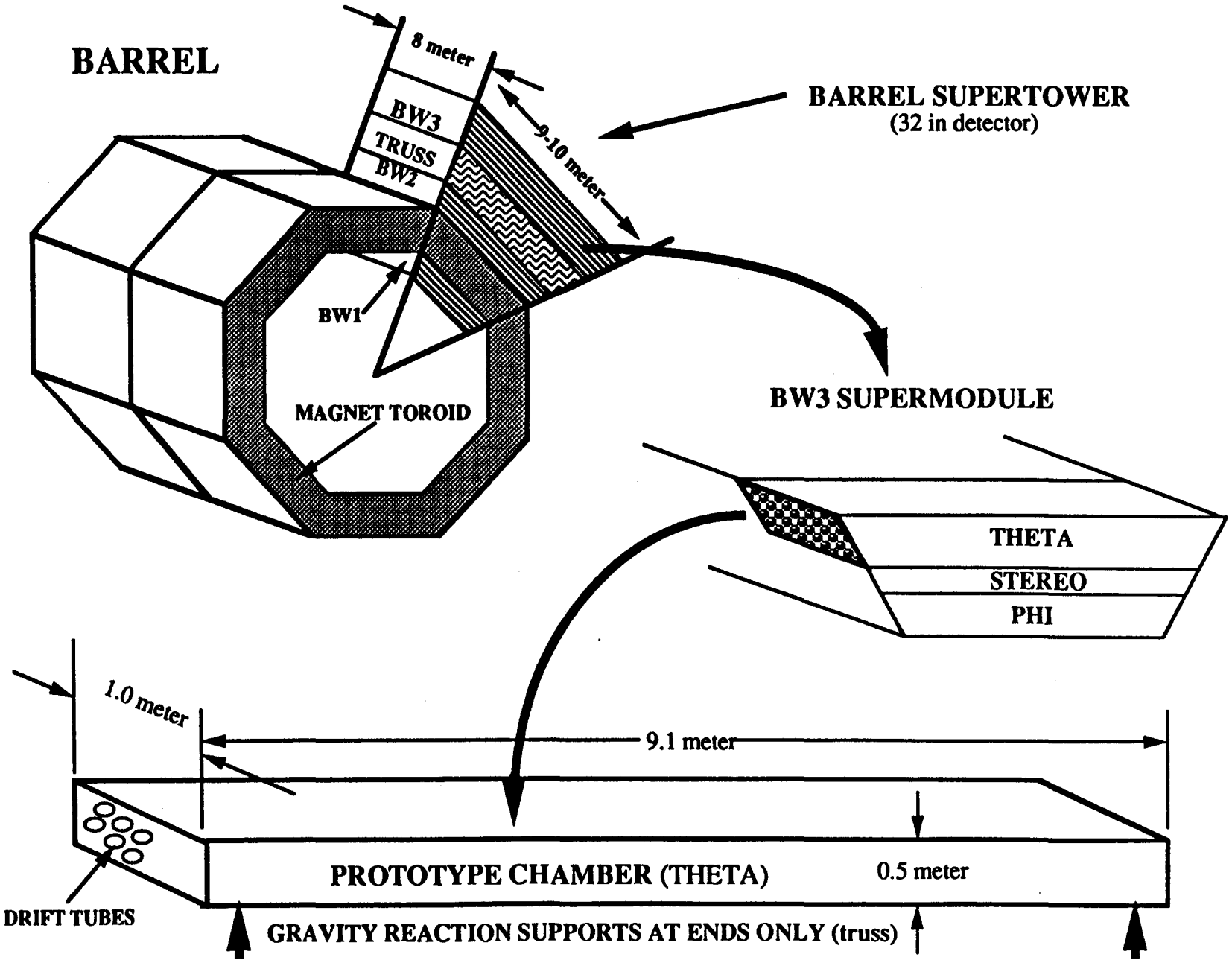

Figure II.A-2. The relationship of the prototype chamber to the full barrel muon system.

B. DRIFT CELL DESIGN

Field Distribution

The prototype cell has an active region cross section of 2 cm transverse to the drift direction and 8 cm along the drift direction. A 50 μm gold plated tungsten sense wire is in the center of this region giving a 4 cm maximum drift distance. Except very close to the wire, each cell is expected to have a resolution limited by the diffusion of electrons in the gas. There should be no loss of resolution from a single sense wire for tracks entering within ± 10 degrees with respect to the normal to the drift direction. The field shaping in the drift region is provided by intermediate field shaping electrodes in the form of copper strips on G-10, fed by an externally mounted voltage divider on one end of the tube. (In the production version, we intend to use silver ink screened onto glass-filled polyester boards.)

The drift cell design should provide an optimized electric field distribution so that the track position versus time dependence is nearly linear over the maximum possible sensitive area. Further, only the portion of the isochrone tangent to the track of a passing particle will contribute to the leading edge of the ionization pulse and be used in determining the drift time. Thus by clever field shaping near the sense wire, and by exploiting the drift velocity versus electric field characteristics of the gas, the cell design should maximize the isochrone radius in order to collect a maximal share of the ionization in the leading edge of the output pulse and minimize the tail. This should be done in a way to accommodate a ±8 degree variation in the track incidence angle.

The CERN Library program POISSON was used for the potential calculations and some of its internal routines were adapted to fit into a field line generator. The quasi-singular sense wire is approximated by requiring an appropriate constant potential on a small (2 mm radius) circle. Timing is done outward from the center wire and is based upon an interpolating look-up table of drift velocity versus field dependence from reported data for several appropriate and representative gases. An additional program was written to calculate the Maxwell stress tensor to establish the electrostatic forces on the sense wire.

The finite mesh used for practical calculation of the potential distributions causes occasional discontinuance of the field lines as they are propagated out from the central circle along the locally-computed potential gradients. This artifact may be seen in the following illustrations but is not expected to affect our conclusions significantly.

Figure II.B-1 is half the prototype model drift region, 4×2 cm^2 in cross section, showing equipotentials, electric field lines and isochrones. In the calculation for this example we have assumed the chamber is filled with Ar-CO_2 (90:10), a common non-flammable drift chamber gas.

As a general principle for a track traversing the tube normal to the drift direction, the larger the radius of curvature of an isochrone, the larger the fraction of ionization electrons that will contribute to the leading edge of the ensuing output pulse. The more readily will that pulse enable the precise recording of the drift time and thus the track location. A desirable feature of this type of drift cell design is the essential constancy of this isochrone curvature, giving a more uniform the output signal size and shape over the bulk of the sensitive volume.

Electrostatic Stresses

To determine the electrostatic force, we calculated fields with the sense wire displaced 0.5 and 1.0 mm up and down, and left and right. Figs. II.B-2 and II.B-3 show the same situation as in Figure II.B-1 except that the wire is displaced up 1 mm in Fig. II.B-2 and to the right 1 mm in Fig. II.B-3. For each case the Maxwell stress tensor was calculated from the POISSON fitted electric field components and its surface integral around the sense wire.The results of these calculations can be summarized in terms of effective "spring constants" (force/unit length of sense wire/unit displacement):

$$k(\text{up/down}) = 0.47 \text{ dyne/cm}^2$$
$$k(\text{left/right}) = 1.23 \text{ dyne/cm}^2.$$

For comparison, the weight per unit length of a 50 μm diameter tungsten wire is

$$f = 0.379 \text{ dyne/cm}.$$

Thus, a 2 mm left or right displacement of the sense wire from center produces a net electrostatic force (1.23)(.2)/0.379 = 65% that of the wire's weight alone. The up/down effect is only 25% that of gravity. Since we are designing to 125 μm maximum sag, this is not expected to present a problem.

The general equation for the shape of a wire of length L in the presence of both f and k, above, can be solved exactly to give a total maximum (central) displacement

$$y_{\max} = \frac{f}{k}\left[\sec\left(\frac{\pi L}{b}\right) - 1\right]$$

where $2\pi / b = \sqrt{k/T}$ and T is the tension in the wire. [This expression yields the familiar result $y_{\max} = (f/8T)L^2$ in the limit of no electric forces, and blows up when L is half of the "wavelength," b.] For the wire in question, 350 g of tension, corresponding to about half the yield strength, gives equivalent "wavelengths," b, of about 54 meters and 33 meters for the up/down and left/right cases, respectively. In a design with a 3 meter unsupported length, the basic gravitational sag is about 125 μm and the electrostatic perturbation adds to it only about 10 μm in the worst (left/right) case.

Timing and Wire Displacement

Using the fields of the basic prototype model tube (Fig. II.B-1) and determining the time intervals (in nanoseconds) for electrons to drift successive 2 mm spaces, yields the result that between about 0.6 cm and 4.0 cm the drift time per 2 mm transit lies within (43±1) nsec. The mean velocity is 46.8 μm/nsec thus the time/distance relationship is effectively linear within about 100 μm over (3.4/4.0) = 85 percent of the tube area.

A similar examination of the effect of moving the sense wire 1 mm to the right found that not only the midline but also that the adjacent "trajectories" had their isochrones shifted 19 nsec. On the other hand, displacing the wire up by 1 mm moved the isochrones only a few tenths of a nsec. One concludes that, as one might expect, it is the sense wire position along the drift direction that is critical. We note that the effect of a wire displacement on the inferred track locations is, at least for the

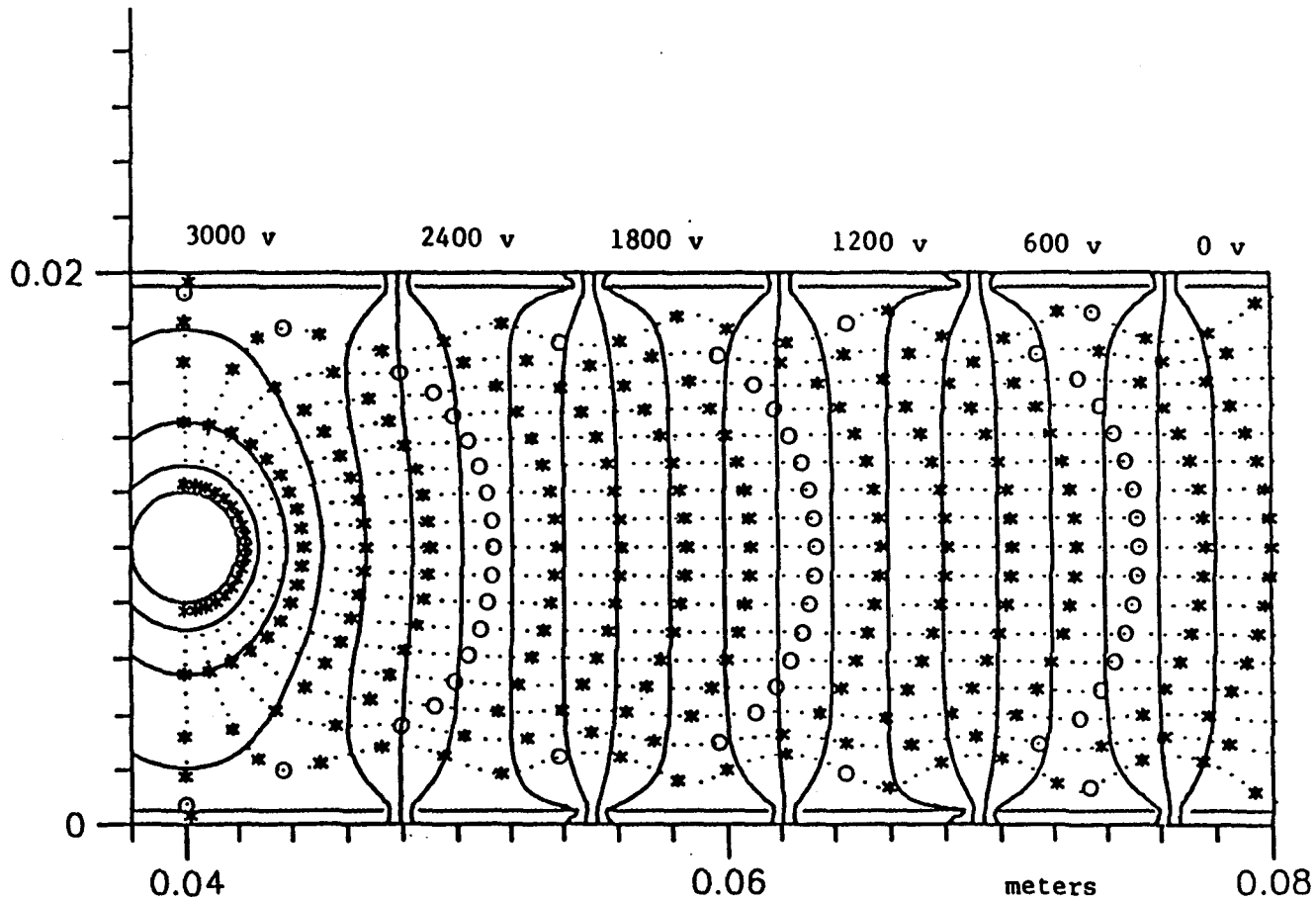

Figure II.B-1. Drift cell for the 4-cm drift prototype using an Ar-CO_2 mixture in a 90:10 ratio with the voltages listed. Equipotentials are shown in solid lines, electric field lines in dotted lines, and isochrones in asterisks every 50 ns and open circles every 250 ns.

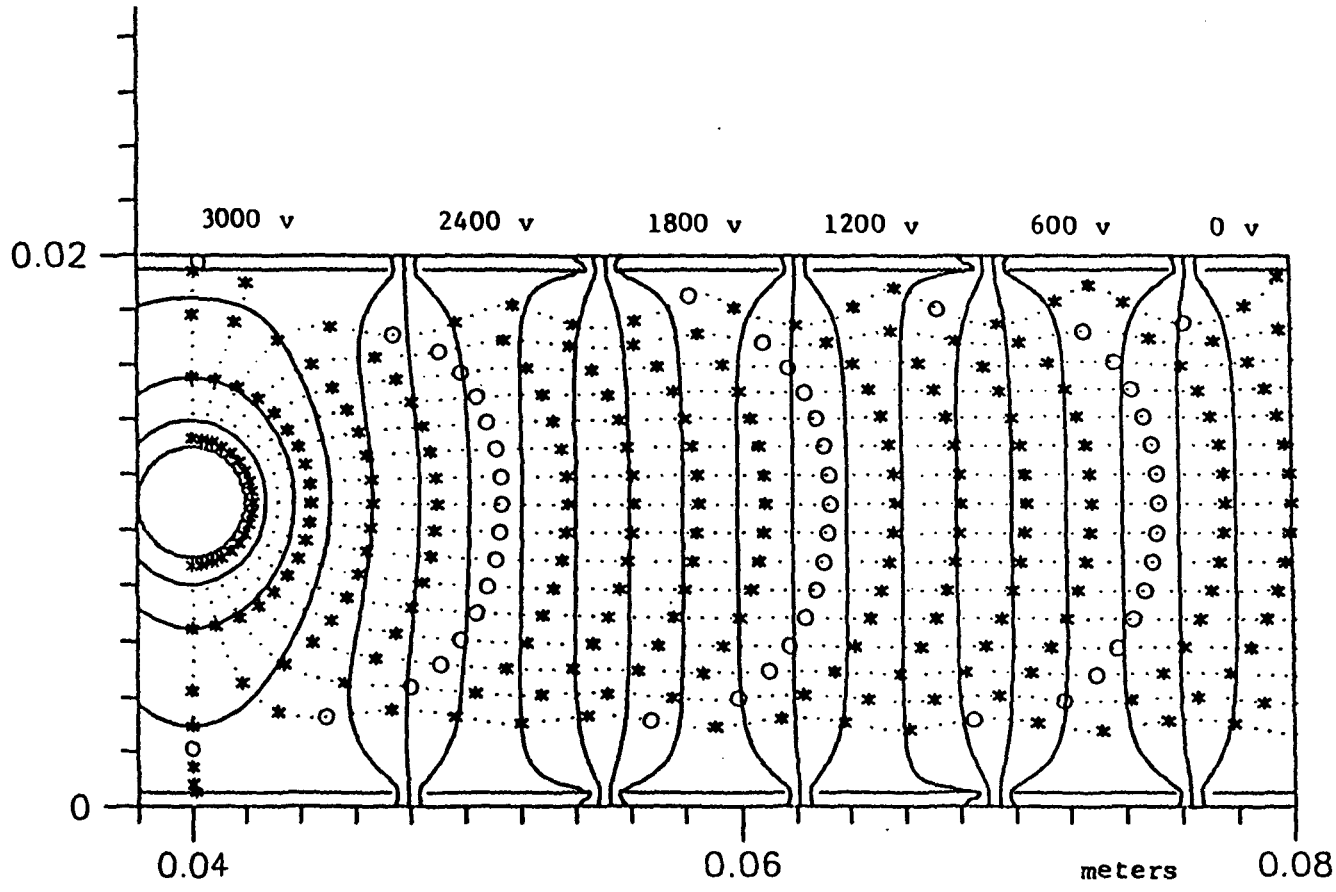

Figure II.B-2. Drift cell for the 4-cm drift prototype as in Fig. II.B-1, except that the wire is displaced up 1 mm.

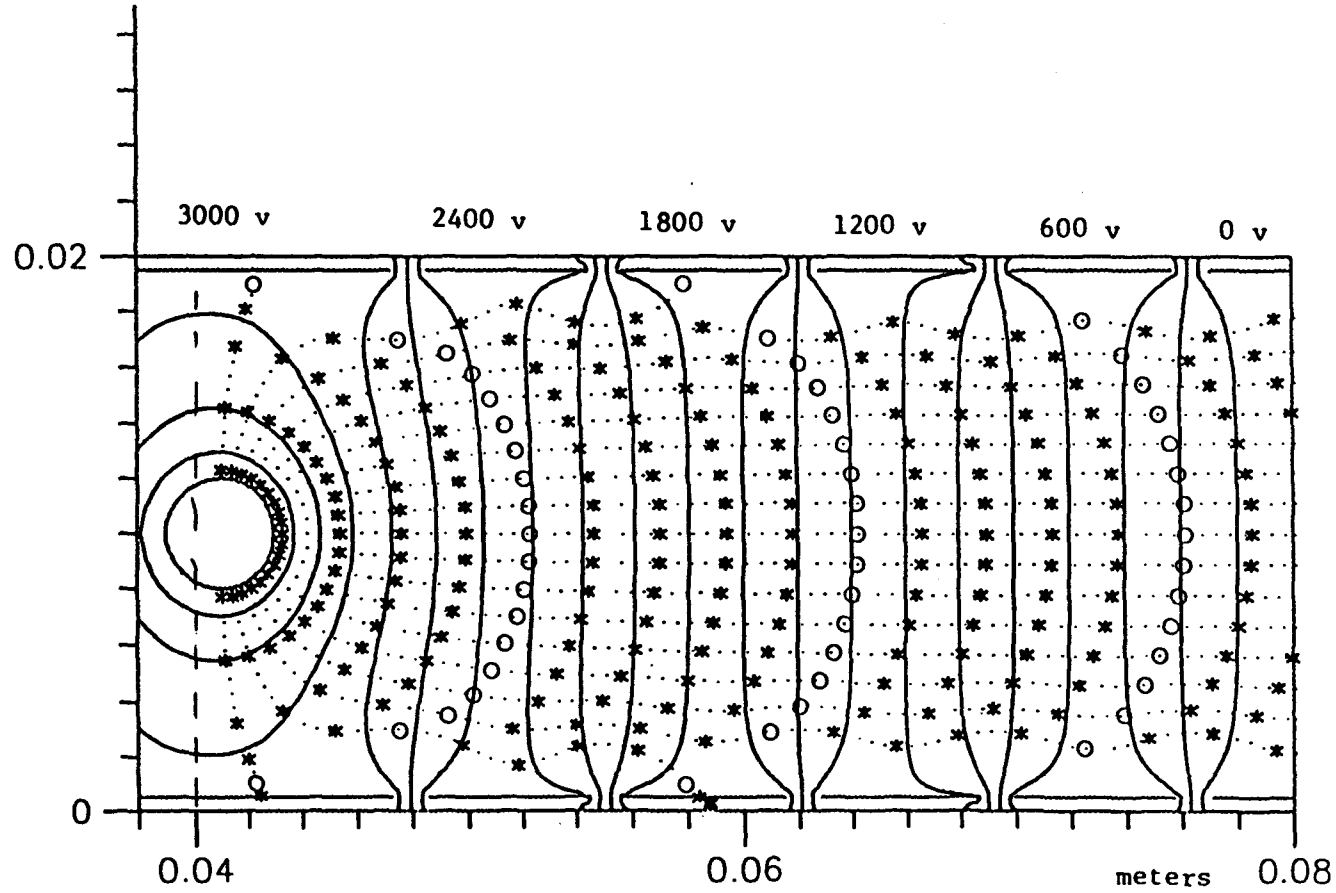

Figure II.B-3. Drift cell for the 4-cm drift prototype as in Fig. II.B-1, except that the wire is displaced to the right 1 mm.

C. TUBE DESIGN

Basic Design

The baseline prototype drift tube is an ellipsoid whose major and minor axes are 4.40 and 2.38 cm. Typical wall thickness is 0.254 cm, with appropriate thickness increases in the vicinity of local groves and notches. The drift tube and end caps form the gas seal. The field shaping boards are 8.0 cm wide and are spaced 2.0 cm apart. The gold-plated tungsten sense wire has a diameter of 50 μm and is pretensioned to 350 grams. It is centered 1.0 cm from either field-shaping board and located precisely between locating keys that mate to grooves in the extruded tubes. The drift tube is shown in Figs. II.C-1a and II.C-1b; the former is an exploaded isometric drawing and the latter is an assembly drawing . Additional details are shown in Figs. II.C-2 through II.C-5. Figure II.C-2 shows the field-shaping boards and how copper clips molded into the endcap make contact with field-shaping boards. Bridges which support the field-shaping boards above and below the clips are shown in Fig. II.C-3, along with the bridge that supports the wires. Details of the end caps and feed throughs are shown in Figs. II.C-4 and II.C-5.

Electrostatic considerations limit the maximum deflection of the tubes and field shaping boards relative to the wire to ~1 mm. The prototype chamber is 9.14 m long with two internal bulkheads which make the maximum unsupported span 3.05 m. Figure II.C-5 plots the transverse deflection of the wire as a function of the wire tension for a 3.05 m span. At a 350 gram preload tension the maximum wire sag is 125 μm.

Extrusion

The tubes are an extruded, heat treated, aluminum alloy 6063-T5, manufactured by Mideast Aluminum Industries. The tubes are extruded by a 1500 ton extrusion press utilizing a 5 inch diameter 24 inch long billet. The manufacturing procedure for each 100 foot extrusion is:

1. The extrusion press extrudes tubes on to a runout table.
2. Tubes are placed on a cooling table.
3. Tubes are checked and dimensional adjustments are made on a stretcher.

4. Tubes are cut to 30 foot ±1/32 inch lengths (9.144 m).
5. Tubes are heat treated at 365° F for 4 hours then slow cooled.
6. Tubes are packed and shipped in wooden crates.

Endcaps, Wire Supports and Field Shaping Boards:

The elliptical endcaps (Figure II.C-4) are injection molded Ryton plastic, 30% glass by volume for stiffness and tolerance stability. Each tube employs two endcaps featuring holes for center electrodes and gas fittings. The high voltage end additionally has molded in beryllium copper gold plated field shaping board contacts. The electrodes are Delrin gold-plated feed through types. The gas feeds are commercial stock brass fittings for 1/8 inch diameter Tygon tubing. End cap dies were manufactured by Anthony Tool and Die, Leominster, Massachusetts. The molded end caps were obtained from Sportsman Plastic Inc, Leominster, Massachusetts.

At intermediate support positions, the wires are supported by a G10 bridge, 8.25 x 0.64 x 0.25 cm thick detailed in Figure II.C-3. These bridges are ground flat to 10 μm and epoxied into tube sidewall slots at four places corresponding to the chamber bulkhead locations. The wire is mechanically centered and epoxied to the bridge. A check is made for wire placement accuracy using a 100X microscope. The expected tolerance is 25 μm.

The field shaping boards are 0.5 mm polyester board with one side bonded by 25 μm of copper. Tracks are scribed, pealed, sanded and cleaned in 10 m lengths.

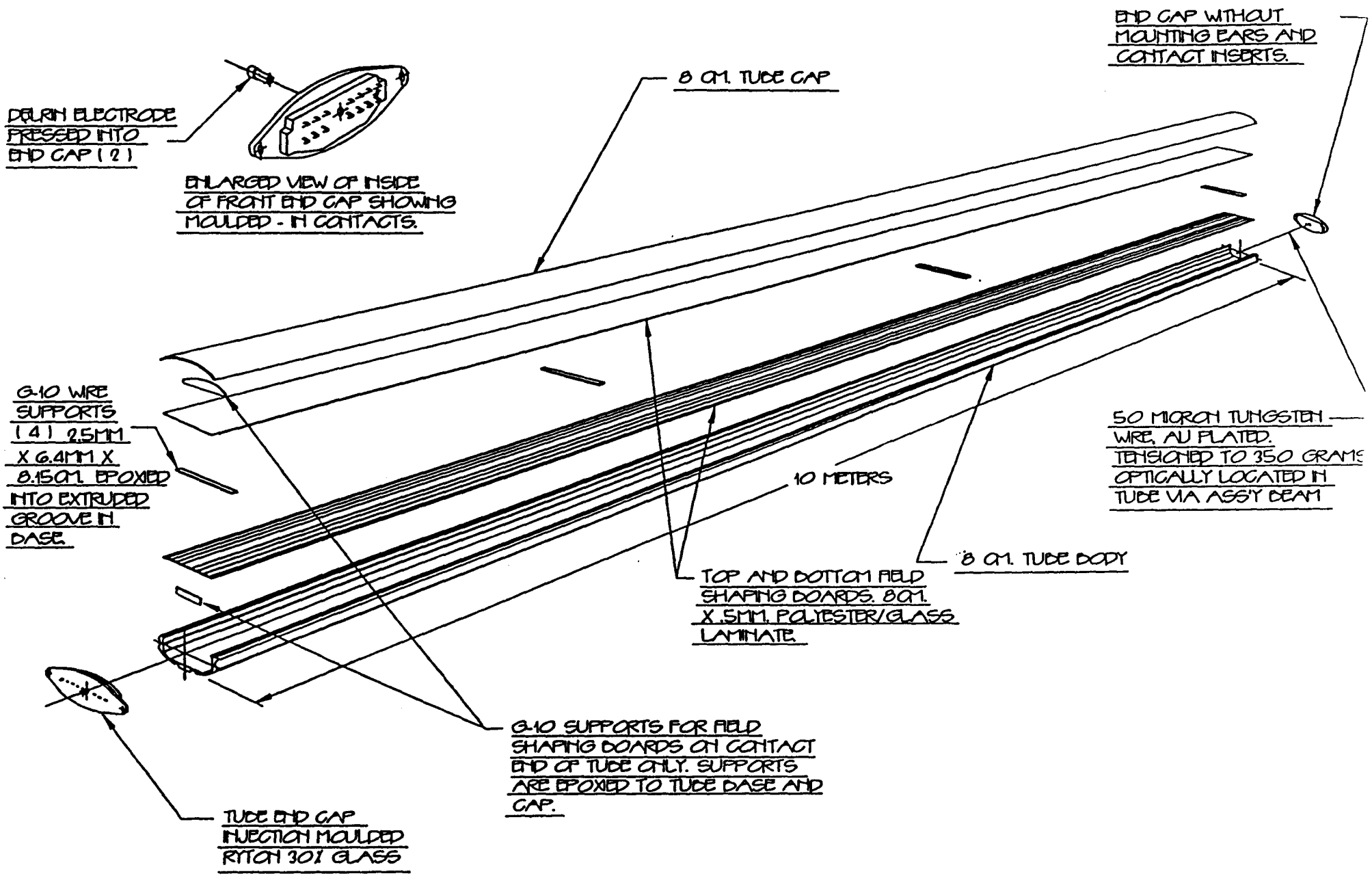

Figure II.C-1a. Exploded isometric view of the prototype drift tube.

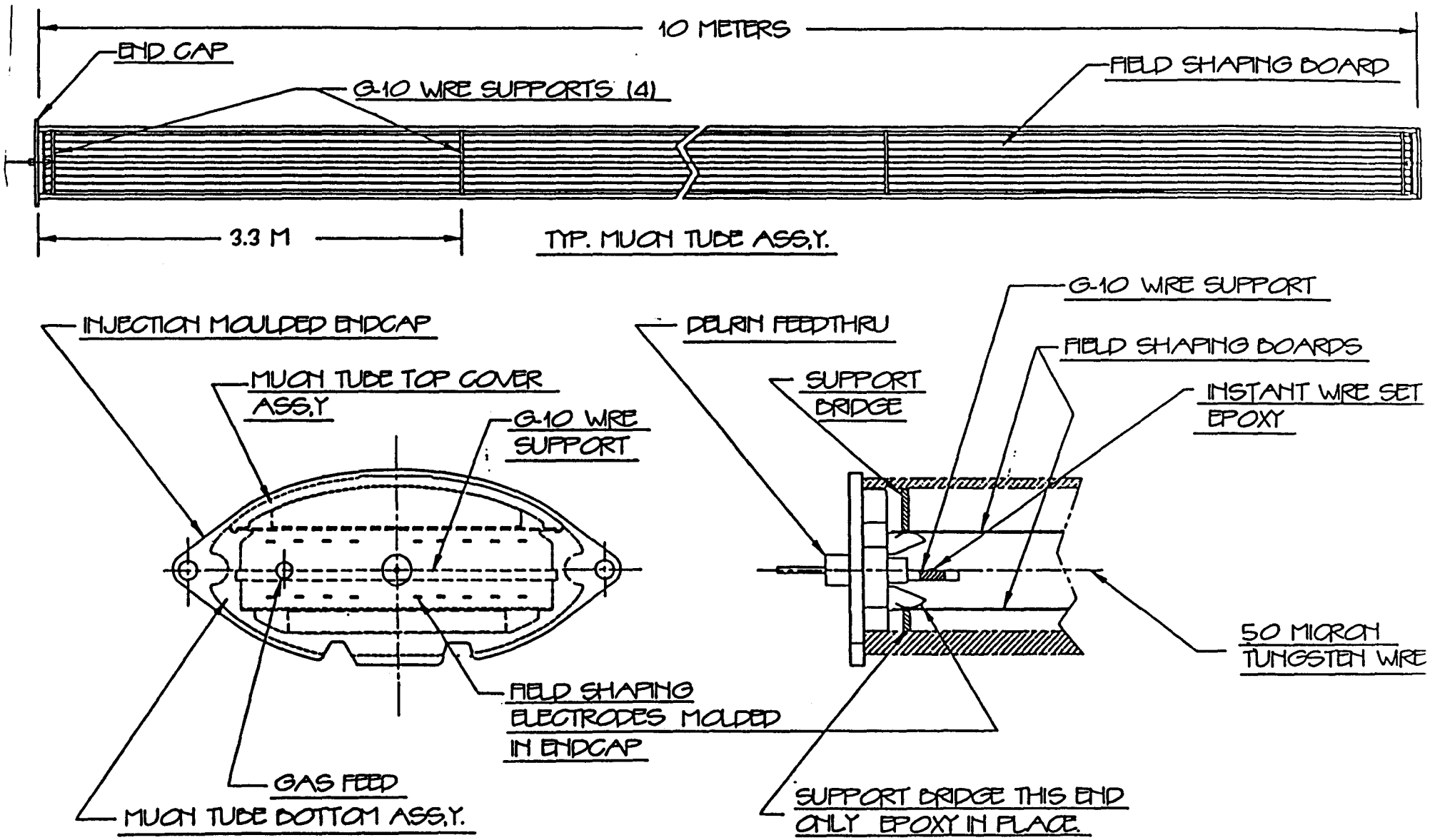

Figure II.C-1b. Assembly drawing of the prototype drift tube.

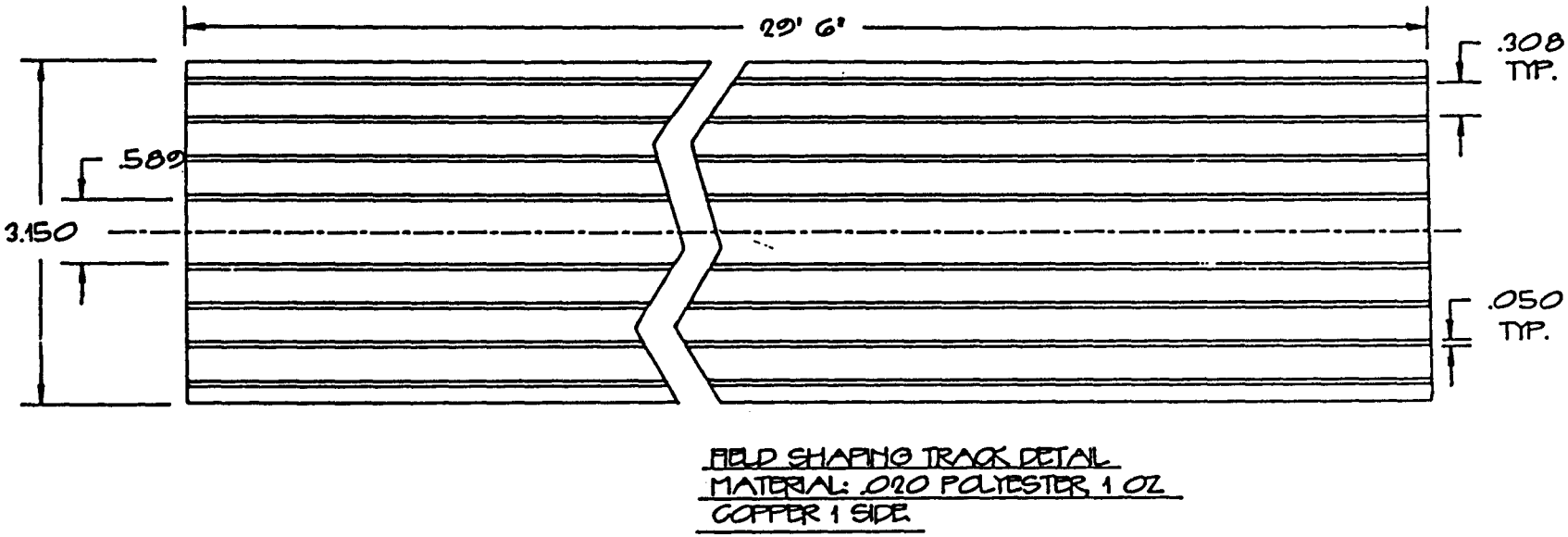

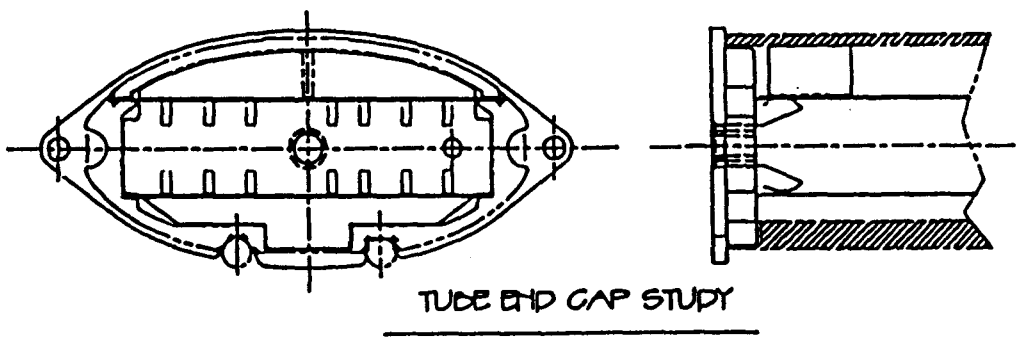

Figure II.C-2. Details of the field-shaping board and.its electrical connections.

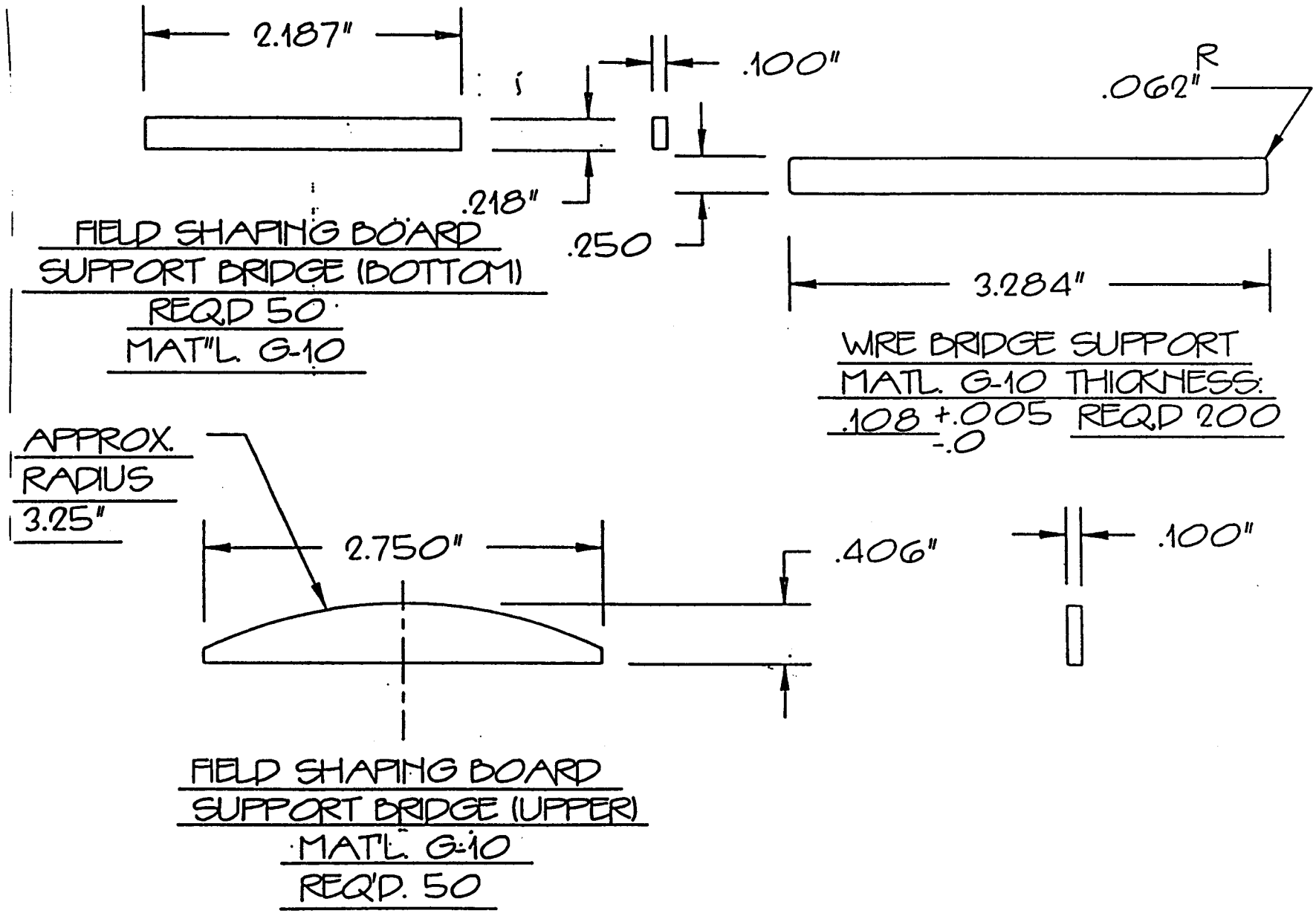

Figure II.C-3. Details of wire and board support bridges.

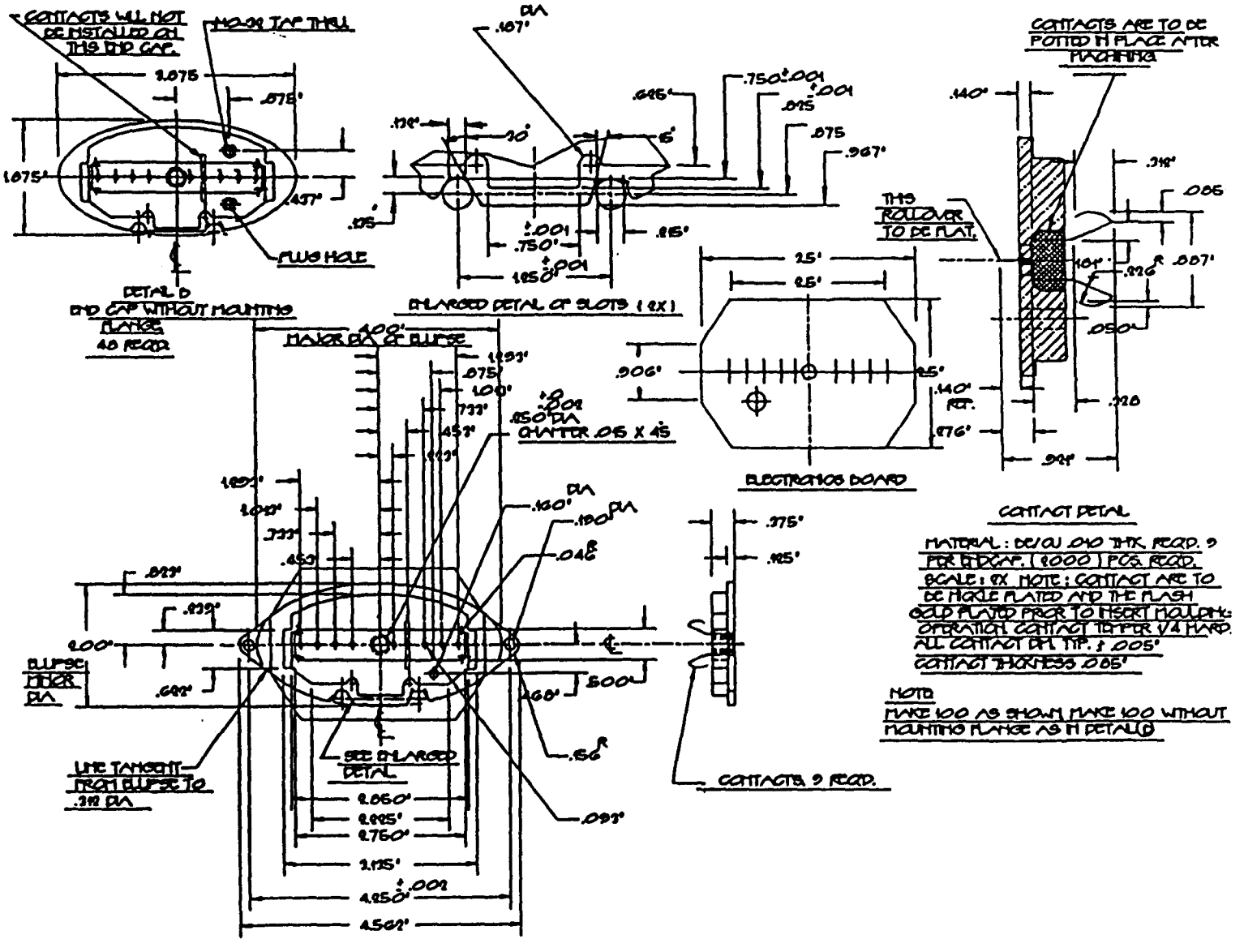

Figure II.C-4. Details of the end caps.

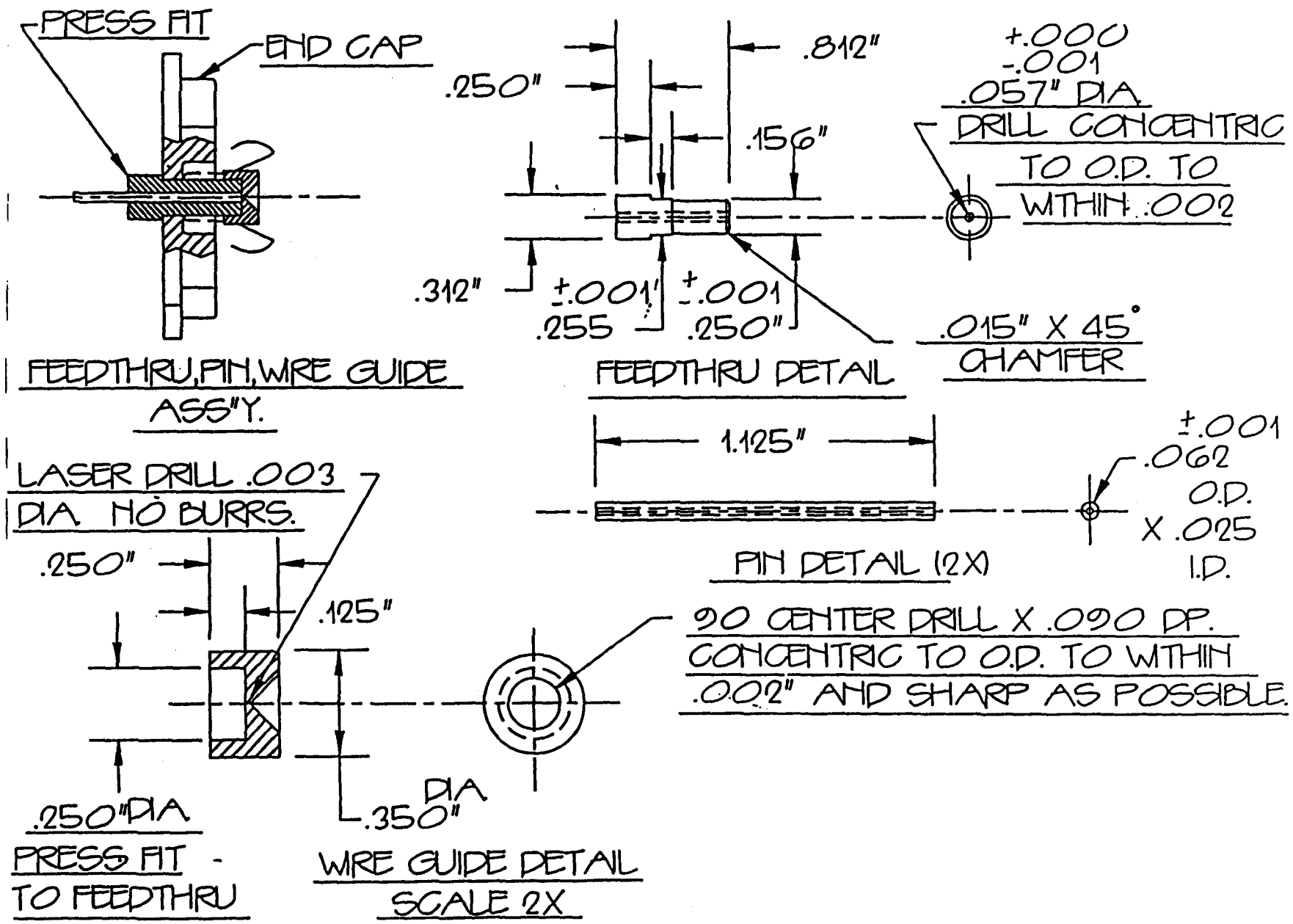

Figure II.C-5. Details of feed throughs.

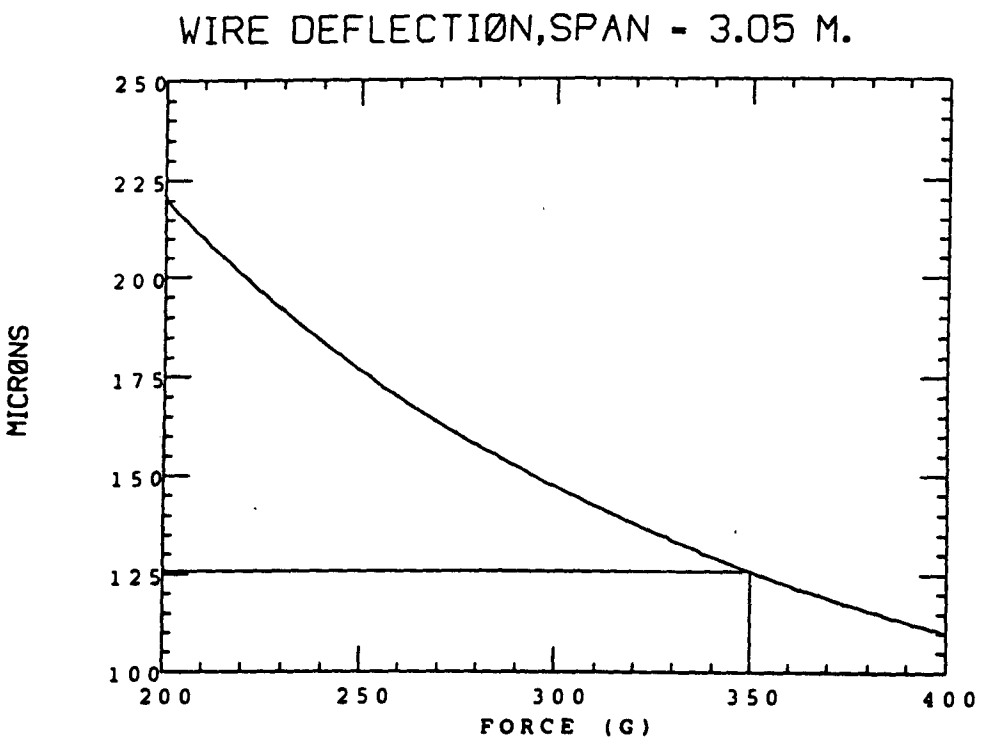

Figure II.C-6 Maximum sag versus wire tension for a 3.05 m span.

Function Plates

Figure II.D-1 shows one type of function plate which can be precisely positioned at any of the four mounting stations. The function plate shown carries a 100X magnification microscope with graduated lens. A wire locating device, illustrated in Fig. II.D-2, attaches to the microscope assembly and brings the wire (under tension) into exact alignment, immediately prior to attachment of the wire to the support bridge. The microscope is used to check the alignment.

Assembly Procedure

The tube assembly process steps:

1. Mount tube on assembly beam, lock down tube at assembly stations.
2. Slide in bottom field shaping board, lock with instant Permabond 200 adhesive.
3. Insert G10 bridges in slots, four places, and lock with instant Permabond 200 adhesive.
4. Apply DP-605 NS adhesive to endcaps and assemble to extrusion body.
5. String 50 μm gold-plated tungsten wire thru endcaps and tension to 350 grams and mechanically crimp.
6. Mechanically position wire at assembly station, check with 100 power microscope to 25 μm, lock with instant Permabond 200 adhesive.
7. Apply long term urethane epoxy DP-605 NS to field shaping board, wire bridge/extrusion slot and wire/bridge joint.
8. Epoxy (DP-605 NS) top field shaping board to top extrusion.
9. Apply epoxy to 30 foot tube and mount top extrusion containing top field shaping board, clamp and remove from assembly station. Store in support rack for curing.
10. X-ray tube to verify wire position.

Three epoxy types are employed:

1. Tack connections to set bridge and wire location use fast setting Permabond 200 adhesive, set up time 10 seconds.

2. Long life high strength bonding for end cap, field shaping boards, wire bridges and extrusion top cover employ 3M Scotch Weld DP-605 NS urethane adhesive using an EPX applicator.
3. Field shaping board grounding to tube body, Bipax #B-A-2902 silver conducting epoxy, manufacturer TRA-CON Inc., Medford, Massachusetts.

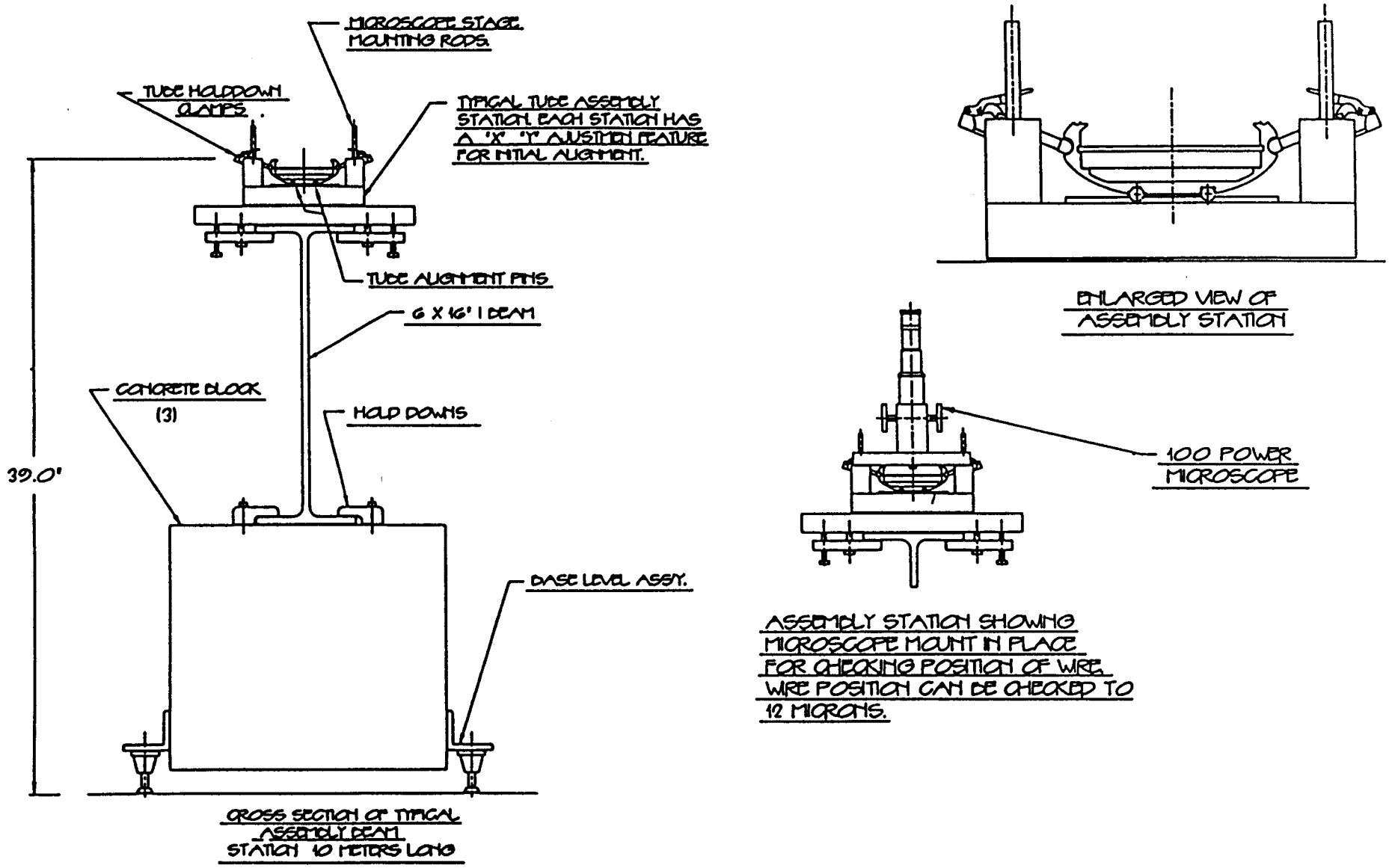

Figure II.D-1. Details of the drift tube assembly station.

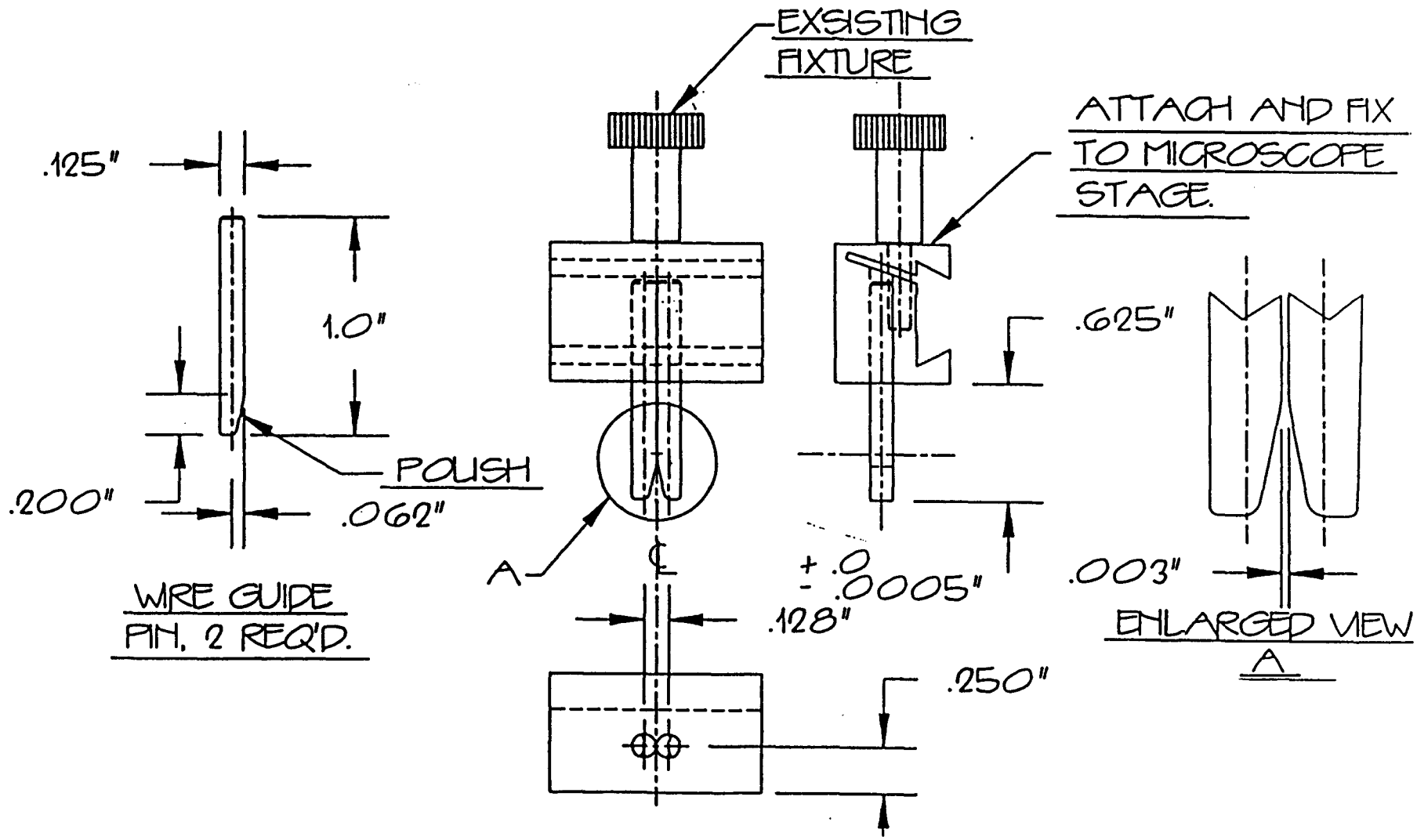

Figure II.D-2. Drawing of the wire locator.

E. BOX DESIGN

Box Stiffness Tradeoffs

To meet the overall requirements on precision, we would like the wire to be straight (or at least in a known position) to about 100 μm. Since the wire is being supported at two intermediate positions, these positions must be in a straight line with the end points to this order deflection. We investigated five potential approaches to building the box to meet this criterion:

1. Build an aluminum box strong enough to meet the requirement directly.
2. Build the box out of a strong exotic material.
3. Fill the box with a potting material to give it sufficient strength.
4. Camber the box to make up for the expected deflection.
5. Make the interior bulkheads actively adjustable.

Figure II.E-1 shows the deflections of the two interior bulkheads (as well as the deflection of the box and tubes at the center of the box) as a function of the moment of inertia ratio between the box and tubes. It is immediately apparent that the chamber center deflection will never be less than about 2 mm, no matter how heavy the box is made. Some small variation is observed by changing the box moment of inertia to area (I/A) ratio, but the bottom line is that increasing the box thickness piles on load very nearly as fast as the stiffness is increased. If we choose a design point near the knee of the deflection curve (about 3-4 mm), a box/tube stiffness ratio of about 10,000 is required. Such a configuration requires 1.5 cm panel thicknesses, and leads to a chamber weight of about 1640 kg , virtually the same as the tube weight. The overall chamber weight would then be approximately 3270 kg for 80 tubes.

The deflection of a single tube under its own weight is 166 mm This illustrates the value of the stiff box in limiting deflections to perhaps 3-4 mm. This range of deflections unfortunately exceeds the tolerance on tube/wire deviation by a wide margin.

A review of other possible materials suggests that a quasi-isotropic P100 graphite/epoxy should be the best practical candidate for a chamber material, with a

specific modulus some four times that of aluminum. A highly oriented composite of the same fiber would provide still higher chamber bending stiffness, with some attendant reductions in off-axis properties. Figure II.E-2 illustrates the effect of using the quasi-isotropic P100 composite in the chamber structure. The deflection asymptote has been reduced from approximately 2 mm to about 0.5 mm, still not meeting the requirement, although it would be satisfactory if the wire did not need internal supports. Even so, this improved performance comes, however, at a very high price in materials (>$200/kg for graphite/epoxy versus approximately $4/kg for aluminum) and additional development effort.

It has been suggested that "potting" the drift tubes together within the chamber structure ought to dramatically improve the bending efficiency, and consequently reduce deflections. An attractive approach to the notion of "potting" the tubes would be to cast the tube array into the chamber with one of numerous available urethane foam resins. A calculation of the deflection of a box made in this way is shown in Fig. II.E-3 for a variety of I/A values. Although the deflection decreases more rapidly with increasing box stiffness than the unpotted cases, the deflection asymptote remains nearly the same at about 2 mm.

In summary, none of the chamber options investigated so far can provide intermediate wire supports which deviate from initial straightness by 100 μm or less. Clearly, an alternative strategy is necessary. One approach would be to camber each chamber and supermodule so that the deflected shape in each of the required orientations would be such as to make the wire supports collinear to within 100 μm. While feasible in principle, this approach is fraught with practical difficulties. Not only would each chamber/supermodule now be of unique form (implying serious logistic problems), but the manufacturing tolerancing of such precise (curved) shapes would be prohibitively expensive. The preferable approach is to make the bulkheads providing tube/wire supports adjustable in service so as to zero the gravity induced deviations from straightness. This implies designing a box with "reasonable" stiffness, such as the knee of the deflection versus moment of inertia curve (deflection approx. 2-4 mm). The intermediate bulkheads would then be adjusted to collinearly with the ends. Since the chambers will be disposed in several different attitudes, position sensing and adjustment capability must be provided in the two principal directions in a bulkhead plane (transverse to wire). Once installed, the movable intermediate bulkheads need not be continuously adjusted, but only

periodically calibrated. The details of alignment and adjustment hardware needed to enforce this compensation scheme will be described in Section II.F.

Prototype Box Objectives and Design Approach

A principal objective of the muon chamber prototype development is to build and exercise a structural system exhibiting, insofar as possible, the mechanical hardware and stiffness characteristics of the typical muon chambers envisioned for the SDC detector supermodules. Since the deformation of the drift tube/chamber combination is proportional to the fourth power of length, inverse third power of height, and is approximately independent of width, it is most important to replicate length and height of a typical supermodule sub-element. For that purpose, the length of the prototype is set at just over 9 meters, the length of a typical theta-chamber in BW3. The depth of the chamber at about 50 cm is such that it can house an assembly of 4φ or 4θ layers. The last dimension, the width of the box can be arbitrary and was chosen for practical purposes at approximately 1.1 m. A schematic of the prototype structural system is shown in Fig. II.E-4 with dimensions and support locations. The drift tubes are arranged in a prescribed pattern (indicated on Fig. II.A-1 above) to respond to physics requirements and are supported by the chamber end walls as well as two intermediate bulkheads.

As the muon chambers will be disposed on the faces of an octagon, the gravity vector affects them in eight different (in some cases anti-symmetric) ways. A single design must therefore be proposed that can withstand any of these loadings and deform within limits imposed by physics performance requirements. Any drift tube supported by the chamber must remain within 1 mm of its nominal "perfect" straightness under any possible gravity orientation, while the wire must be straight to within 100 microns. As was shown above, an active compensation scheme is necessary to insure drift tube dimensional stability by correcting excessive deformations. These deformations may be due to gravity or other sources such as thermal, creep, and fabrication (esp. welding) induced misalignments.

The overall support system of muon chambers is provided by a truss system that offers support points only at the ends of the muon chambers. To emulate these conditions the prototype chamber must span between A & D (Figure II.E-4) without excessive deformations that would further add to the tubes deflections inside. As

we established above, a compensation system for the internal bulkheads is a necessity. One obvious approach would be to reduce the excessive box deflections by use of external actuators taking support on the underlying truss, a solution that essentially adds redundant intermediate supports and departs from the original design approach (kinematic mounts). A more elegant technique however consists of compensating for the box deformations by moving the tubes inside the box itself. This solution was selected and found especially attractive because of the very large difference in stiffness between all the drift tubes and the supporting box structure (1 to 171 ratio). By pushing against the box the intermediate support bulkheads can move the drift tubes to insure adequate positioning with very little effect on the box itself. This concept allowing correction in two perpendicular direction enjoys generality and thus is applicable to all chamber orientations. In addition the actuation of the bulkheads may correct misalignments caused not only by gravity but compensate also for thermal, creep and fabrication/welding induced effects.

The biggest drawback of this concept is the need to measure precisely the position and alignment of the drift tubes in the box so as to trigger the proper corrective actions. The design and calibration of an optical alignment system is therefore incorporated and its details are discussed in Section II.F of this report. The "cohabitation" of sensing optics, movable bulkheads (supporting close packed tubes) and activation hardware render the mechanical design details of the prototype aluminum box somewhat complex. Accessibility for initial alignment and calibration is only one of many issues that need to be addressed in designing a completely self adjustable muon chamber.

Prototype Box Configuration

Having decided that compensation of the tube/wire supporting bulkhead positions was the best design strategy, the prototype chamber was configured to exercise the alignment and compensation system as well as the basic drift tube and layout performance. The prototype tube layout has previously been shown as Figure II.A-1, and comprises 48 of the 8 cm x 2 cm drift tubes arranged in an overlapping array, tube cross-sections tilted 10 degrees with respect to the chamber walls. Within the box, the tube array is supported on four precision NC-milled bulkheads. These bulkheads are machined to accommodate the tubes through clearance holes which contain location features. These features fit into grooves

extruded into the drift tube cross-section. The bulkheads are further machined to accommodate the four channels of optical components required to sense the relative positions of the two intermediate bulkheads. The two end bulkheads are fixed to flanges set in slightly from the box ends, while the two intermediate bulkheads are set at the third-points of the box beam span.

These intermediate bulkheads are attached in an adjustable fashion to picture frame angle stiffeners welded to the box panels. As shown in the next section their transverse position inside the box can be adjusted plus or minus 1 cm in both bulkhead principal directions. These movable intermediate bulkheads must be attached to the chamber structure in a manner that allows precise adjustment of the transverse position, while maintaining tight parallelism tolerances with respect to the end bulkheads. The attachment scheme must further permit positive locking of the final adjusted position. A novel 2 degree-of-freedom flexure was designed to perform the function of holding the adjustable intermediate bulkheads, but initial cost estimates suggested that it would be too costly. A simple backup scheme was then formulated incorporating a locking eccentric cam mechanism. This latter eccentric is the baseline for the prototype and is shown in Fig. II.E-5. Obviously, the intermediate bulkheads must be provided with attachment provisions for the actuation and locking mechanism. These hardware trades are discussed more fully in the next section. Figures II.E-6 and II.E-7a illustrate the prototype end and intermediate moveable bulkhead geometries, respectively. Figure II.E-7b shows the fixed picture-frame bulkhead to which the intermediate bulkhead attaches.

The chamber structure supporting the tube array is a stiffened box; with dimensions of 9.28 meters length, 1.09 meter width, and 0.49 meter height. The box top and bottom panels are 3/8 inch 6061 aluminum plating, while the side panels are 1/2 inch plate. In order to avoid panel buckling (oil canning) problems, the box is further stiffened by rectangular bars welded to the top and bottom panels and running longitudinally, as well as transverse "picture frame" stiffeners at approximately 0.5 meter centers. Plan and side views of the prototype chamber structure (one-half length) are shown on Fig. II.E-8, and an end view is shown on Fig. II.E-9. It will be apparent that the sides and bottom are welded at the corners through intermediate angle sections. The stiffeners and bulkhead attachment frames are similarly welded to the top, bottom, and side panels. The total prototype

weight will be slightly over 2300 kg., with 1000 kg in the tubes and 1100 kg in the box structure (allowing an additional 10% misc.).

Set in from either end of the box approximately 7.5 cm is a picture frame bulkhead or transverse stiffener. To these frames the precision milled end bulkheads are bolted with some freedom to shim both the transverse position and the out of plane angle. These shim adjustable features are intended as contingencies against potential end bulkhead out of parallel (or square) due to box welding. On the top of the chamber at either end and above the intermediate bulkheads are arranged removable "hatches", which are intended to allow access to the optical devices and adjustment features while the box is resting on the construction tooling. When the hatches are removed, the torsional rigidity of the box will be quite small, allowing easy correction of any built-in twist. These hatches will be fastened about their perimeter at 7.5 cm centers (using 1/4 inch screws) to the flanges formed by the box corner angles and transverse stiffeners.

The overall chamber center deflection when end-suspended in the horizontal attitude is predicted to be 2.0 mm. The intermediate bulkhead deflection is predicted as 1.6 mm. In this situation, the box ends tilt over (downward) approximately 0.001 radian. These estimates are likely to be somewhat optimistic, since the hatch joints will not provide perfect load transfer (and stiffness). To cover the potential increase in deflections due to unaccounted flexibilities, as well as fabrication deviations that may need correction, the bulkhead adjustment range has been specified as ± 1 cm using the eccentric cam adjustment mechanism.

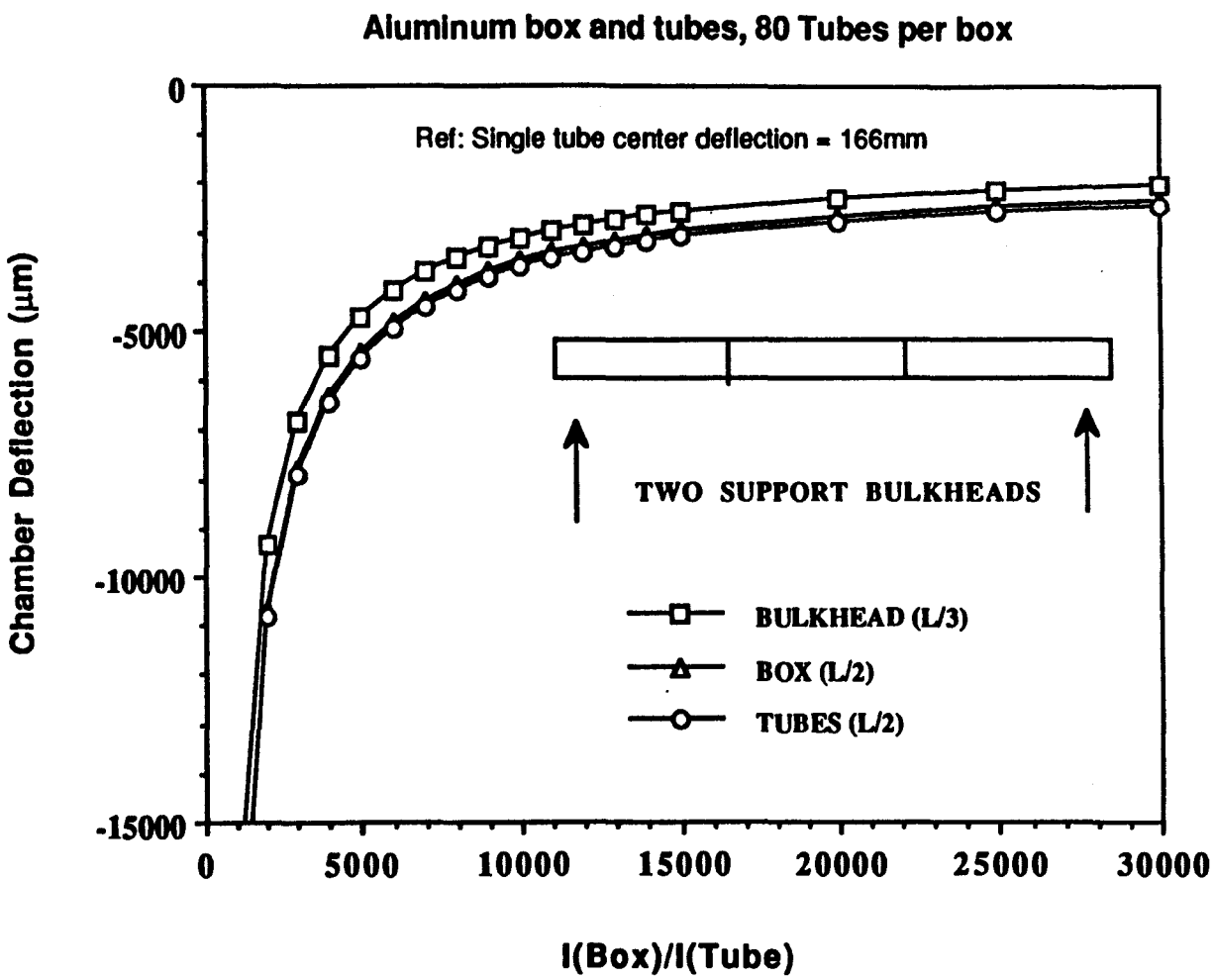

Figure II.E-1. Chamber and box deflections versus stiffness ratio for an aluminum box.

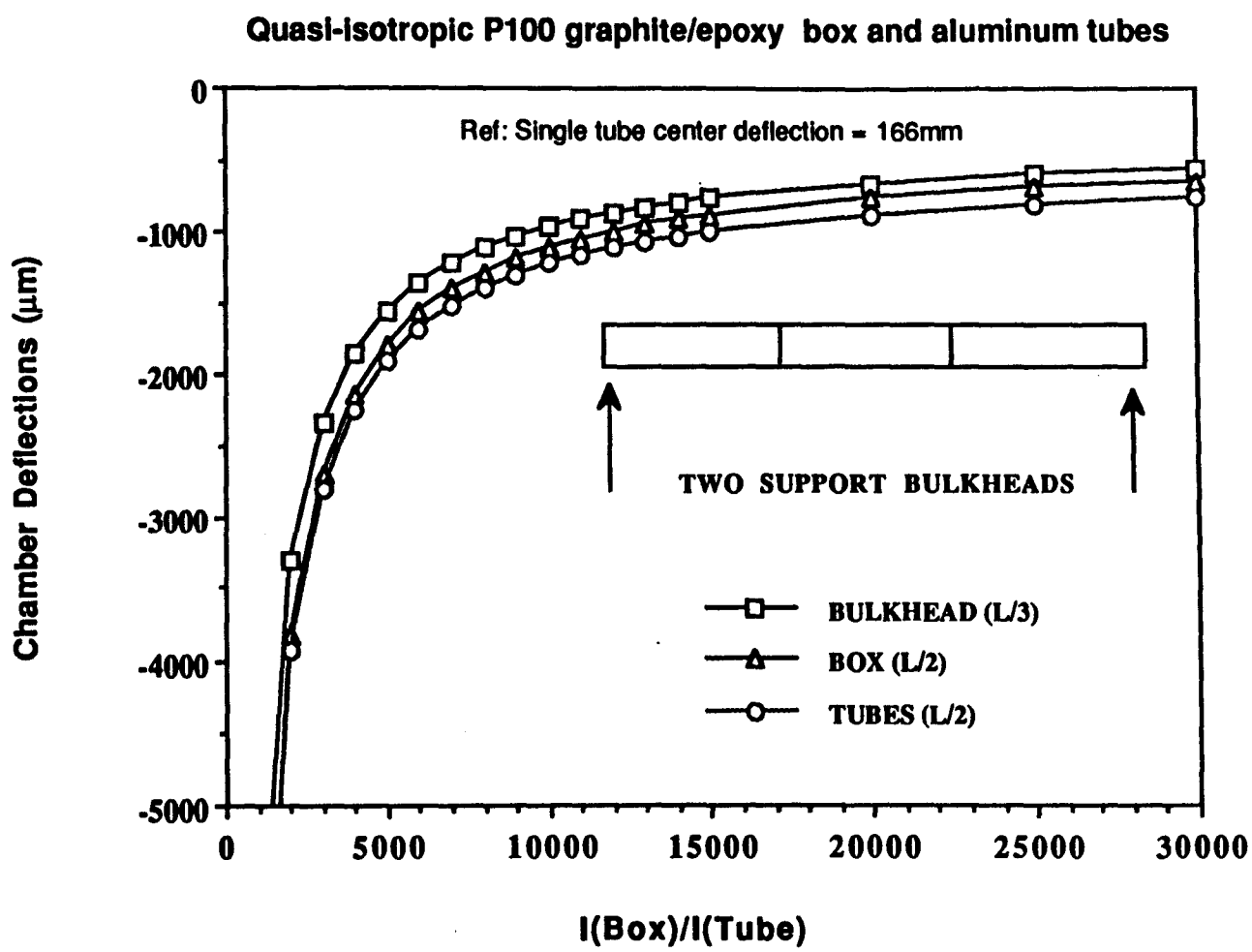

Figure II.E-2. Chamber and box deflections versus stiffness ratio for a graphite/epoxy box.

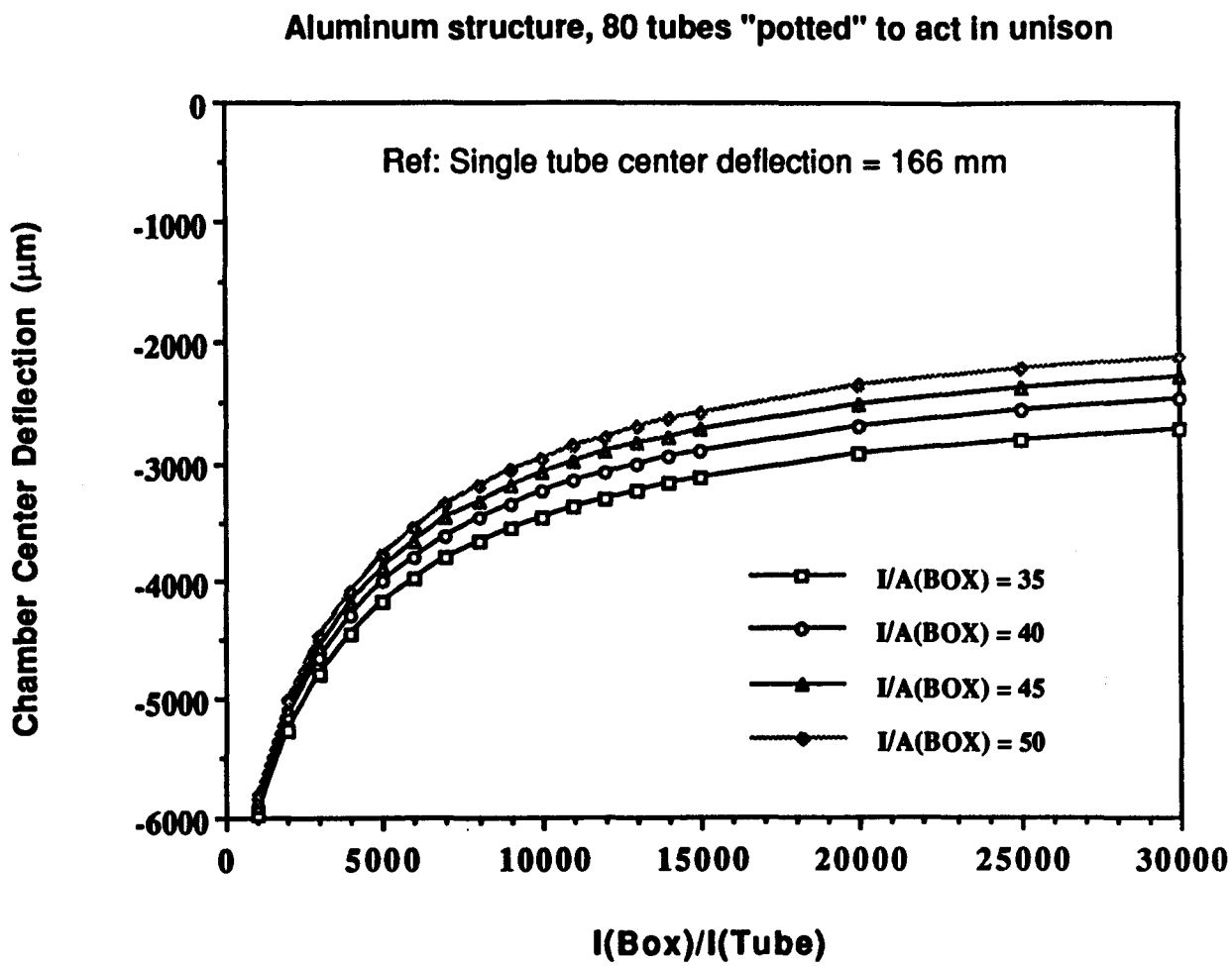

Figure II.E-3. Chamber center deflection for tubes potted together.

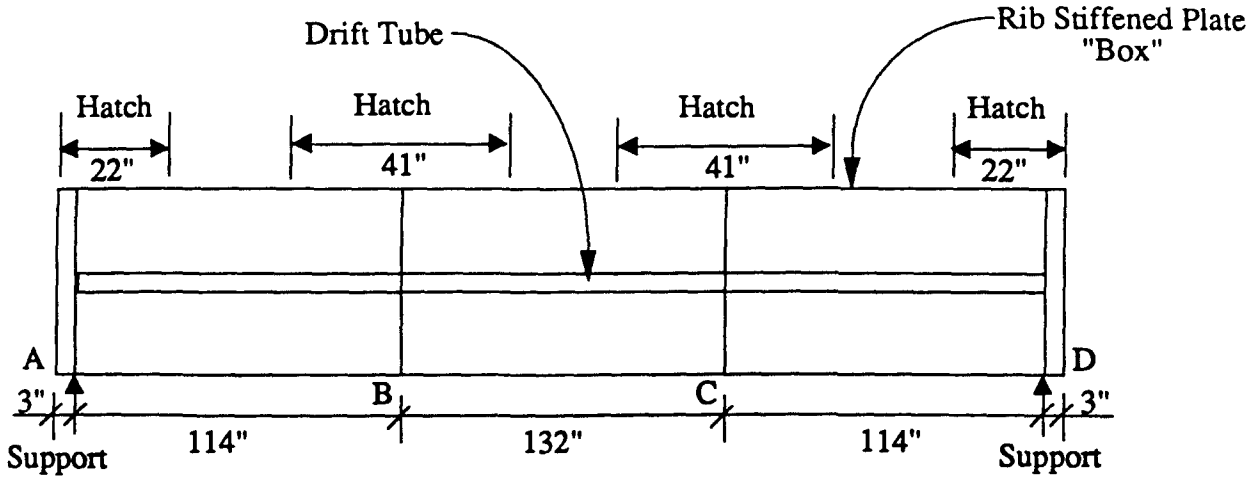

• **PROTOTYPE CHAMBER – SCHEMATIC**

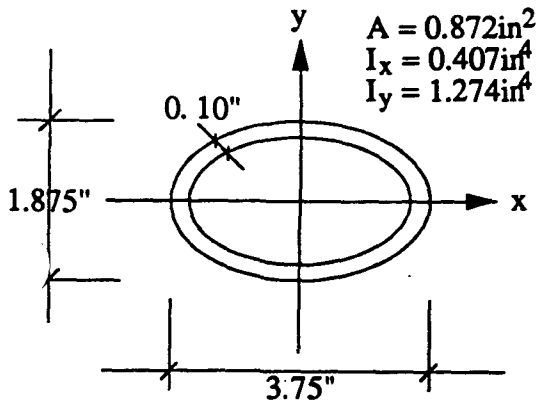

• **DRIFT TUBE**

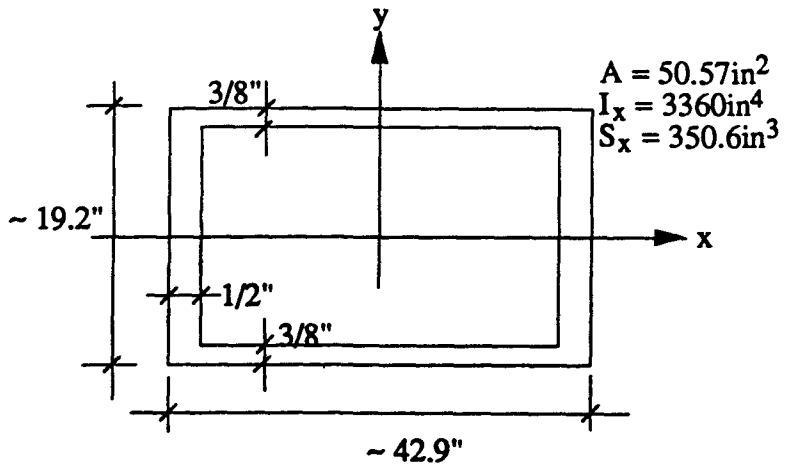

• **CHAMBER BOX**

Figure II.E-4. Prototype chamber box schematic.

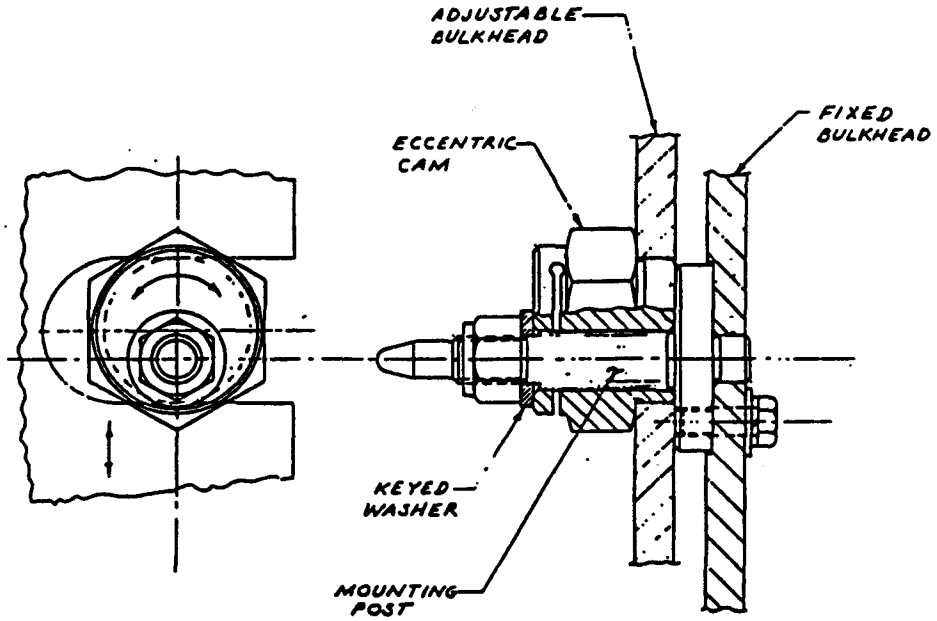

Figure II.E-5. Prototype bulkhead adjustment eccentric.

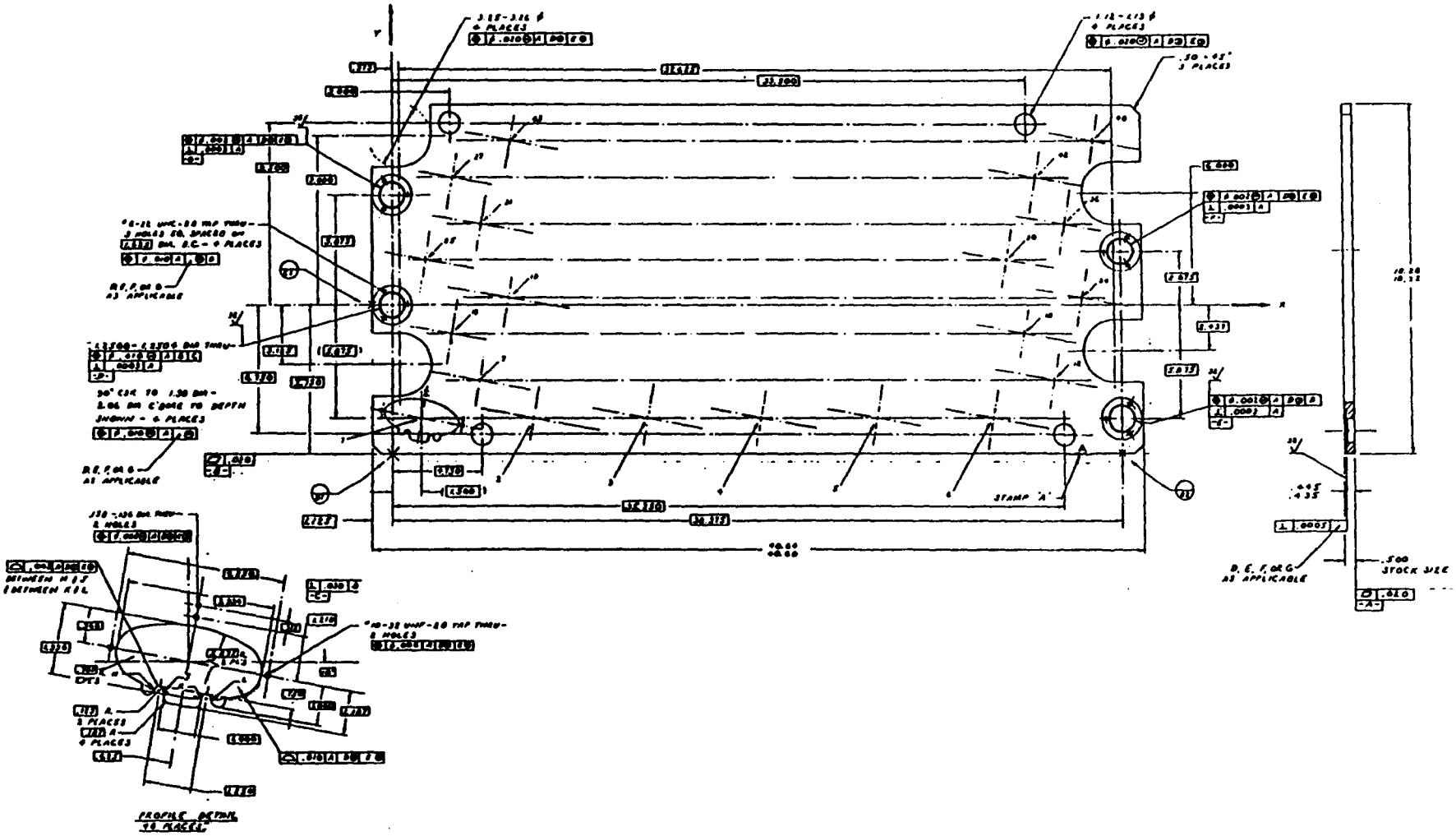

Figure II.E-6. End bulkhead.

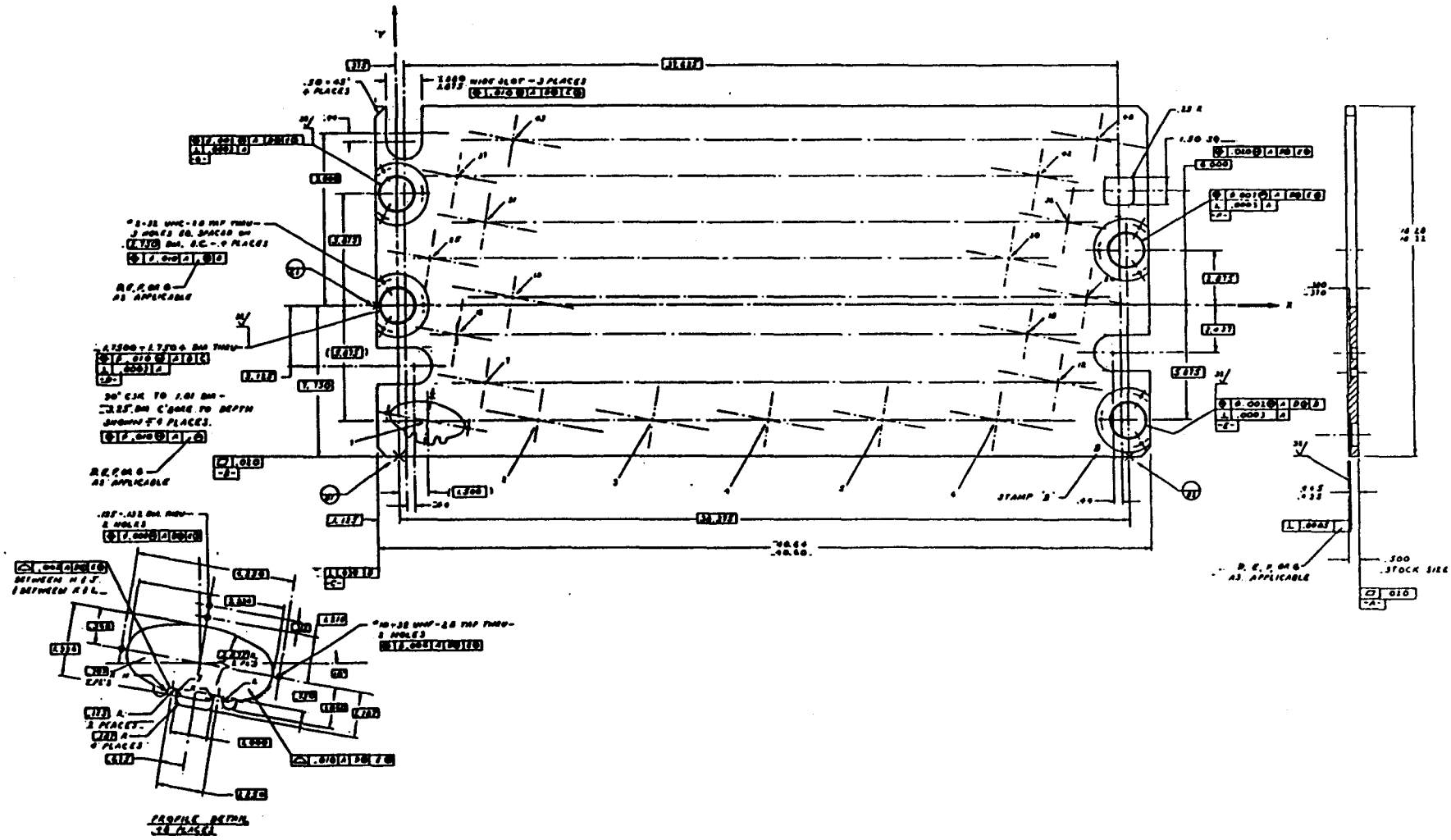

Figure II.E-7a. Intermediate moveable bulkhead.

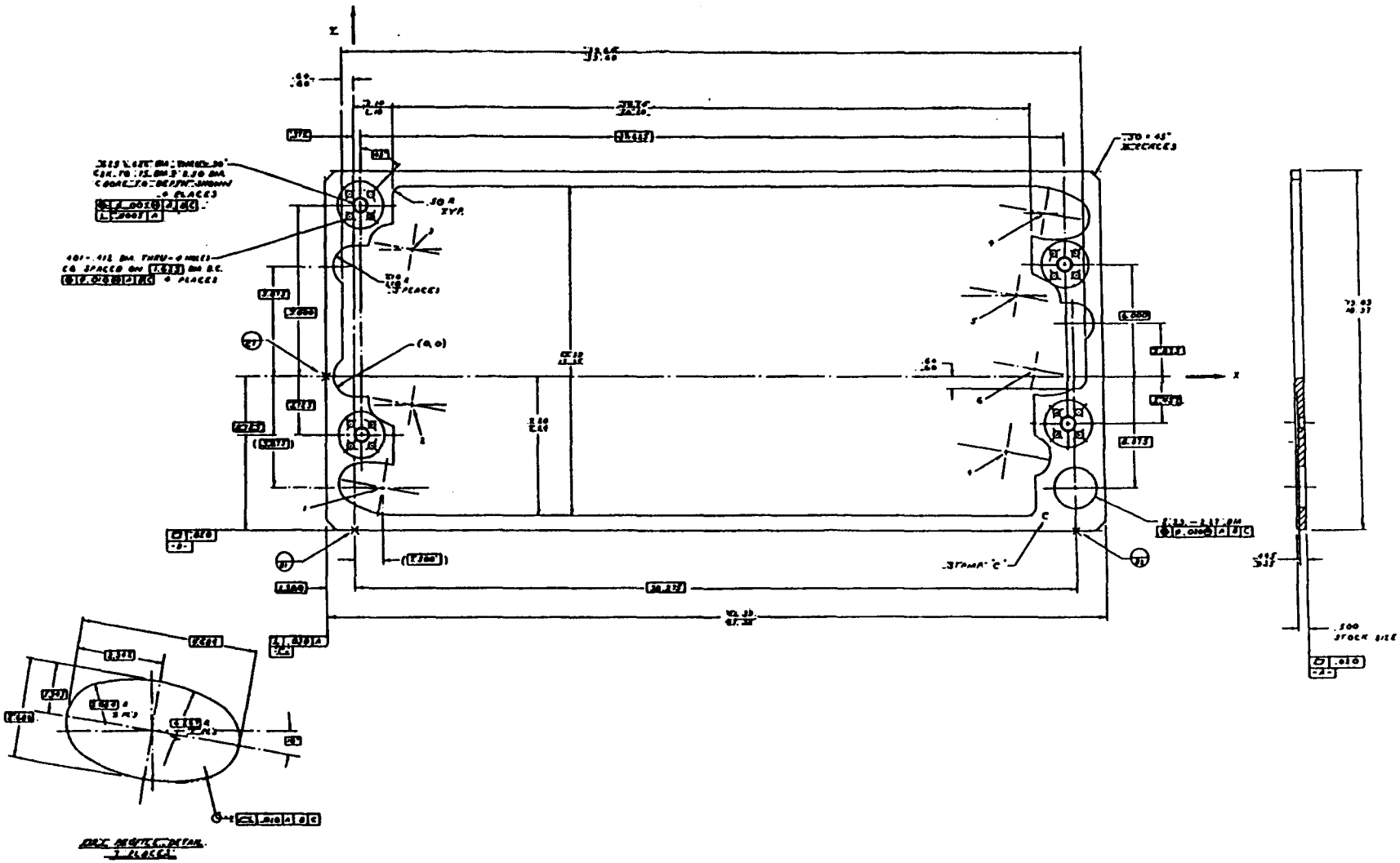

Figure II.E-7b. Intermediate fixed bulkhead (picture frame).

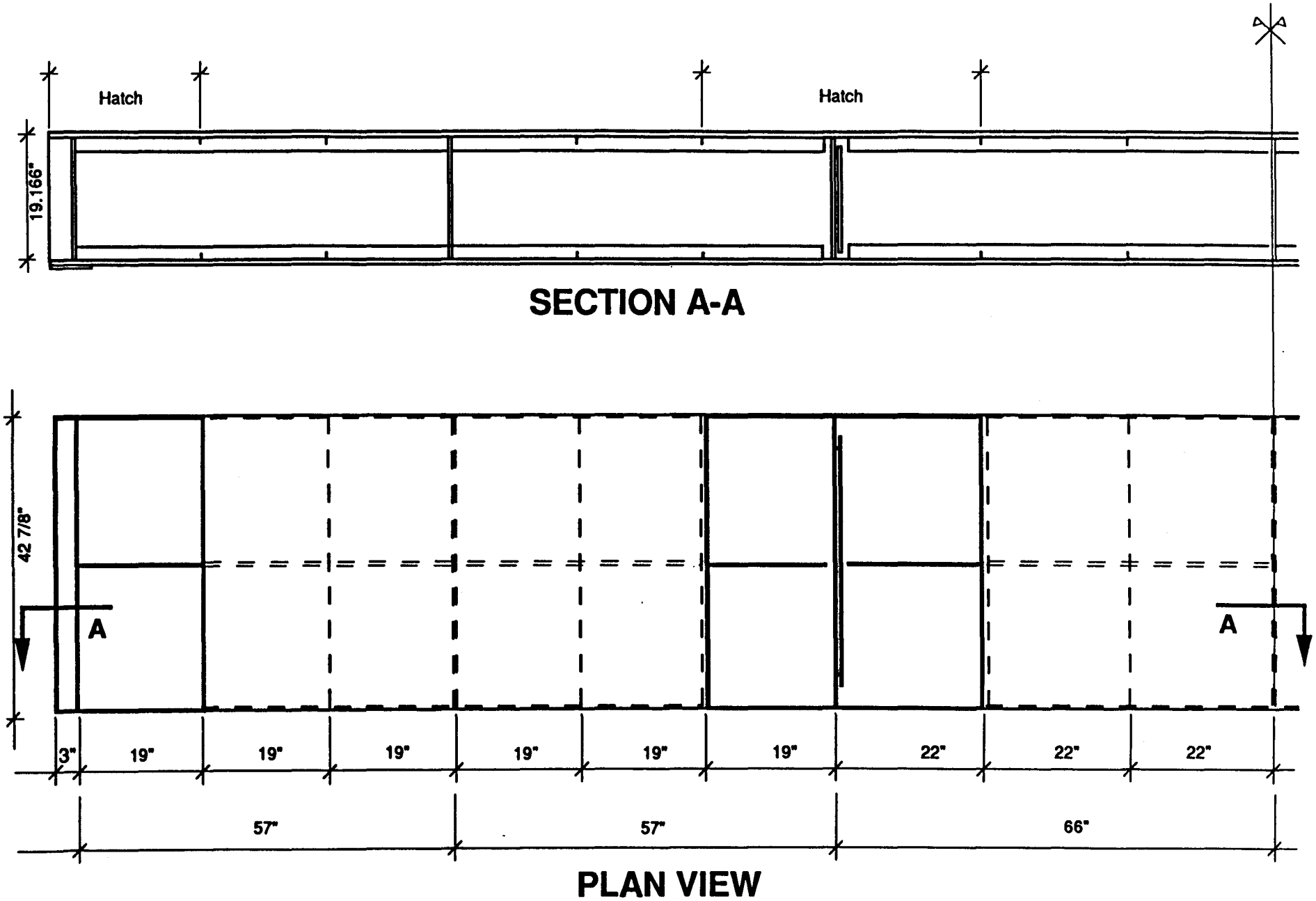

.05" = 1"

Figure II.E-8. Prototype box design schematic.

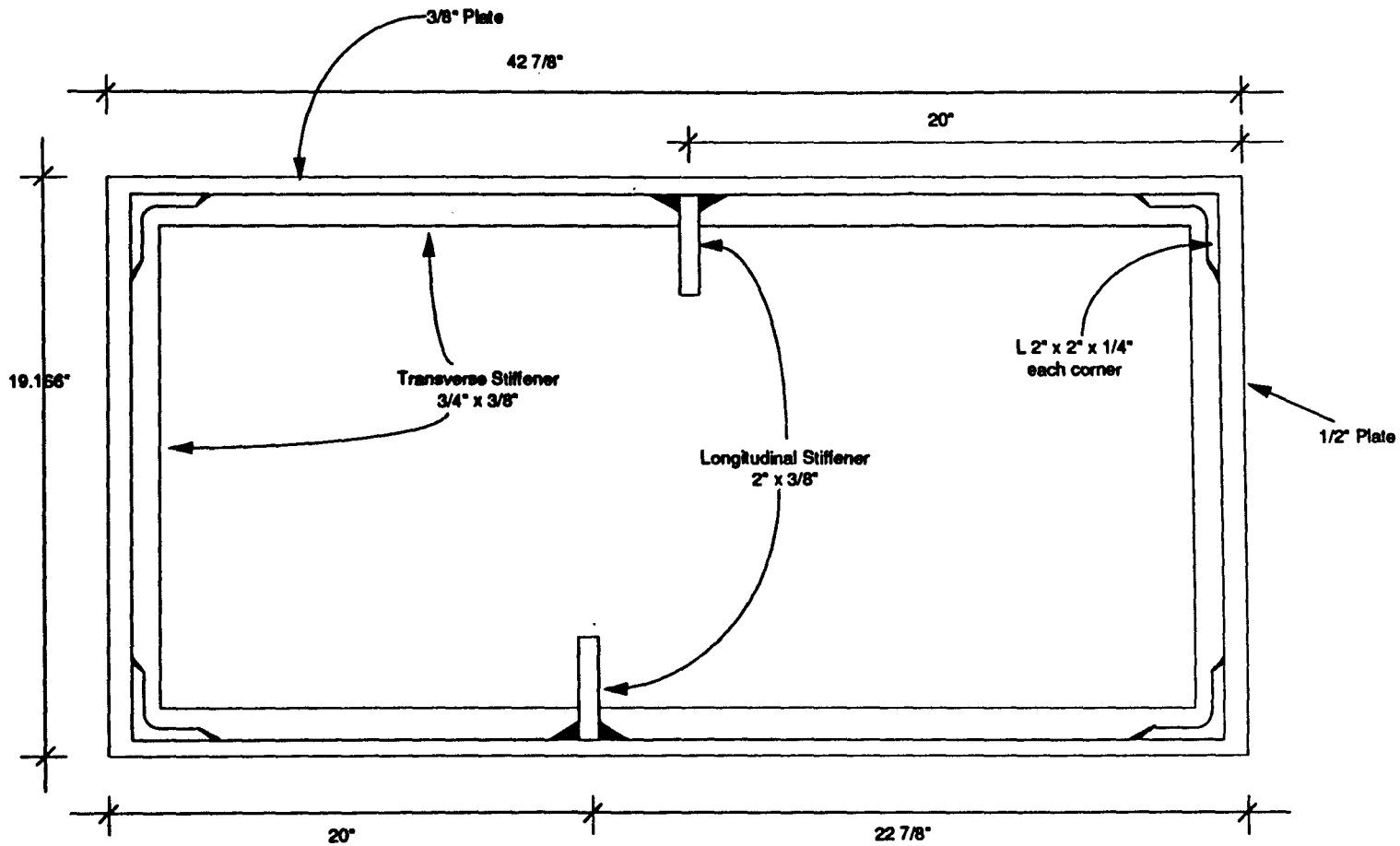

Figure II.E-9. End view of the prototype box.

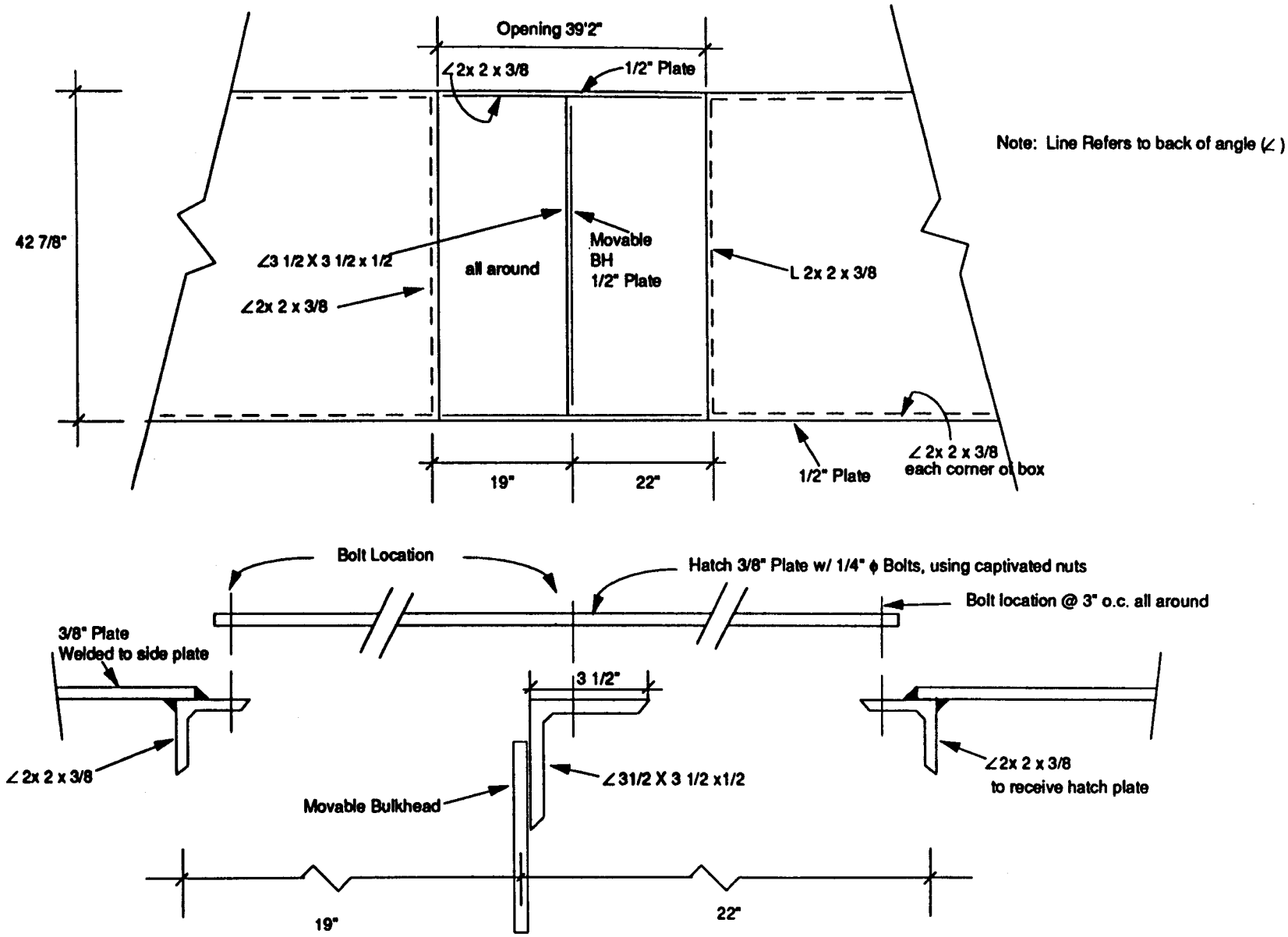

Figure II.E-10. Hatch configuration and connection details

F. Alignment System

Design Concept

As described above, the drift tubes and wires are supported at both ends and at two intermediate locations by precision NC-machined bulkheads. These bulkheads and their tube location features ensure that the tube ends are positioned to within the machining tolerance (< 25 μm) with respect to their array neighbors. The intermediate precision bulkheads likewise ensure the relative tube positions at the third-points of the chamber span. The box is supported by the end bulkheads, and knowledge of the support point positions will ensure knowledge of the wire end points from the accurate fabrication of the bulkheads. Sighting fiducials will be placed on the chamber ends to provide this global reference. We assume that the box is supported at three points in a kinematic manner, and a fourth support point is provided in a semi-kinematic fashion to prevent excessive twist in the box. The alignment is therefore split in two parts, (1) the "external" alignment of the box support points, and (2) an "internal" alignment to maintain the straightness of the wires within the acceptable tolerance.

To limit the excessive sagitta due to sagging of the wires, two intermediate bulkheads are used, supporting the tubes (and therefore the wires through wire supports in the tubes) at the bulkhead locations. Again, the relative positions of the wires at the intermediate bulkheads in any transverse direction is maintained at the design values by the rigidity and accuracy of the bulkheads and the wire supports. The intermediate bulkheads are adjustable and can be translated in any direction perpendicular to the wires. The internal alignment is thus reduced to the proper positioning, in two orthogonal directions perpendicular to the wires, of the intermediate bulkheads. Figure II.F-1 shows a schematic cross-section of the chamber under gravity load, indicating that the goal of the internal alignment system is to maintain points A, B, C and D in a straight line. The bulkhead deflections have been exaggerated in order to stress the need for an alignment system which is independent of the bulkhead tilt. The intermediate bulkhead deflections are approximately 1.6 mm as indicated in the previous section, with an end bulkhead tilt of approximately 0.001 radian. A tilt of 0.001 radian produces a translation of the line of sight perpendicular to the bulkhead equal to 3 mm at 3 m.

This offset is of the same order as the expected bulkhead deflection, showing the importance of designing a tilt insensitive alignment system.

The internal alignment solution adopted, shown on Fig. II.F-2, is a combination of simple optical alignment channels each comprising a Light emitting Diode (LED) source, a lens, and a lateral detector sensing the position of the LED image. Two such channels (for x and y coordinates and in plane rotation) are needed for aligning one intermediate bulkhead with respect to the end bulkheads, therefore a total of four channels are needed for the prototype chamber. The source and detector centers are used as references, and the alignment consists in bringing the optical center of each lens on the line defined by the centers of the LED and the center of the detector (zero output position). Tilts of component due either to tilt of the bulkheads, or due to mounting misalignment, do not produce any error in the sensed translation as long as the rotation is about the center of the component and relatively small (a few degrees).

In order to ensure that the straightness of the four monitoring optical channels will provide the straightness and parallelism of the wires, the center of each component in the optical channels must be accurately referenced to the positions of the wire supports on each bulkhead. This is done by mounting and permanently centering each component in a holding cell which has accurate external reference diameter, and providing accurate mounting holes for these cells in the bulkheads. These intermediate holding cells have been designed for the prototype chamber at Draper Laboratory and are illustrated in Figs. II.F-3, II.F-4, and II.F-5 for the LED, lens, and quad cell or lateral detector, respectively. The permanent centering operation for each component in its respective cell is done prior to assembly, with routine optical bench procedures, and may even be eliminated if factory centered components are available (which will be true in general for large purchases).

The focal length of the lens for proper imaging of the LED on the detector is selected using the lens equation:

$$1/p' + 1/p = 1/f$$

where p and p' are the distances from source to lens and lens to detector respectively. With $p = 3.06$ m , and $p' = 6.76$ m , we get $f = 2.1$ m. The image of the source is magnified by the amount :

$$M = p' / p$$

The size of the geometrical image of the source is therefore:

$$d'_{geom} = d\,M$$

where d is the diameter of the source. If the lens is translated by an amount D, perpendicular to the direction defined by the centers of the source and detector, the image of the source moves by an amount

$$D' = D\,(1 + M)$$

in the same direction, and it is the displacement D' which is sensed by the detector. All the numbers used here are controlled by the dimensions of the box and the positions of the intermediate bulkheads.

The four optical channels described above will provide an error signal for any sensed misalignment in the x and y translations as well as the inplane rotation. If a nonzero misalignment is detected, mechanical means must be provided to remove it. The intermediate bulkheads of the prototype chamber are mounted to the box structure via eccentric cam-type devices as shown on Fig. II.E-5. The mounting post or stem is rigidly attached to the fixed "picture frame" bulkhead. An eccentric cam is provided which slides over the fixed stem and engages a slotted hole in the adjustable bulkhead. The eccentric cam is provided with an integral nut to facilitate alignment via a wrench inserted from the near end of the chamber. Turning the nut will rotate the cam, providing vertical or horizontal actuation of the bulkhead. The operator will be observing an oscilloscope or other device indicating quad-cell output to obtain adjustment feedback. The fixed stem is also provided with a locking nut, turning against a keyed washer so as to firmly hold a desired cam position, without disturbing it in the process. It is anticipated that first one direction of adjustment would be aligned with the other fixed, and then the process would be reversed.

Component Hardware Tradeoffs

In order to provide the required accuracy at the minimum cost, a preliminary trade-off selection for the different components has been carried out.

a) Lens selection : As mentioned in the previous paragraph, the focal length is restricted by the mechanical dimensions of the box. In order to maximize the light gathered by the lens, its diameter D is selected to be the largest one compatible with the bulkhead design. This leads to a clear aperture diameter of approximately D = 38 mm. The half acceptance angle is:

$$q = \tan^{-1}(D / 2p)$$

corresponding to an acceptance numerical aperture:

$$N.A. = \sin(D/2p)$$

With the given dimensions of the box, we obtain $N.A. = 0.0062$ and $q = 0.357°$. These numbers show that only a small portion of the source output will be gathered by the lens. The imaging f-number is:

$$f_{\#} = f / D$$

therefore $f_{\#} = 55.1$ .This is a large f-number, and the aberrations of the lens will have a negligible effect on the size d' of the image of the light source. Therefore this image size is

$$d' = \sqrt{d'_{geom}{}^2 + d'_{diff}{}^2}$$

where d_{diff} is the size of the diffraction spot due to the lens;

$$d'_{diff} = 2\, l\, f_{\#}$$

where l is the wavelength of the light source.

b) Detector options : Three types of detector can be used for sensing the displacement of a spot of light. First a mosaic of detectors associated with a centroid-finding processor. This approach allows for large capture range, large linear range, and is geometrically very stable, but unfortunately very expensive. A second approach is to use a quad-cell which is essentially a planar photodetector with its sensitive surface cut in four adjacent quadrants, creating four separate photodiodes. The centering in this case is done by sensing the relative amount of light falling on

the quadrants. The relative output near the center of the detector is approximately proportional to the displacement, over a region equal to the size of the image of the source, as long as the image of the source is totally included in the sensitive surface of the detector. This type of detector is available from several manufacturers in this country, is relatively inexpensive, has a high precision near the zero position and has a stable absolute zero position dictated by its construction. The third type of detector is a lateral-effect photodiode. It is a single photodiode with planar active area and output leads at the four corners. The position of a spot of light falling on the active area is derived from the relative diffusion of the photon-generated electrons appearing at opposite corner leads. The currents generated are proportional to the distance between the contact points and the centroid of the spot of light This type of detector is also available from several manufacturers in this country, but is more expensive than the quad-cell, and it is in general noisier for the same amount of light. The output of quad-cell and lateral-effect photodiodes are compared on Fig. II.F-6. Both detectors have the same capture range (approximately equal to the size of the active area) and the quad-cell has a smaller linear range over which the output is proportional to the position. The quad-cell has a better position resolution in its linear range than the lateral detector because of its higher sensitivity (slope), and lower noise. For a quad-cell the trade-off is between the lateral linear range and resolution. The linear range is approximately equal to the image spot diameter d', and the resolution near null is:

$$\text{Quad-cell resolution(near null)} = \frac{K}{SNR}\frac{d'}{2}$$

where SNR is the signal to noise ratio when the spot is centered, and K is a constant related to the light distribution in the spot image, $0.5 < K < 1$.

$$SNR = \frac{\text{Signal response}}{\text{Noise rms}}$$

$$\text{Noise rms} = \sqrt{(\text{Johnson noise})^2 + (\text{Shot noise})^2 + a^2_{1/f}}$$

within the bandwidth of the amplifier. Johnson noise and shot noise have a white spectrum, and $a_{1/f}$ is a noise term whose spectrum is proportional to the inverse of the frequency of operation over the bandwidth of the electronics.

For the lateral-effect detector the lateral range is nearly equal to the diameter of the active area. The resolution equation is similar to the equation for the quad-cell, with d' replaced by the the diameter of the active area. The noise equation is also similar with larger terms. For this type of detector, the position of the "center" or zero position is largely dependant upon the associated electronics. There is a potential long term drift or environmental drift of the electronics. Also, the electronics have to be matched to the one used during the centering of the detectors in their cells. Finally the effect of the non uniform harsh environment (high magnetic field for example) may affect the zero position and therefore the accuracy of the alignment.

c) Detector Electronics Options: The typical electronics necessary to process the output of a position sensor using quad-cell or lateral-effect photodiode is composed of one low noise transimpedance (current to voltage) amplifier for each quadrant or output of the detector, followed by two differential amplifiers, one for the x-direction and one for the y-direction. When the amount of light available is limited, electronic noise must be kept to a minimum. This is achieved with the detector operating in photovoltaic mode, i.e., without bias.

An improved electronics option can be constructed by modulating the (LED) source at >200 Hz, and sensing the detector output with narrow bandpass electronics centered on the LED modulating frequency. This approach has the advantages of eliminating the $1/f$ noise, minimizing white noise, and eliminating ambient light effects. The significantly lower noise associated with modulated sensing allows tradeoffs to lower power sources (LEDs). A breadboard of this modulating electronics has been built at Harvard University and is currently being evaluated in a prototype alignment system at Draper Laboratory.

d) Light Source Trade-off: The basic tradeoff in light sources is between LEDs and Laser Diodes. This tradeoff is basically a question of light output versus cost, with LEDs of suitable type at less than $100 and Laser Diodes at approximately five to ten times that level with appropriate power supplies. Since the bench testing to date

indicates sufficient signal with LEDs, the tradeoffs have been reduced to a selection between competing LEDs. The wavelength of the source should be near the silicon detector peak of 0.8-0.92 μm. The source should also be relatively insensitive to tilt misalignment. This latter requirement is best served by a source having very short focal length (ball) lens, rather than the more traditional long focal length lens which maximizes the apparent source size. While a large apparent source will put more light through the lens, it will be more sensitive to tilt misalignment, with less energy in the final image than a system with very short focal length. This tradeoff is illustrated in Figure II.F-7.

e) Bulkhead Adjustment Scheme: Two issues must be addressed regarding bulkhead adjustment: 1) the means used to hold the movable bulkhead square and parallel with respect to the chamber structure (end bulkheads), and 2) the means used to provide the adjustment force and feedback control. In the former issue, several schemes were considered for holding the bulkheads, including:

- Two degree of freedom flexure,
- Sliding wedges in "picture frame" tracks,
- Transverse screw adjustment with movable/fixed through bolting for locking,
- And the above described eccentric cam baseline.

The eccentric cam approach was chosen largely for its low cost and historical use on previous experiments. The cam-type systems suffer in terms of sensitivity by comparison to the various direct screw or wedge systems, by virtue of the shallow helix angle mechanical advantage of the screw. The eccentric can, however, be manipulated from the end of the chamber without recourse to a right angle drive, such as would be required for any screw-type system.

The second issue of tradeoff in the bulkhead adjustment is whether to utilize servomotors and closed loop electronic control in making the adjustment, or close the loop through human intervention. Cost and reliability factors strongly suggest the man-in-the loop approach, although this necessarily precludes final adjustment of bulkheads after assembly on the toroid. For the prototype system, a manual approach has been chosen, with actuation via 3-meter long wrenches and the sensitive application of muscle power. Should later studies indicate the desirability of closed-loop feedback control of the bulkhead adjustments, it will be necessary to

revisit the choice of actuation mechanism. It is likely that a screw-type system will be preferable to the baseline cam system for servomotor installations.

Prototype Design Specifications and Costs

Based upon the design tradeoffs and breadboard testing, the following commercial items have been chosen for the prototype:

- Quadrant photodiode from UDT, model # SPOT9DM1, operated in photovoltaic mode (no bias), 25 mm cell diameter, 10 mm diameter active area, cost approximately $80/each (4x).
- Lens from Melles-Griot, model #O1LMP059, 50 mm diameter, 38.1 mm diameter clear aperture, cost approximately $30/each (4x).
- Light emitting diode (LED) from Motorola, model #MFOE1102, Al-Ga-As, λ = 820 nm, 250 μm spot size, cost approximately $35/each (4x).

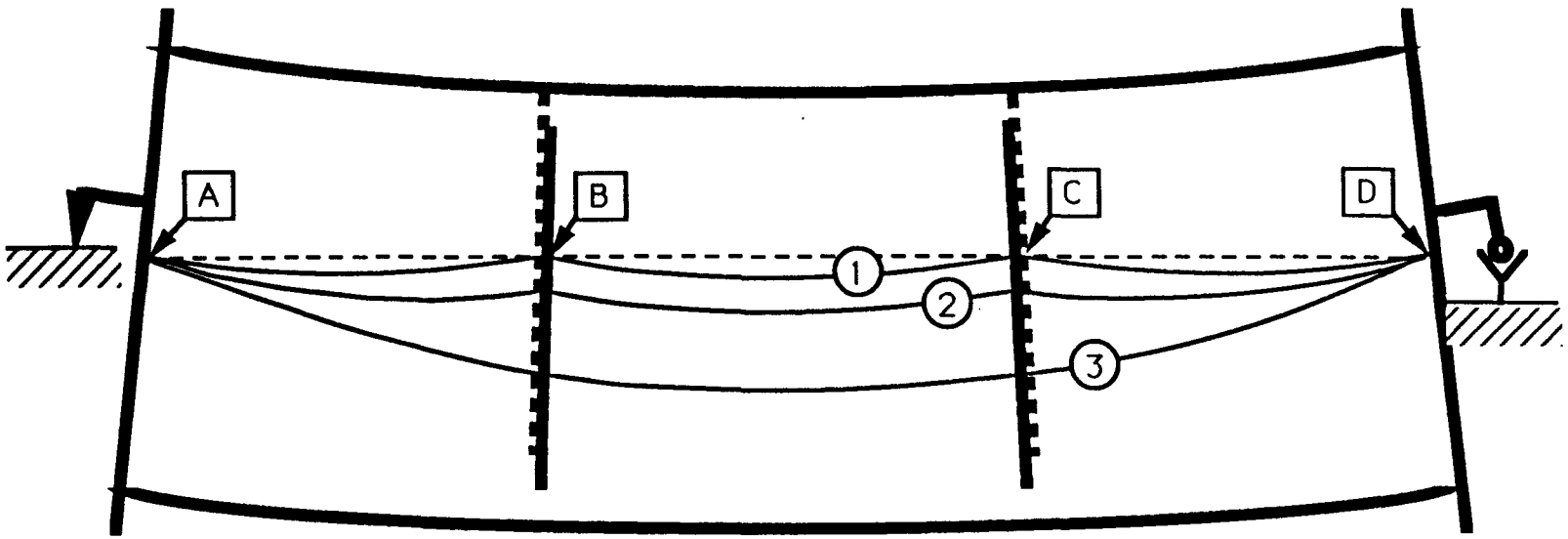

1 After correction

2 Before correction

3 Unsupported wire

Movable bulkhead shown in dashed line after correction

Figure II.F-1. Schematic chamber deformation and compensation concept.

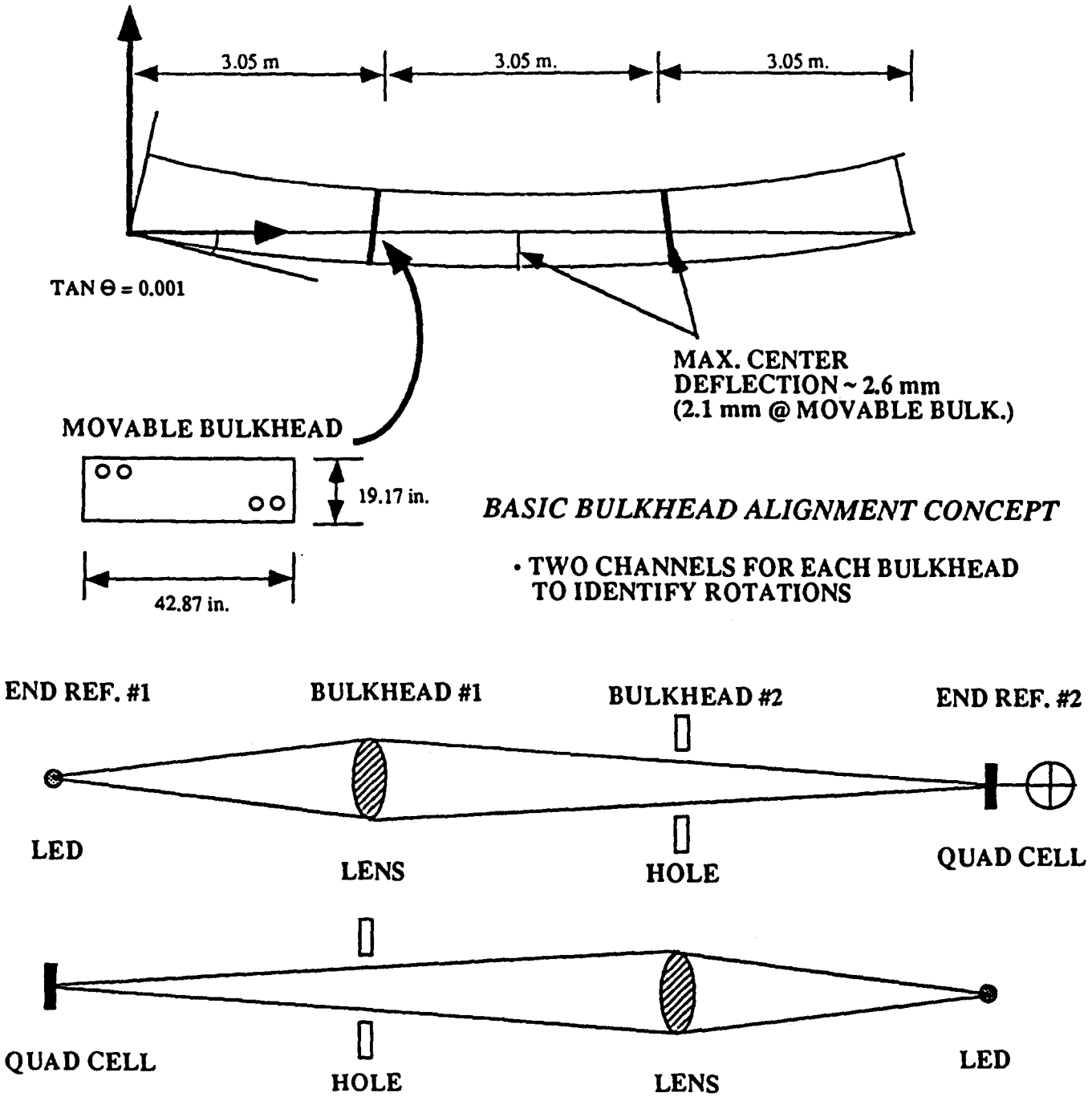

Figure II.F-2. Schematic of the prototype alignment system.

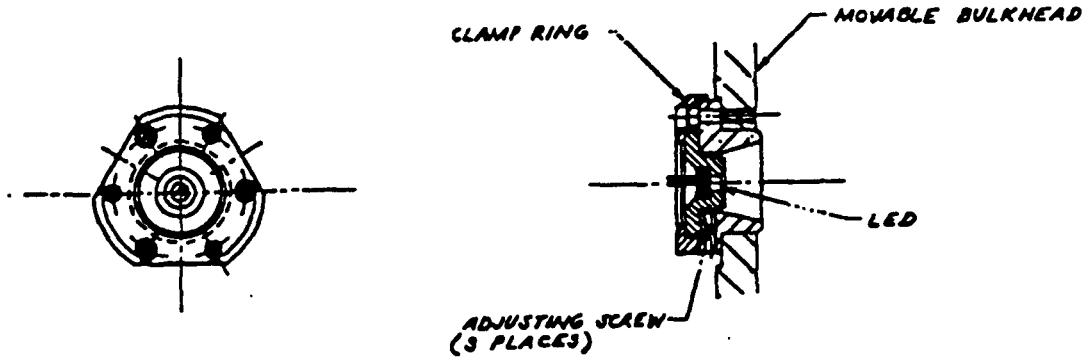

Figure II.F-3. LED mount for prototype alignment system.

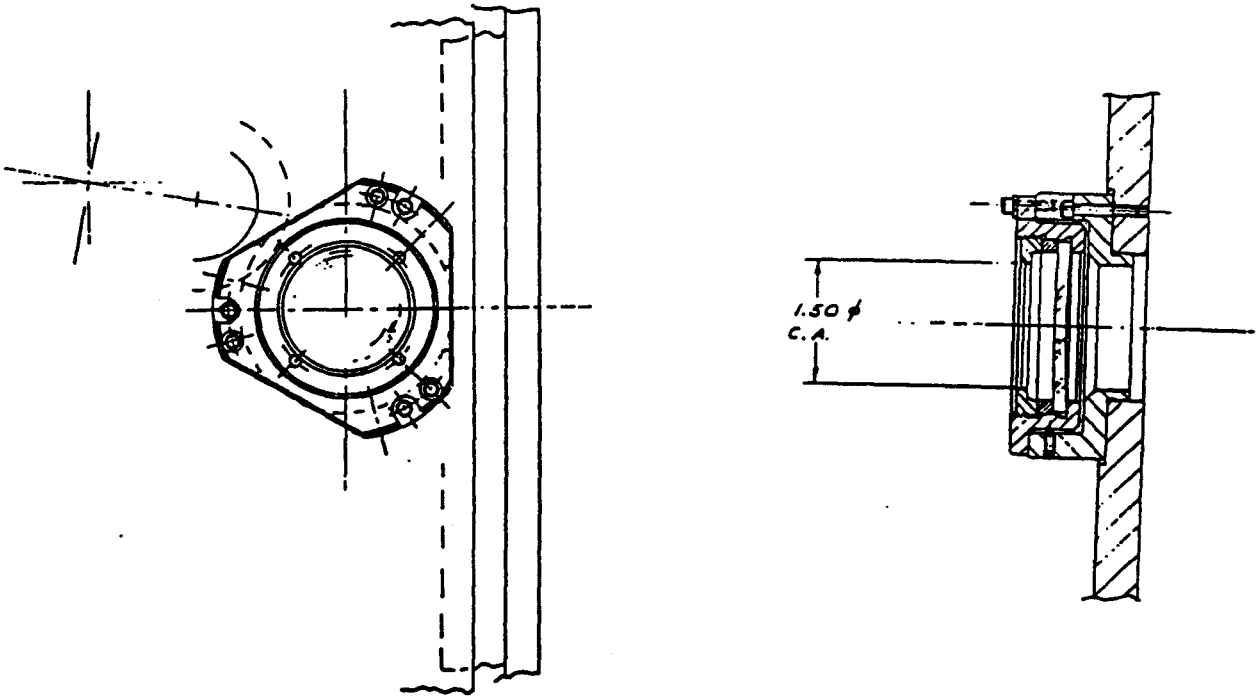

Figure II.F-4. Lens mount for prototype alignment system.

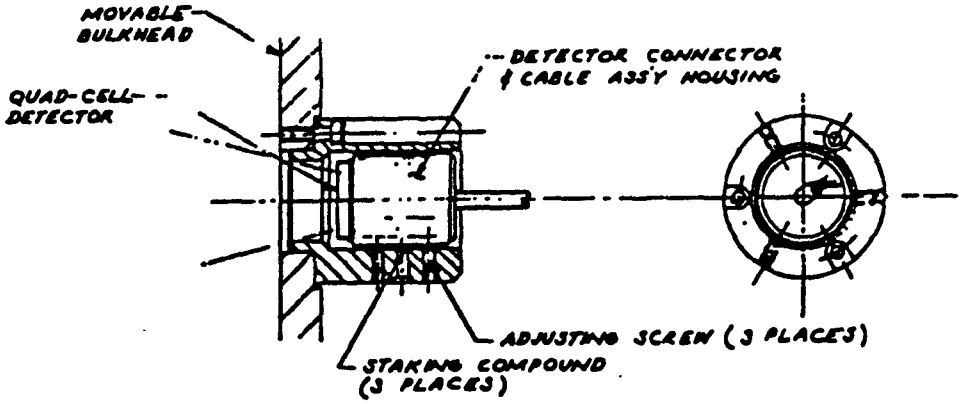

Figure II.F-5. Quad-cell detector mount for prototype alignment system.

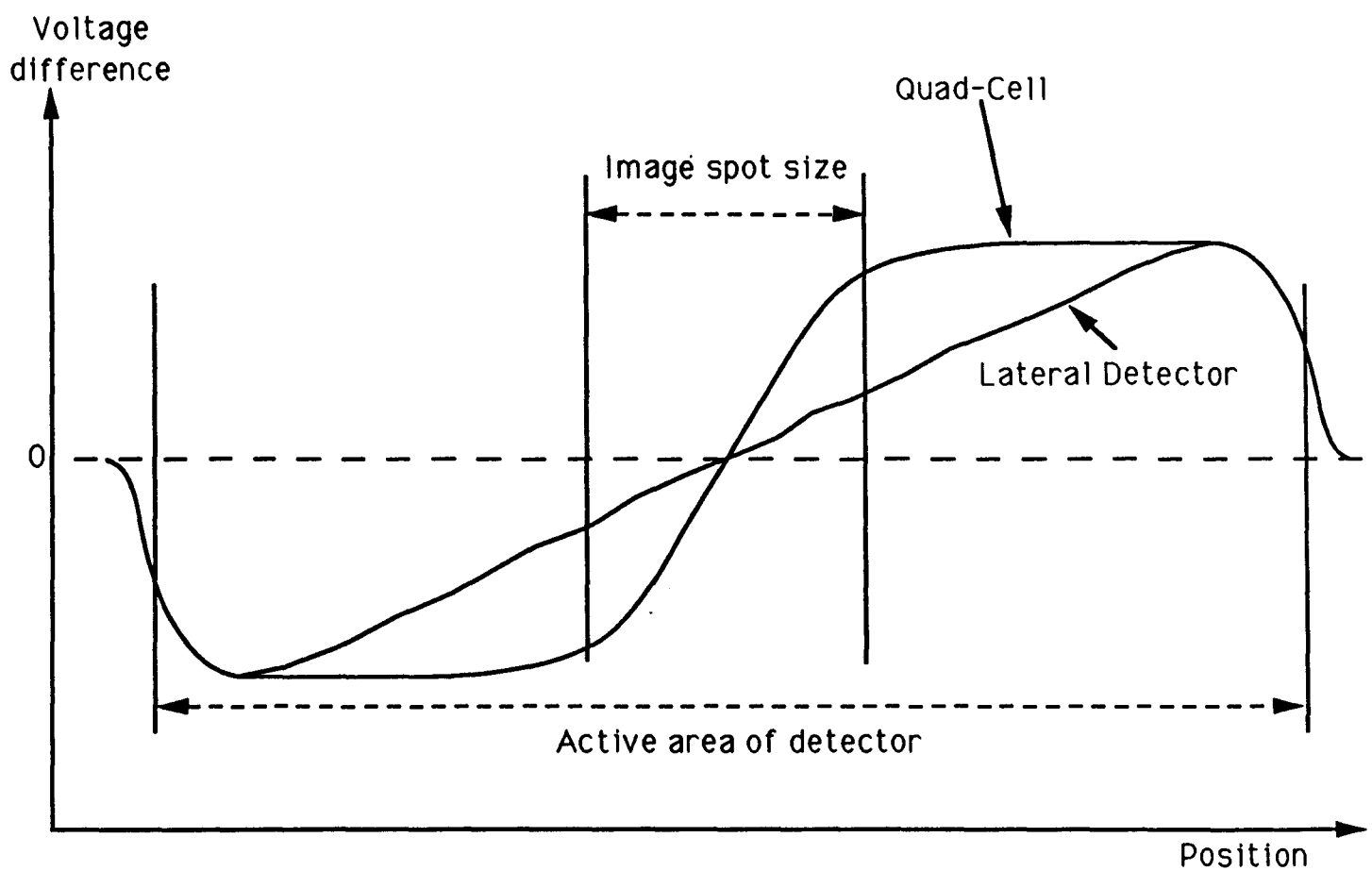

Figure II.F-6. Comparative output of quad cell and lateral effect detectors.

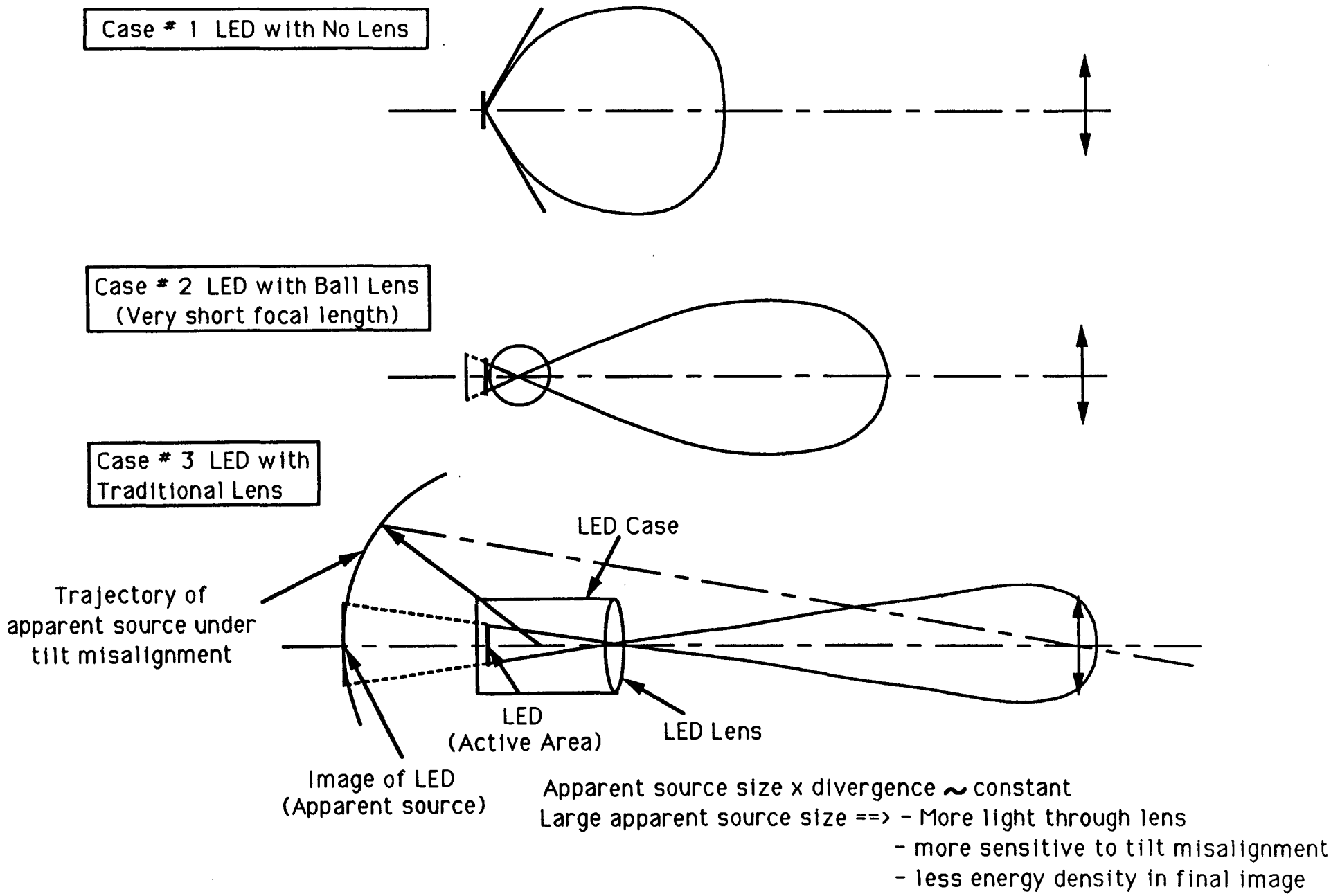

Figure II.F-7. Light source tradeoffs.

G. BOX ASSEMBLY

Assembly Table and Alignment/Holding Fixtures

The prototype box will be built in the high bay area of the Harvard High Energy Physics Laboratory. A rigid and flat assembly table has been constructed there using two pre-existing steel I-beam beds and a heavy duty rolling table with adjustable-height legs and lockable casters. The basic arrangement is shown on Fig. II.G-1, indicating the overlap of the box outline on the beds and the provision of excess table length at each end to accommodate alignment instrumentation. The upper surfaces of both steel beds and the intermediate table have been levelled and rendered coplanar by shimming to a theodolite reference. In order to safely accommodate the assembly tooling, 1.0 inch thick aluminum plates have been attached to the steel beds and table to provide a working surface four feet wide. These aluminum plates have been shimmed to preserve a planar surface upon which to build the prototype chamber. Figure II.G-2 shows half-length side and plan views of the assembly table.

It is envisioned that the bottom plate will first be assembled in sections on the table and welded. Edge angles will then be welded to it, and machinists' squares and clamps used to fix the end and intermediate "picture frame" bulkheads in place for welding. Once the bulkheads are welded square to the bottom plate, they will serve as self-fixtures for welding on the side plates. The basic concept calls for minimal specialized fixturing, relying on a bootstrap fabrication approach. Specialized tools required include: autocollimator, right angle tools with mirror mounted, right angle clamps, flats, level, laser and flat mirrors.

Precision Bulkhead Quality Control

The precision bulkheads, illustrated on Figs. II.E-6 and II.E-7, are being machined at the Boston University Physics Department shops on a large NC milling machine. B.U. will provide partial inspection of the finished bulkheads using a coordinate measuring machine (CMM). The key dimensions to be checked are the contours of the locating features on each

tube cutout indicated on the inset to Fig. II.E-6. An alternative approach to checking bulkhead dimensions is being considered, in which a precision plug having the outline of the drift tube cross section is inserted into each hole in the bulkhead to be checked. This plug would have a visible fiducial placed at the nominal wire location in the cross section. The procedure in this case would be to set up the bulkhead to be checked in a vertical orientation, with a theodolite sighted nearby to view the face of the bulkhead. The plug would be inserted into each tube hole in turn, and the coordinates of the fiducial measured and noted. In this way, the relative orientations of the tube/wire positions could be checked with respect to the optical alignment system channels.

Construction Procedure

Basic Assembly Concept

The basic concept pursued in the prototype chamber assembly was to divorce, insofar as possible, the tube relative location precision from the stiffened box structure fabrication. This concept was the only practicable choice when initial fabrication estimates suggested that a welded structure of the size proposed would likely possess misalignments of the order 0.6 -1.2 cm. While it is believed that significantly closer tolerances can be achieved in welded structures, the cost appears to be prohibitive.

Initial Layout and Alignment

a) Check part availability and dimensions

b) Align tables for overall flatness

- gross positioning and height adjustment of the three tables. Use a level also so that the three tables are parallel.
- fine leveling: starting with table A and using an autocollimator with level and retroflat mounted on right angle tool. [Two autocollimators could also be used, or a theodolite mounted outside of the table.]

- adjustment of table B. successive approximation of height and level.
- adjustment of table C: Join B and C with the flat iron, and repeat procedure.

Welding Procedures and Alignment Checks

- layout bottom plates and center approximately
- visually align component plates and recheck flatness
- welding of bottom (tack first, then seam)
- position end-bulkheads and set up optical lines of reference
- align bulkhead with machinists tool square and clamp
- locate laser or theodolite to sight through hole normal to bulkhead
- welding of end bulkhead
- position picture frames, align and square with theodolite
- tack-welding of sides and picture frames
- verify fit of cover
- final welding of sides and picture frames
- verify fit of cover after removal of box restraints
- replace box restraints
- reestablish optical lines of reference

Bulkhead Attachment Procedures

The intermediate bulkheads are positioned longitudinally using the eccentrics as a template. Transversely they are approximately located visually and loosely supported in place. By construction, at this stage they should be automatically normal to the z axis. The eccentrics and the drive mechanisms are attached.

-position intermediate bulkheads
-align longitudinally using eccentrics as template
-loosely support and align transversely (visually is accurate enough)
-attach eccentrics and drive mechanisms
-remove support and verify operation of eccentric for range (ruler) and sensitivity (optical alignment). Verify sensitivity at different

positions within the range using auxiliary lens and detector. Verify that mid-range of eccentrics correspond to nominal position

-verify again fit of cover

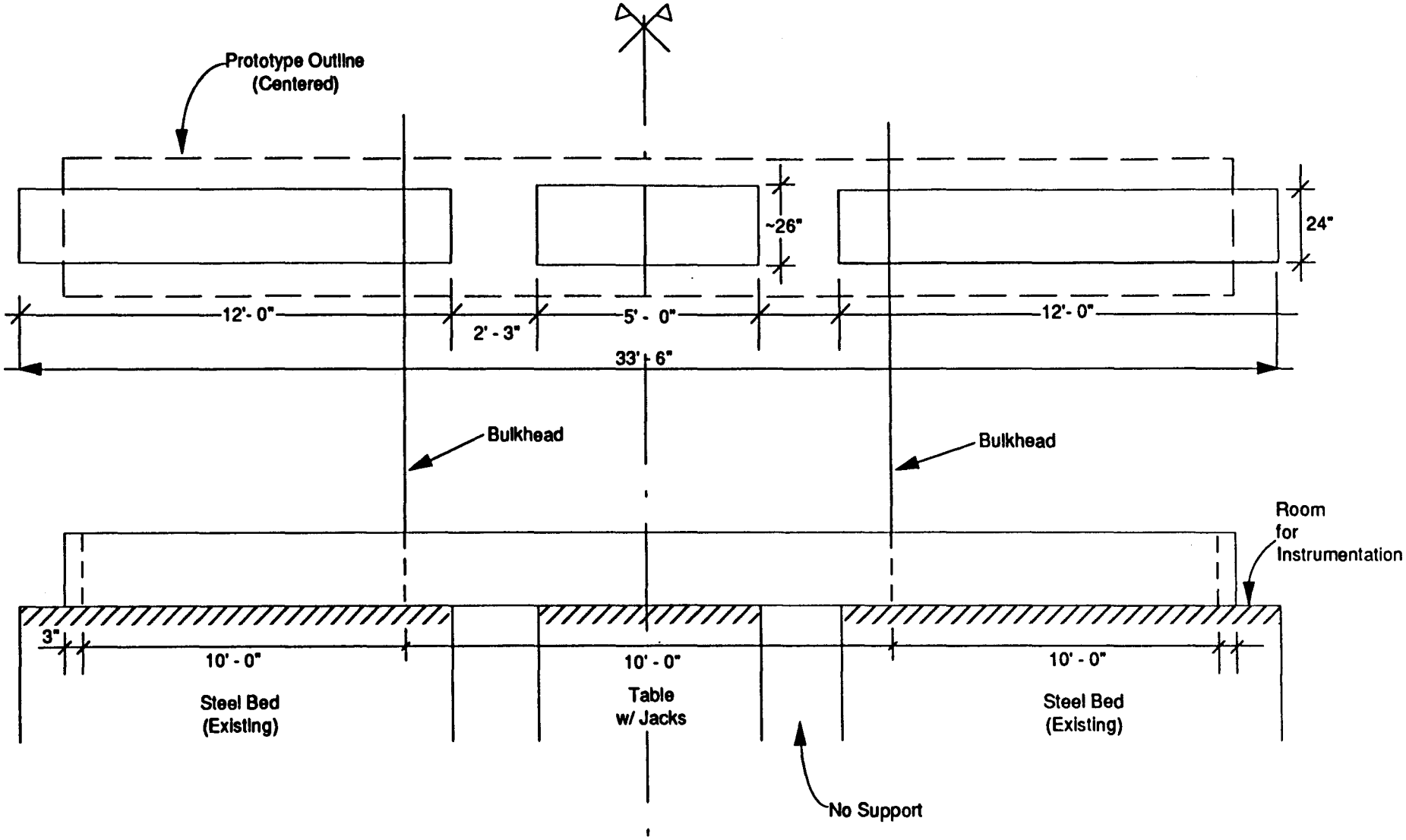

NOTES:
- Tubes are 30' long
- Box is 30' - 6" long as shown (3" each side)
- New spans: 10'- 0 " for tubes
- Bulkheads fall on "hard" steel bed

Figure II.G-1. Schematic of the box assembly table.

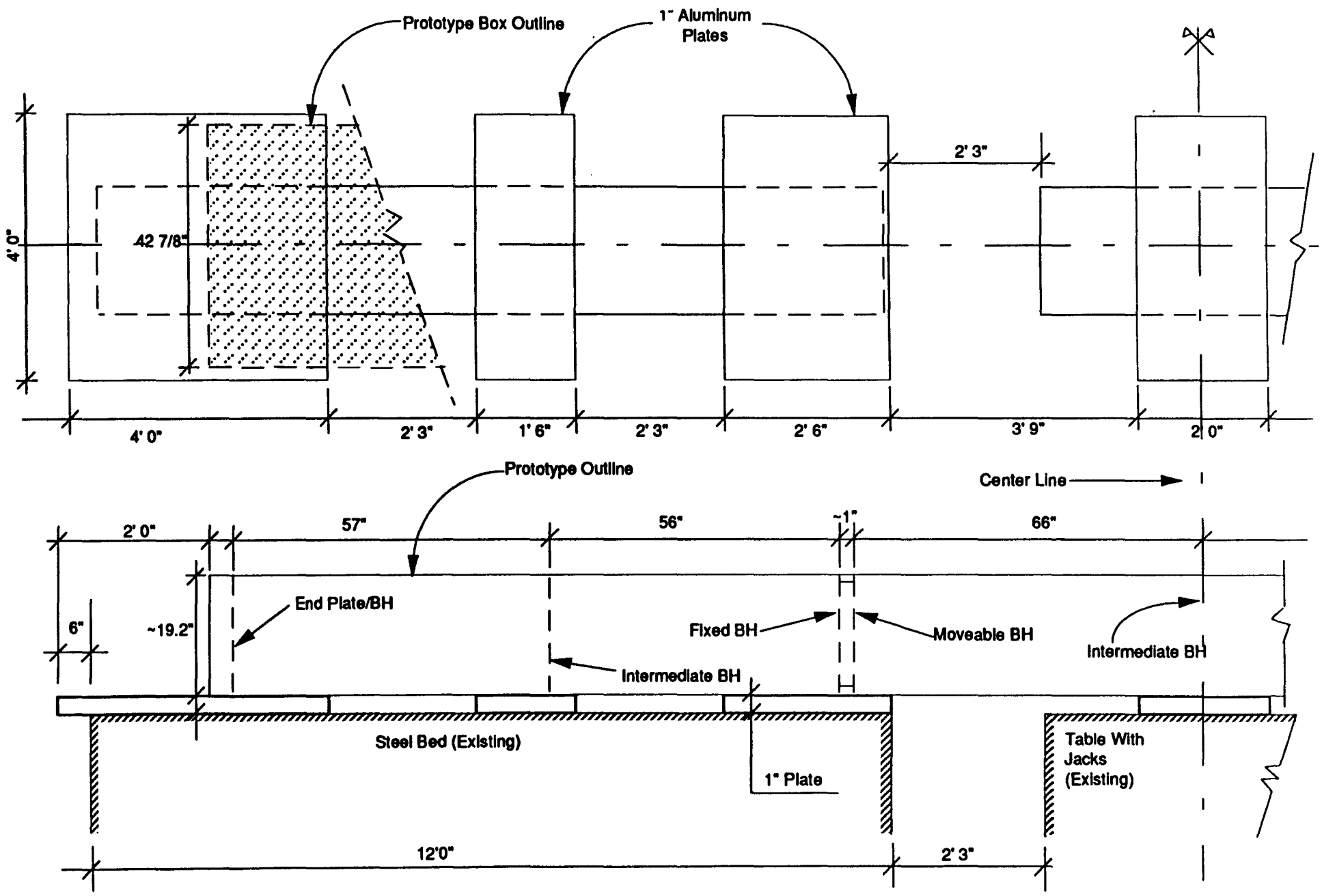

Figure II.G-2. Prototype box assembly table arrangement

H. DESIGN VERIFICATION

We will subject the drift tubes to a four stage quality assurance program after they are produced. These tests ensure that a tube will perform properly within the expected tolerances. A similar quality assurance program has already been used by the Harvard group in the production of almost two thousand muon drift tubes for the CDF experiment at Fermilab. All of the CDF tubes had to pass the quality assurance criteria, and a subset (approximately 10%) of the tubes were also tested under operational conditions on a cosmic ray test stand. All of the tubes subjected to the cosmic ray test performed flawlessly indicating that the quality assurance tests were successful.

Leak Testing

First the tubes are leak tested by doing a pressure lifetime measurement. This depends on the fact that:

$$\frac{dN}{N} = \frac{dP}{P}$$

where N is the number of gas molecules and P is the absolute pressure. It assumes that the temperature and the volume are constants. The absolute pressure is atmospheric, i.e. approximately 400 in (of water). We measure N in terms of cubic feet of gas at atmospheric pressure, and in these units N is approximately 1.5 ft^3 for one tube. Therefore we can give the leak rate in terms of the pressure gradient:

$$\frac{dN}{dt} = \left(\frac{1.5\ \mathrm{ft}^3}{400\ \mathrm{in}}\right)\frac{dP}{dt}$$

Thus a pressure gradient of 1 in/hr corresponds to a leak rate of 4×10^{-3} ft^3/hr. We also know that the leak rate will be proportional to the differential pressure (relative to atmospheric) inside the tube. We eventually plan to run with 1 in of over pressure, so if we test with 6 in of over pressure any observed leak rate will be six times normal:

$$\frac{dP}{dt} < \frac{1\,\text{in}}{\text{hr}}\{\text{test}\} \Rightarrow \frac{dN}{dt} < 6\times10^{-4}\,\frac{\text{ft}^3}{\text{hr}}\{\text{normal}\}$$

The nominal gas flow rate in the experiment will be one tube volume change per day which translates to 6×10^{-2} ft^3/hr. Therefore a pressure gradient of 1 in/hr in a test with 6 inches of over pressure corresponds to a leak rate which is 1% of the nominal flow rate of one tube volume change per day at 1 in of over pressure.

We will consider the above limit to be the goal for individual tubes. This can be done practically by observing the absence of a pressure drop over a shorter period of time, e.g. $dP < 0.1$ in over six minutes. It is also possible to leak test a number of tubes in parallel. Any tube failing the test will be repaired and then retested.

High Voltage Testing

Several tests are done to ensure the high voltage integrity of the tubes. The first set are done before the tubes are assembled to check the grid boards. The second set are done to test the completed tubes.

The field-shaping boards are subjected to two tests before the are inserted in a tube. First the overall integrity of the board is tested by subjecting it to a set of resistively divided voltages just as under actual running conditions. The only difference is that the voltages are 50% higher than normal. Second the gaps between the strips on the board are tested by grounding alternate strips and putting high voltage on the strips in between. This makes it possible to test the gaps to an over voltage of five times normal. If abnormally high current (or breakdown) is observed in either of these tests the grid board being tested is rejected.

After the tubes have been assembled and leak tested with nitrogen, a second set of high voltage tests are performed. First the grid is again tested with resistively divided voltages which are 50% above normal. In this test the anode wire is set to the same voltage as the center strip of the grid. If a grid fails this test by drawing too much current it was probably damaged in the assembly process. Second the anode wire is raised to a voltage of several hundred volts above normal relative to the center grid strip. If the wire draws too much current at this point it normally indicates a small speck of dust on the wire. This condition can often be repaired by

gradually raising the voltage over a period of time or reversing the voltage. However, if the wire does not hold voltage or if the grid is not behaving normally it is necessary to reject the completed tube.

Wire Tension Testing

After the completion of the high voltage testing the wire is subjected to a tension test. In this test a U-shaped permanent magnet is placed around the tube at several locations and an alternating current is driven down the anode wire by a variable frequency oscillator. When the current is driven at the natural vibration frequency of the wire a vibrational resonance is induced by the field of the magnet. The point of resonance is easily observed by connecting an oscilloscope across the two ends of the anode wire. The tension of the wire can then be calculated from the observed resonant frequency using the relation:

$$\text{frequency} = \frac{\sqrt{\dfrac{\text{tension}}{\text{linear density}}}}{2 \times \text{length}}$$

The wires are strung with a tension of 350 g (times g). Since the length of the wire in the tube is subdivided by the three wire supports the effective half wavelength of the vibration is approximately 330 cm. As the density of the (predominantly) tungsten wire is .00037 g/cm,we expect a resonant frequency of 45 Hz. We would like the tension to be correct within 10%, which means that the measured frequency for this test must be within 5% of the nominal value. Otherwise the tube is rejected.This test must be performed at three locations on each tube so that the wire tension is checked between each of the wire supports.

Wire Position Tests

After the assembly of a drift tube the position of the tungsten wire must be verified to 25 μm in the direction parallel to the drift direction and to 0.1 mm in the direction perpendicular to the drift. This test is done with an x-ray camera to locate the tungsten wire inside the drift tube with respect to the alignment grooves.

The prototype drift tube has a total thickness of 1 cm and the Tungsten wire has a 50 μm diameter. The transmission of x-rays through the aluminium and through the tungsten was computed from tables and is shown in Fig. II.H-1. 71 keV is just above the tungsten K-shell absorption edge. From Fig. II.H-1, it is clear that a 70 to 80 keV x-ray source will produce the highest contrast negatives. Although good pictures should be possible down to almost 30 keV, if the increase in film sensitivity is considered. Safety considerations and the availability of cheap used dental x-ray machines lead to the choice of 50 keV for these measurements.

Dental x-ray sources require extensive filtering and have low intensity. These devices do not regulate the accelerating voltage but use the tube as a rectifier resulting in a pulsed electron beam energy modulated by $\sin(\omega t)^2$ at 60 Hz. The x-rays (bremsstahlung) are of course spread towards even lower energies, but the standard aluminium filter of the tube cuts out most radiation below 25 keV. Typical dental x-ray devices use an electron beam of 5 to 20 mA, with 50 to 90 keV peak. The exposure times are up to 3 sec, and 2 to 4 pictures can be taken per minute.

The test procedure is to use a clamp type devise to be mounted around the drift tube, as shown in Fig. II.H-2. The two rods are identical to the mounting rods of the bulkheads, this positions the clamp precisely with respect to the grooves. The clamp will be fitted with two film holders as shown and pairs of tungsten wires will be imbedded into the clamp, above and below, as well as to the left and right of the drift tube. They will be positioned precisely with respect to the positioning rods and symmetrically with respect to center wire. By taking x-ray pictures from the top and from the right that show all five wires, we can determine both the x and y coordinates of the center wire. The result will be independent of the film position, independent of any film shrinkage, and most important independent of the position of the x-ray source head. With the drift tube on the assembly I-beam the clamp can be moved to different positions with the x-ray head rolled along a simple track. A focussed light beam fixed to the head allows one to position the x-ray tube properly. Finally top/bottom and left/right markers as well as a serial number will be exposed onto the negative for positive identification.

An x-ray photograph of a 50 μm tungsten wire in a prototype tube is shown in Fig. II.H-3. The photograph was taken with 50 keV x-rays. The wire in the drift tube is in the center, and the two outer lines are from fiducial tungsten wires below the

drift tube separated by 12 mm. The position of the lines can be determined to between than 10 μm, resulting in an accuracy of ±15 μm in the location of the sense wire.

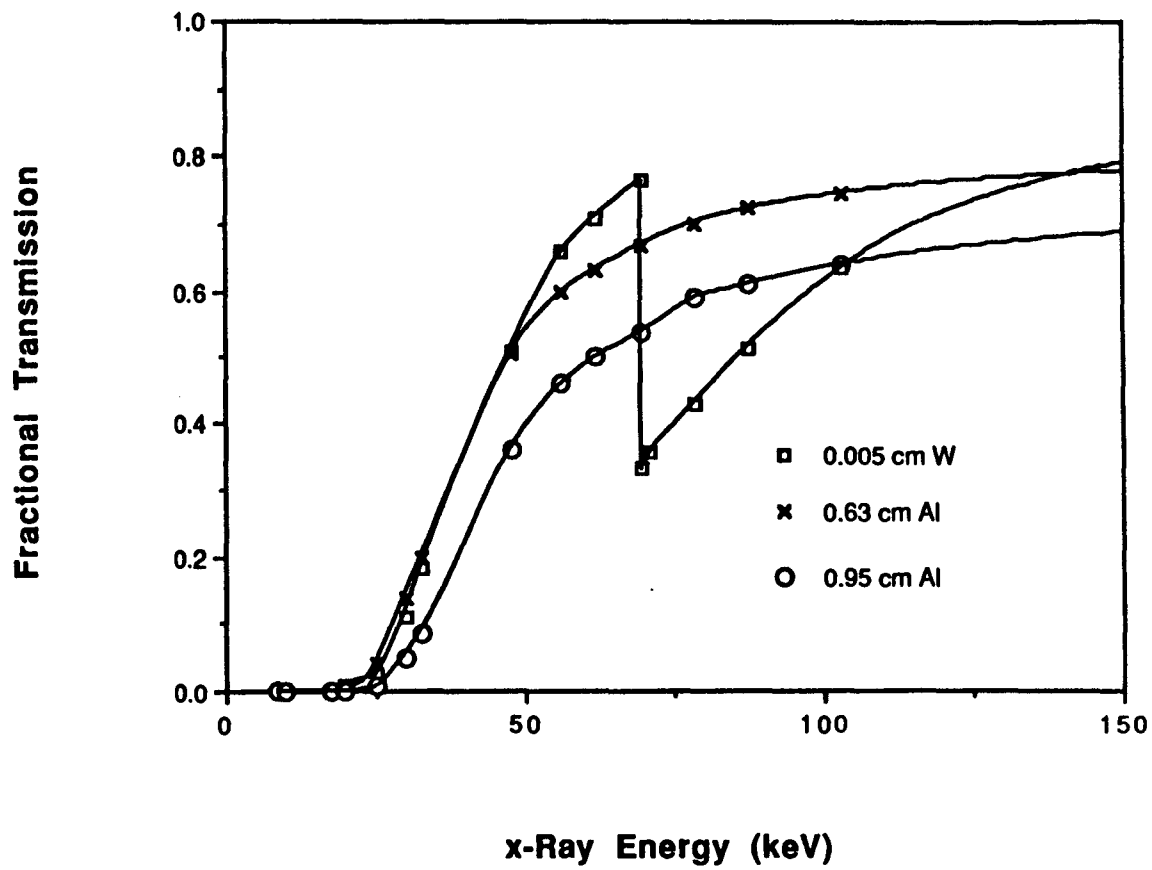

Figure II.H-1. Transmission of x-rays.

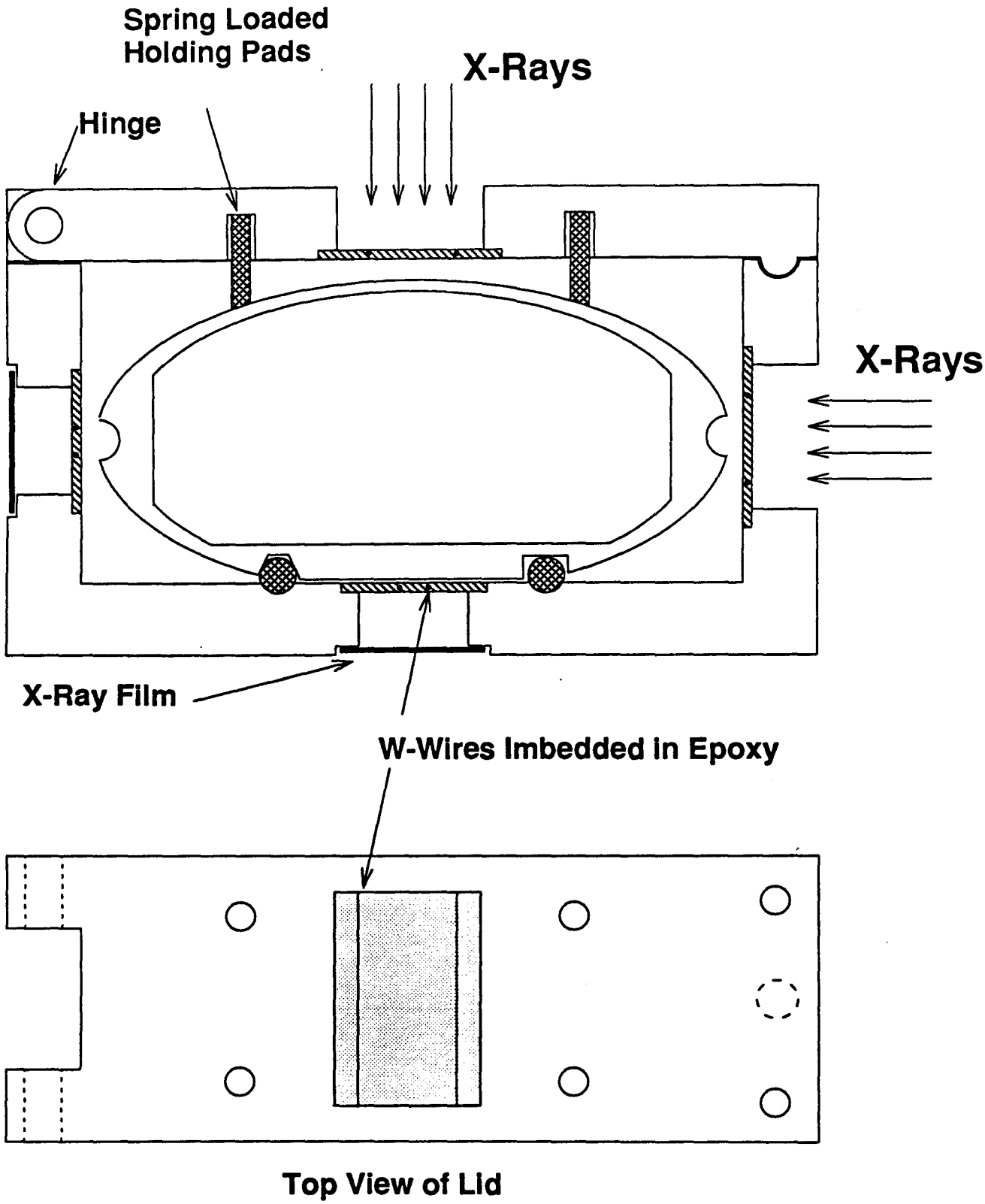

Figure II.H-2. x-ray film and fiducial holder.

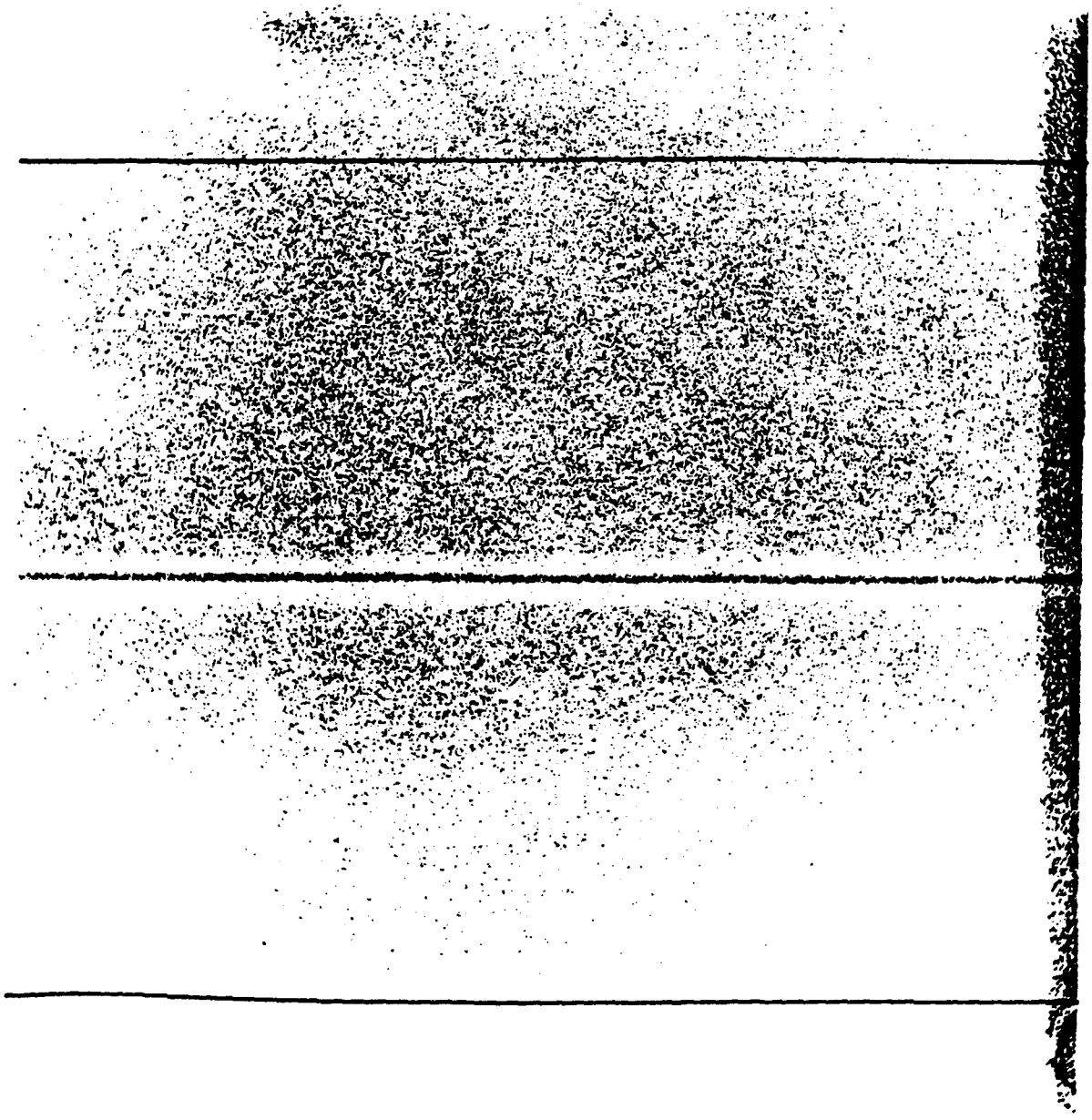

Figure II.H-3. x-ray photograph of a 50 μm tungsten wire inside an aluminum drift tube. The outer lines are tungsten fiducial wires.